DESIGN AND FABRICATION OF MULTIFUNCTIONAL POLYMER BASED NANOCOMPOSITES FOR BONE TISSUE ENGINEERING

CHEN LING

Ph.D

The Hong Kong Polytechnic University

2014

THE HONG KONG POLYTECHNIC UNIVERSITY

DEPARTMENT OF INDUSTRIAL AND SYSTEMS ENGINEERING

Design and Fabrication of Multifunctional Polymer Based Nanocomposites for Bone Tissue Engineering

CHEN Ling

A thesis submitted in partial fulfillment of the requirements for the degree of Doctor of Philosophy

August 2013

CERTIFICATE OF ORIGINALITY

I hereby declare that this thesis is my own work and that, to the best of my knowledge and belief, it reproduces no material previously published or written, nor material that has been accepted for the award of any other degree or diploma, except where due acknowledgement has been made in the text.

_____ (Signed)

CHEN LING (Name of student)

Abstract

Abstract of thesis entitled "Design and Fabrication of Multifunctional Polymer Based Nanocomposites for Bone Tissue Engineering"

Submitted by CHEN Ling

For the Degree of Doctor of Philosophy

at The Hong Kong Polytechnic University in August, 2013

Biodegradable polymer scaffolds with drug delivery function have received great research attention in bone tissue engineering due to their biocompatibility and biodegradability as temporary support systems for cell adhesion, growth, differentiation and tissue regeneration. The drug release systems of the scaffolds can deliver biologically active molecules with the desired behavior, so as to reduce the amount of drug administration and shorten the therapeutic period. Scaffolds with shape memory effects have been considered as smart materials for potential applications in minimally invasive surgery. Efforts have also been devoted to the development of composite scaffolds combining biodegradable polymers and bioactive ceramics with enhanced osteoconductive properties and mechanical strength. However, there is still no best method for three-dimensional scaffold fabrication and the influences of bioactive inclusion and porosity of the scaffold on drug delivery behavior, shape memory effect, biodegradability, bioactivity and cellular response have not yet been well addressed. The purpose of this study is to develop a technique to produce a multifunctional porous composite and investigate the influence of bioactive inclusion on its mechanical

properties, biodegradability, drug release behavior, shape memory effect and cellular response for bone tissue engineering.

Among the developed fabrication technologies, the solvent casting/particulate leaching method is the most commonly used scaffold fabrication method due to its simplicity, efficiency and ability to independently control the porosity and pore size of the scaffold. Nevertheless, it is limited to fabricating scaffolds with uniform pore distribution. To solve this distribution problem, a method using polymer coagulation, thermal compression molding and salt leaching has been reported however, the problem of decomposition of the active drug and polymer may be induced. In this study, a new technique has been developed to fabricate multifunctional scaffolds. This technique, called PC-DC technique, applying polymer coagulation (PC) and drug coating (DC) to solvent casting/particulate leaching method and using cold compression molding instead of conventional hot compression molding. This low temperature composite technology can contribute to a wider range of choices of drug loadings, since thermal decomposition of drug inclusion and polymer matrix can be avoided. This technique not only independently controls the pore size and porosity of the scaffolds, but also reduces solvent residual. A uniform distribution of pores throughout the polymer matrix can be achieved by this technique.

Poly(ethylene glycol)/dexamethasone (PEG/Dex)-coated porous poly-D-L-lactide/nano-hydroxyapatite (PDLLA/nano-HAp) composites with homogenous pore networks and controllable porosity and pore size have been fabricated by the PC-DC technique. The compressive moduli and strengths of the composites were improved by the nano-HAp

addition, which were close to those of cancellous bone. The improved wettability of the scaffold by PEG/Dex coating and nano-HAp filling was confirmed. The drug loading ability and total drug release amount of the scaffolds increased with increasing porosity level and/or the nano-HAp content. The improved bioactivity of the scaffolds was validated by the apatite formation on the scaffolds with nano-HAp addition after incubation in simulated body fluid (SBF). The compressive moduli and strengths of the scaffolds after incubation in SBF were affected by the combination of degradation, weight loss, apatite deposition and incubation time. Nano-HAp incorporation can decelerate the polymer degradation and mass loss. Moreover, the PDLLA/nano-HAp scaffolds showed a pH compensating effect to reduce the risk of chronic inflammation complications. Cyclic thermomechnical and physical shape recovery tests were firstly conducted to investigate the shape memory effect of the porous PDLLA/nano-HAp scaffolds. The results showed that desirable shape memory behavior could be achieved when the nano-HAp fracture was 10 wt%. Good biocompatibility, bioactivity and osteoconductivity of the PDLLA based samples were confirmed by investigating the ability of the scaffolds for MG63 cell adhesion, proliferation and differentiation.

This study provides a new technique for the fabrication of multifunctional biodegradable drug loaded bone scaffolds with shape memory function, which is highly desirable in the bone repair applications. The findings of the study not only lead to a better understanding of the effects of nano-HAp, structure factor, surface coating on the mechanical properties, degradability, drug release behavior, shape memory effects and the cellular response of the composites in bone tissue engineering, but also provide guidelines for design and fabrication of the multifunctional composites with

controllable properties for certain application requirements. A finite element model simulating the behavior of the scaffolds implanted into a human body and animal model experiments for further evaluation of the in vivo performance of the composite scaffolds are recommended for future study.

Acknowledgements

I would like to express my sincerest thanks to my supervisor, Prof. Chak Yin TANG for giving me this great opportunity to join his group and broaden my research horizon. The lessons I learned from him were not only in regard to scientific knowledge, but also responsibility, perseverance, and integrity, which will bring me lifelong benefits. Without his constructive advice, clear guidance and continuous support over the past four years, I would not have completed this research. I am forever grateful for everything that he has done for my continuous improvement.

My sincere gratitude is also accorded to my co-supervisors, Dr. Da Zhu CHEN of Shenzhen University and Dr. Chi Pong TSUI of The Hong Kong Polytechnic University (PolyU), for their selfless help, valuable suggestions about the experimentation and documentation in this study. I would like to express my particular gratitude to Mr. S.Y. Lau (PolyU) in the Materials Engineering Laboratory, Mr. Hardy LUI (PolyU) in the Material Research Centre, for their patience and thoroughness in instructing me to use those equipments for my research.

My appreciation is expressed to Dr. Mo YANG (PolyU) in the Interdisciplinary Division of Biomedical Engineering for his professional advice and providing the resources in his laboratory. I would also like to thank Ms. Xuan LIU (PolyU) from the Institute of Textiles and Clothing, who taught me the basic cell culture techniques and provided indispensible assistance for the *in vitro* biological tests. Special thanks go to Dr. Harry KU and Dr Francisco CARDONA of the Centre of Excellence in Engineering Fibre Composites (University of Southern Queensland) for their guidance and

assistance during the three-month *Research Student Out-going Attachment Programme*.

My final acknowledgement should be reserved to my family: my parents, who raised me and supported me; my husband, who trusted and encouraged me all the time. Their unyielding support gave me confidence and strength to overcome every difficult moment and finish this thesis.

Table of Contents

List of Figures

List of Tables

Chapter 1. Introduction

1.1 Background

Bone tissue which provides the human body with physical support, has the function of protecting the internal organs and housing biological elements for hematopoiesis, as well as keeping the acid-base and electrolyte balance (Sommerfeldt 2001). These functions, together with the unique ability to adapt its mass and morphology to functional demands and to effect repairs without leaving scars, make it the ultimate smart material (Salgado et al. 2004). That explains why bone is considered to be one of the most important tissues in the human body. However, bone deficiency or failure resulting from bone metastases, congenital defects, and trauma is considered as a major human health problem, especially due to the aging of the population worldwide. This can significantly alter people's body balance and quality of life. According to a new market report published by Transparency Market Research, the population aged 60 years and above is expected to double by 2020 that represents the key driver of global orthopedic biomaterial market, which is estimated to reach a market worth USD 5,519.9million in 2019 (Medtronic Inc., 2013). Therefore, it is critical for both physicians and scientists to get a deeper understanding of the biological aspects of bone and develop appropriate strategies to solve this health problem.

Even though some progress has been made in the bone regenerative medicine field, standard therapies, such as autograft and allograft applied for orthopaedic defect treatments (Rose & Oreffo 2002). The autograft is a part of bone taken from a patient's own body to complement host repair, while an allograft is a bone harvested from one

donor and implanted into the patient. However, both autograft and allograft suffer from certain limitations (Giannoudis et al. 2005). Autograft is restricted owing to the inadequate amount of autograft material and the donor site morbidity. And allograft is limited by the shortage of donors and higher rates of side effects and/or infection occurrences (Chen et al. 2002). Other therapies such as synthetic prostheses and medical devices cannot substitute all the functions of bone or they may show a significant rate of complications, like resorption of bone transplants and inflammations (Chen et al. 2001). Repairs or reconstructions of large bone tissue defects have always been a thorny problem for surgeons. Hence, improved clinical strategies and adequate bone replacements for full recovery of the patients are imperative.

Tissue engineering is defined as "an interdisciplinary field that applies the principles of engineering and life sciences in the development of biological substitutes that restore, maintain, or improve tissue function" (Langer & Vacanti 1993). Bone tissue engineering potentially provides an alternative approach to treat the loss or malfunction of bone tissue without the restrictions of current therapies. Differing from the traditional biomaterial (metal, ceramic, and polymer) implantation approach, tissue engineering aims to make use of the self-healing potential of human tissue to induce the new tissue regeneration. There are three general strategies for tissue engineering: (i) Implantation of isolated cells or cell substitutes; (ii) Implantation of tissue-inducing substances; and (iii) Implantation of scaffold with cells within it (Langer & Vacanti 1993). As bone is a 3D structure, and cells do not grow in a 3D fashion, a 3D scaffold mimicking bone structure should be used so that new tissue can be grown in a 3D manner, especially for a large bone defect. Therefore, in bone tissue engineering, more attention has been paid

to the third strategy that involves isolating cells from the patient, followed by culturing of the cell in temporary 3D scaffolds, regeneration of the new tissue and replacing the biodegrading scaffolds.

Three-dimensional porous scaffolds play an important role in tissue engineering that they serve as a temporary template for cell interaction and formation of a bone-extracellular matrix to provide structural support until a new tissue formed (Chen et al. 2002, Hutmacher et al. 2007, Liu et al. 2007). Design and fabrication of these scaffolds becomes one of the most significant challenges in tissue engineering. Considering the sensitiveness and complexity of a human body, scaffolds need to retain several features as follows: (i) the chemical composites of the scaffold should be biocompatible in case that they cause unresolved inflammatory responses, minimal immunity or cytotoxicity; (ii) three-dimensional architecture with predefined shape, controllable interconnected porosity and desired pore size are needed to direct cell growth and immigration; (iii) good mechanical properties are imperative in order to help the scaffold support the patients during their normal activities; (iv) the degradation rate of the scaffold needs to match the new tissue growth rate so that scaffold can provide sufficient support during the full regeneration process of the impaired tissues (Rezwan et al. 2006, Chung & Park 2007, Bose et al. 2012). Biomaterials used for orthopedic applications are mainly metals, ceramics, and polymers. Within the category of polymers, biodegradable polymers attract much more attention because they can be gradually degraded and replaced by the newly regenerated tissues which can avoid secondary surgery to remove the implants after tissue recovery or when the drug supply is depleted (Liu et al. 2007, Biondi et al. 2008). However, scaffolds derived from unfilled polymers are lack of osteoconduction

and mechanical strength. Recently, composites derived from the combination of bioactive ceramics and biodegradable polymers have been developed to improve these properties (Boccaccini et al. 2005, Zhang et al. 2009, Chuenjitkuntaworn et al. 2010). Efforts have also been devoted to the development of scaffolds with drug release function. This kind of scaffold in or near the damaged bone can not only act as a physical support but also release growth factor, anti-inflammatory drug or antibiotic to provide the benefits of high therapeutic efficacy and fast recover rate (Kim et al. 2004, Biondi et al. 2008, Mourino & Boccaccini 2010). Scaffolds with shape memory effect (SME) have also been investigated and considered as intelligent scaffolds with potential applications in intelligent medical devices, and implants for minimally invasive surgery, since they can be precisely positioned in the body in a temporary small shape and gain their application-relevant shape after implantation (Lendlein & Langer 2002, Gunes & Jana 2008, Leng et al. 2011). However, the influences of bioactive inclusions on the drug delivery behavior, shape memory effect, biodegradability and cell response of multifunctional scaffolds have not yet been well addressed.

Over the last two decades, several fabrication technologies have been developed for processing biodegradable polymers into three-dimensional porous scaffolds, for example, fiber bonding, emulsion freeze drying, solvent casting/particulate leaching, gas foaming/particulate leaching, phase separation, high-pressure processing, electrospinning, solid freeform fabrication (SFF) (Hutmacher 2001, Hollister 2005, Liu et al. 2007). The pore size, porosity, surface topography, and even mechanical properties of scaffolds can be affected by the fabrication methods applied for scaffold preparation. Currently, no best fabrication method has been developed, while all the

methods have their own advantages and limitations. For example, both electrospinning and phase separation have the advantages of easy processing and can fabricate scaffolds with high porosity; nevertheless, they have the same problems with residual solvent which can be harmful to human tissue. SFF can fabricate scaffolds with predefined porous architecture using a data file created by computer aided design software; however, fabricated scaffolds generally have limited pore size and insufficient mechanical strength (Ravichandran et al. 2012). Furthermore, directly mixing the drug with the polymer is a commonly used method to obtain drug delivery scaffolds (Kim et al. 2003), and it is limited for water soluble drug loaded scaffold preparation using the particular leaching method. A new method need to be developed for fabrication of composite scaffolds with biocompatibility, controllable pore size and porosity, improved mechanical properties, biodegradability, bioactivity, drug release function, and shape memory effect to improve the performance of the bone scaffolds to the greatest extent.

1.2 Objectives

This study aims to develop a technique to fabricate a multifunctional porous composite with similar mechanical strength to that of natural bone, controllable shape memory behavior, osteoconduction and drug release function, for bone tissue engineering.

The main objectives of this study are listed as follows:

- To develop a new processing method for multifunctional polymeric composite fabrication;
- To study the effect of processing conditions on the microstructure and drug

release behavior, and the mechanical properties of the composites;

- To study the influence of fraction of the inorganic filler phase on the mechanical properties, drug release behavior, biodegradability and shape memory behavior of the composites;
- To investigate the effect of bioactive inclusions on the bioactivity of the fabricated composites in simulated body fluid (SBF) by apatite deposition on their surface; and
- To investigate the influence of the drug coating, bioactive inclusions and porosity of the composites on human osteoblast-like cell attachment, proliferation, and differentiation.

To achieve these objectives, multifunctional porous dexamethasone (Dex)-releasing poly(D-L-lactide)/nano-hydroxyapatite (PDLLA/nano-HAp) composite was fabricated as a model composite system for bone tissue engineering. It could not only act as a temporary physical support, but also release Dex to prevent inflammation. Its degradability and shape memory effect could avoid secondary surgery and had high potential for minimum invasive surgery which might reduce the pain of a patient and shorten the therapy period. A method which involves polymer coagulation, cold compression molding, particulate leaching and drug coating (PC-DC technique) was developed in this research for scaffold fabrication. Poly(D-L-lactide) (PDLLA), a US Food and Drug Administration (FDA) approved biodegradable polymer, has been fabricated into porous scaffolds for various tissue regenerations (Wu et al. 2008b, Xu et al. 2009), and was chosen as the base material. However, scaffolds developed from unfilled polymers are limited by low mechanical strength and osteoconductivity.

Calcium phosphate (CaP) is the major mineral composition of natural bone and possesses osteconductive properties (Douglas et al. 2009). Hydroxyapatite (HAp) is one of the most frequently used CaP in bone tissue engineering due to its great bioactivity. Compared with micro-HAp, nano-HAp with a larger surface area exhibits improved mechanical properties of the composites due to the strong hydrogen bonding interactions between the nano-HAp and the polymer (Zhou et al. 2007, Ren et al. 2008). Therefore, nano-HAp was chosen as the reinforcing and bioactive phase in the polymeric matrix. Dex was selected as the drug releasing model because of its great effect in inducing and maintaining the osteoblastic phenotype of exposing stem cells and its high anti-inflammatory capacity (Yoon et al. 2003). The microstructure, mechanical properties, bioactivity, degradability, shape memory behavior, drug release function, and cellular response of the multifunctional Dex-releasing PDLLA/nano-HAp composites were investigated.

1.3 Need and Significance

Development of polymeric scaffolds with appropriate chemical composition, structure, and functions is critical for their success in tissue engineering applications (Armentano et al. 2010). Considerable work has been done to fabricate scaffolds with the goal of achieving high degrees of porosity and good control over pore size, morphology, degradation and drug release rate so as to facilitate cell attachment, proliferation and tissue in-growth. Recently, biodegradable polymeric composites incorporated with a nano-sized bioactive ceramic phase have achieved much recognition as bone scaffolds because both the mechanical and osteoconductive properties of the scaffolds have be improved. Shape memory polymers (SMPs) have been considered as an intelligent

material with potential applications in implants for minimally invasive surgery since they can be precisely positioned in the body in a temporary small shape and attain their application-relevant shape after implantation (Wischke & Lendlein 2010). In view of this effect, development of multifunctional polymer based composites with degradability, shape memory effect, and drug release function is indispensable in bone tissue engineering. These multifunctional scaffolds may have a high potential in the field of orthopedics to treat large bone defects by providing a substrate for the cell adhesion, growth and releasing bioactive molecules to promote bone regeneration. A comprehensive understanding of the relationships among the pore structure, drug delivery, degradation, mechanical properties, shape memory effect, and cellular response of the multifunctional scaffolds was achieved. Patients will benefit greatly by single surgery, less pain and fast healing time by the shape memory effect (minimum invasive surgery) and controllable degradability (avoiding second surgery) of the scaffolds. The risk of future surgery will be reduced due to minimum invasion with increased scaffold functionality and reliability.

This study provides a novel way for the fabrication of multifunctional scaffold material with drug releasing function, shape memory effect, and controllable biodegradation rate. This technique not only independently controls the pore size and porosity of the scaffolds, but also shortens the scaffold fabrication time by reducing the solvent evaporation time in the polymer coagulation, salt leaching and solvent casting steps. Solvent residual can be reduced by polymer coagulation and vacuum drying. The low temperature fabrication technique, avoiding thermal decomposition of the drug inclusion and polymer matrix, contributes to a wider range of drugs and polymers for

fabricating drug releasing biodegradable porous shape memory polymer composites. Moreover, the subsequent PEG/Dex coating process is an alternative approach to fabricate drug loaded scaffold, especially for water soluble drugs. The multifunctional scaffold material fabricated in this study has the advantages of controllable biodegradability of the scaffold thereby avoiding secondary surgery for taking out the implants after tissue recovery; similar mechanical properties and microstructure structure to human cancellous bone; the drug releasing function provides relatively high therapeutic efficacy and a faster recover rate; excellent bioactivity and biocompatibility facilitating cell adhesion, growth, and differentiation; reduction of surgery risk by minimal invasive techniques.

Chapter 2. Literature Review

After describing the background and research objectives of this study, an overall review of the substantial literature is presented in this chapter. Basic knowledge of bone biology, which is fundamental for bone scaffold fabrication, is placed at the beginning of this chapter. The biological, chemical, and biological requirements of a bone scaffold are then explained. To fulfill the requirements of a bone scaffold, selection of the material and fabricating method is essential. Therefore, the development of bone scaffold materials, the current available fabrication techniques, as well as their limitations and research trends, are discussed at the end of this chapter.

2.1 Bone Biology

2.1.1 Bone Structure and Function

In order to fabricate a scaffold mimicking natural bone structure for bone tissue engineering, understanding the structure and function of such tissue is the first step. Bone is a stiff skeletal material providing the principal support and protection of the body. Bone has the major role in load bearing and prevents fractures caused by fatigue. The protection function of bone is widely recognized, especially in vital areas (e.g. head). Dense-porous-dense sandwich structures can be found in the cranial vault, which can absorb maximum energy to avoid serious injury. In addition to these two major functions, bone is a hematopoietic organ to produce red blood cells throughout one's life. Moreover, hormones, fibroblast growth factor 23 and osteocalcin, secreted from the bone have the function of mediating phosphate metabolism and energy metabolism (Burr & Akkus 2014).

Bone is composed of 60% mineral (primarily apatite), and its organic component contributes about 40% to its composition. Almost 95% of the organic material is collagen (type I, III, V collagen) and the rest is proteoglycans and numerous non-collagenous proteins. Bone is organized as a multiscale composite material, from the nanometer to millimeter scale. The micro- and macrostructure of a human long bone were illustrated by Park & Lakes (1992). At the macroscopic level, bone is a composite material comprising dense cortical (or compact) bone and more porous cancellous (or spongy, trabecular) bone. Cancellous bone is typically found in the ends on long bones with a cortical bone formed outside the shell. At the microscopic level, cortical bone is composed of Haversian systems (or osteon) which is made up of from 4-20 concentric lamellae around the Haversian canal carrying a blood vessel, nerves, and lymphastics. At the nanostructural level, bone is made up of collagen fibers with apatite crystals. The collagen/apatite fibrils are the basic components arranged into lamella sheets (Burr & Akkus 2014). Cancellous bone also consists of lamellae arranged approximately parallel to the trabecular surface.

2.1.2 Bone Cells

After describing the bone structure and functions, a brief introduction to the cells of bone tissue and the cells used in bone tissue engineering are described. Cells involved in the formation and remodeling of bone tissue include four different types: osteoblasts, osteocytes, bone lining cells, and osteoclasts.

Osteoblasts are fully-differentiated cells that originated from either bone marrow stromal cells or mesenchymal stem cells (Marie 2008). Osteoblasts cells are derived from preosteoblasts when the preosteoblasts are stimulated by some factors, such as bone morphogenetic proteins, for differentiation (Zaidi 2007). Osteoblasts are usually found lining areas of newly developed unmineralized tissue and are composed primarily of collagen type I. They are responsible for the formation of bone.

Osteocytes are the main cellular components of bone and can be found in the whole body of the bone, surrounded with a mineralized matrix. They are the fully mature osteoblasts. An osteocytye is a cell responsible for maintaining the mineralized tissue through limited abilities of both synthesis and resorption of the matrix.

Bone lining cells are found in the lining surface of bone. They form a thin layer covering both the inner and outer surface of bone. Bone lining cells are flat, slender, elongated and inactive. They are responsible for preparing the surface of bone by removing nonmineralized collagen fibrils, and then deposit a smooth layer of collagen over the bone surface (Matsuo & Irie 2008).

Osteoclasts are bone-destroying cells, whose role is the resorption of bone. They are large and multinucleated cells differentiated from the hematopoietic stem cells found in circulating blood. They exhibit two distinct plasma membrane regions: a ruffled portion and a sealing region (Väänänen et al. 2008). Osteoclasts disappear and presumably die after they have done their job.

Bone tissue engineering is the application of biological, chemical and engineering principles to repair, restore or regenerate bone tissue using the three basic elements of biomaterials, cells, and growth factors (Laurencin et al. 1999). Cells have the functions of forming replacement tissue and forming bone tissue engineering constructs. Selection of a reliable source of cells to be seeded onto the scaffolds and expanded into high numbers before implantation is of importance in tissue engineering.

Osteoblasts harvested directly from biopsies taken from patients (autologous cells) are the most obvious choice for bone tissue engineering because of their nonimmunogenicity. However, the isolation of osteoblasts is time consuming and it is limited by the low cell number obtained from the host tissue and the low expansion rates of the osteoblasts. Moreover, in certain bone related disease or for an elderly patient, autologous cells may not be appropriate for transplantation (Heath 2000). Using cells obtained from a non-human donor (xenogeneic cells) is an alternative method to harvest enough cells numbers. However, xenotransplantation has serious limitations, such as immunogenicity of the cells, possibility of the transmission of infectious agents and the ethical issues (Platt 1996).

Stem cells have been demonstrated to be an attractive cell source for bone tissue engineering because they are undifferentiated cells and are able to generate virtually all other cell types when using the appropriate differentiation factors, such as biological, physical and chemical stimuli (Blau et al. 2001). *Embryonic stem cells (ES)* are found in the Inner Cell Mass of the blastocyst. They can differentiate into nearly all cells that arise from the three germ lines, but not the embryo (Preston et al. 2003). For bone tissue

engineering, osteoblasts can be differentiated from ES cells with the help of dexamethasone, as reported by Buttery (2001). Multipotent stem cells also known as adult stem cells (ASC) can be found in the fully differentiated tissues, such as muscle, cartilage, bone, the nervous systems and, probably, the liver and pancreas (Heath 2000). They can differentiate into cell lineages from the tissue in which the ASC resides. In addition, ASC have been found to have a higher degree of differentiation plasticity (differentiate into muscle, brain, and fat cells) (Toma et al. 2001).

Human mesenchymal stem cells (MSC), stem cells that reside in bone marrow, have drawn much interest in the bone tissue engineering field. These cells have the name mesenchymal stem cells, given by Caplan (1994), who reported that these cells could be easily isolated, expended and directed to differentiate into cells with mesenchymal origin and form bone, cartilage, fat, and other tissues. MSCs have been used not only in bone tissue engineering research but also in clinical trials (Li et al. 2006). *Ex vivo*-expanded MSCs combined with three-dimensional porous biomaterials carriers have been implanted into a sheep skull to directly repair a cranial defect (Shang et al. 2001). Moreover, systemic infusion of MSCs into subjects with osteoporosis has led to the attenuation of the disease (Ichioka et al. 2002). The use of MSCs in bone tissue engineering applications offers powerful novel tools in the clinical strategy development for the site-specific bone defects repair and the attenuation of bone disorders (e.g. osteoporosis).

Additionally, in bone tissue engineering research, human clonal osteoblast cell lines are widely used as osteoblastic models. The most commonly used osteoblast-like cell lines

include SaOs2, MG63, Te85 (HOS), and U2OS (HTB96). All these cell lines are derived from osteosarcomas but differ in their responsiveness to certain hormones. Osteosarcomas are malignant tumors of bone derived from cells of the osteoblast lineage. They are poorly differentiated and pleomorphic with high mitotic activity. The reason for their widespread use as osteoblast models is that osteosarcoma cells can express osteoblastic genes, synthesize bone matrix proteins and respond to calcium-regulating hormones (Gartland et al. 2005).

2.1.3 Bone Repair

Bone is a tissue with the ability of defect-healing to regenerate new tissue and blood vessels and maintain physical and biological functions. In order to fabricate a suitable scaffold to treat bone damage, it is essential to understand the bone healing process. Bone fracture commonly occurs due to falls, accidents or sports injuries. It is taken as an example to study the bone repair. There are four stages of secondary fracture healing: inflammatory response, soft callus formation, hard callus formation and bone remodeling (Li & Stocum 2014). Stage 1: When trauma occurs, the blood supply of the bone is disturbed and a hematoma (blood clot) forms. Platelets trapped in the hematoma release a platelet-derived growth factor (PDGF) and a transforming growth factor (TGF-β) to initiate an inflammatory response. At Stage 2, the periosteal MSCs begin to produce new vessels, proliferate and differentiate into osteoblasts. The hematoma is replaced by fibrocartilage. After that, the cartilage is replaced by hard callus; and the osteoblasts form woven bone on the calcified matrix at Stage 3. At the final stage of bone repair, a remodeling process proceeds with hard callus resorption by osteoclasts and lamellar bone formation by osteoblasts.

The repair of bone critically depends on the defect size. A defect heals spontaneously when it is a non-critical size. However, a critical size defect cannot completely be repaired and filled with new bone tissue by the bone self-healing ability (Meyer & Wiesmann 2006). Research is currently in progress to develop bone-like scaffolds containing cells and/or bone growth factors that helps bone regeneration after implantation, for critical defect healing and is known as bone tissue engineering (Chung & Park 2007). The requirements of a bone scaffold are studied and presented in Section 2.2.

2.2 Requirements of Scaffolds for Bone Tissue Engineering

To succeed as a bone regenerating scaffold, it should: (i) be biocompatibility inducing minimal immune response or cytotoxicity; (ii) posses bioactive surface properties which promote cell adhesion, bone bonding and stimulate osteogenesis; (iii) have precise controllable interconnected porous structure with predefined shape, porosity and pore size that can allow cell ingrowth, immigration and differentiation; (iv) exhibit mechanical properties similar to those of the replacing host bone to support the patients' normal activities; (v) have a controllable degradation rate which matches the new tissue growth rate; and (vi) be sterilisable for clinical use (Rezwan et al. 2006, Chung & Park 2007, Bose et al. 2012). The details of these requirements are described as follows:

2.2.1 Biocompatibility

Biocompatibility is the single most important factor that distinguishes a biomaterial from any other material. "Biocompatibility is the ability of a material to perform an

appropriate host response in a specific situation" (Donaruma 1988). This means that the material should perform an appropriate response to the tissue without eliciting an immune response, not simply to exist in the human body, and the appropriateness may be different from one situation to another.

As a scaffold for bone tissue regeneration, biocompatibility is also an important requirement. When a scaffold is exposed to a living organism, there is a natural tendency for the living organism to respond to this foreign object. Many interactions may occur at the scaffold-tissue interface. The interactions, such as coagulation, immune surveillance, healing, inflammation, mutagenicity, and carcinogenicity, between a host and an implanted scaffold are extremely complex. These biologic responses to materials are important considerations in the design of medical devices, such as scaffolds. The host response is influenced by the material characteristics which are also considered in the context of the biocompatibility (Williams 2008). The major material characteristics include chemical composition, structure, morphology, crystallinity, elastic constant, wettability, porosity of the bulk materials, surface composition, surface engineering, surface electrical properties, corrosion parameters and ion release profile (for metal), degradation profile and degraded product toxicity (for polymer and ceramic) and the ware debris release profile (Williams 2008).

To develop a scaffold for tissue engineering, understanding of the molecular mechanisms of the interactions, controlling the interactions, and optimizing the scaffold need to be considered. Therefore, the biocompatibility of the scaffold must be evaluated. The biocompatibility tests can be divided into two levels: biosafety and biofunctionality

(Pizzoferrato et al. 1995). The first level tests are concerned with the biosafety of the materials in terms of cytotoxicity, hemotoxicity, genotoxicity and histotoxicity. The tests at the second level are designed for biofunctionality issues, to assess the host response evoked by the materials in a specific application. The second level tests include cytocompatibility, immunocompatibility, hemocompatibility, histocompatibility, and infectability (Zhang 2004). The basic testing methods can be found in the International Standards Organization 10993 standards: international standards for biological evaluation of medical devices. Understanding the historic context and the biocompatibility of materials used in biomedical field will facilitate the design and fabrication of new medical devices.

An *in vitro* test (test with cells cultured outside body) is usually done before an *in vivo* test (test in body), because it is cheaper and less time consuming; *in vivo* results are difficult to obtain and have a lot of restrictions. The interaction between cells and biomaterials *in vitro* can mimic that *in vivo*. *In vitro* cytotoxicity tests are used in evaluating a wide range of devices and materials for medical applications (ISO 10993-5-2009). There are three types of test: extract test, direct contact test and indirect contact test. The methods used in cytotoxicity determination can be grouped into four categories: morphological means for cell damage assessments; chemical measurements of cell damage; cell growth assessments; specific aspects of cellular metabolism measurements.

2.2.2 Bioactive Surface Properties

Chemical compositions of the scaffold surface are related to the cell attachment and dictate the protein adsorption behavior with cellular interactions (Dos Santos et al. 2009). The initial cell adhesion plays a decisive role in determining cell survival. The cells continue to grow and differentiate only after the adhesion is achieved. Once the scaffold is implanted, its surface will be covered with the body fluid and protein layer. The cells will attach to the surface through various biomolecules in the adsorbed layer. The important molecules called integrins, a kind of cell surface receptor, can be absorbed on the scaffold surface when it has appropriate chemical properties. These integrin receptors can transmit biochemical signal between the intracellular and extracellular compartments. After the integrin receptors interact with the cells, focal adhesions will be formed. Hydrophilicity or wettability, which is controlled by the chemical compositions of the scaffold surface, influences the cell adhesion. Techniques such as self-assembled monolayers (SAMs) have been used for the tailoring of surface chemistry. It was shown that the in vitro osteoblasts adhesion and differentiation were better on hydrophilic surfaces than on hydrophobic ones (Keselowsky et al. 2005). Chemical gradient polymers mixed with hydrophobic and hydrophilic plasma polymers were recently developed and investigated (Zelzer et al. 2008). The results from this study also confirmed that the hydrophilic part of the polymer is more cytotropic (having an affinity for cells).

After focal adhesion, the cells will spread and migrate to find a more suitable place to secure their shape stability and future developments. Not only the chemical composition, but also the topography of the scaffold surface, can control and affect cell response to

the bone implant materials, such as cell adhesion, migration, and proliferation (Anselme et al. 2010). A phenomenon named ‘contact guidance’ has been observed when there is a systematic orientation of the cells in the direction of grooves on the substrate (Chen et al. 2007, Ismail et al. 2007). It has been shown that the enhancement of microstructural roughness could facilitate the osteogenic cells migration on the materials surface (Du et al. 1999, Albrektsson & Johansson 2001). Osteoblast-like cells, such as MG63 cells, show positive interaction with substrates with rougher surfaces (Lincks et al. 1998), nevertheless, contradicted findings are also reported (Setzer et al. 2009). This is due to the influence of the cell model used in different studies.

All these indicate that the cytotropic surface properties are important for a bone scaffold. Surface modification of the bone scaffold is one of the promising strategies to achieve the desired biological response. Numerous technologies have been developed for surface modification. The surface of a scaffold can be functionalized with some bioactive molecules, such as protein or peptides, either by physical adsorption or chemical modification (Shin et al. 2003). The collagen, cell adhesive protein, peptide and growth factors adsorbed onto the surface of the scaffolds show a positive effect on cell attachment, growth and differentiation (Patel et al. 2008). Arg-Gly-Asp (RGD) is the most commonly used peptide for surface modification to enhance cell adhesion (Hersel et al. 2003). Kokubo (1991) reported that the formation of a bonelike apatite layer on the surface of an artificial biomaterial after being implanted in the body is the essential requirement for bonding to living bone. Oyane (2003) reported that the apatite formation in a simulated body fluid (SBF) can be reproduced as the artificial biomaterial implanted in a living body. Therefore, the biomimetic apatite formation on

the artificial biomaterials after soaking in SBF not only has been used to assess the bioactivity of materials, but also becomes a strategy to improve the surface bioactivity of materials (Song et al. 2004). Apart from these chemical methods, some physicochemical methods such as glow discharge gas plasma treatment and ion irradiation have been used to modify the surface composition, and surface energy to improve cell adhesion (Wan et al. 2004).

2.2.3 Macro-architecture and Mechanical Properties

Highly porous interconnected three-dimensional scaffolds with a minimum pore size of 100 μm facilitate cell migration, and proper transportation of nutrients and metabolic wastes (Hutmacher 2000). The architectural characteristics of the scaffolds are usually determined by the fabrication method.

Porosity and interconnectivity are the important parameters for bone tissue engineering scaffolds because they directly affect the diffusion of physiological nutrients and gases into the scaffold resulting from the activity of the cells. Kuboki (1998) reported that the porosity of scaffolds is crucial for bone formation since no osteogenesis is induced in solid hydroxyapatite, while in the porous hydroxyapatite new bone formed after 2 weeks implantation. Increased porosity is benefit for nutrients and oxygen diffusion, resulting in increased cell proliferation (Khademhosseini & Langer 2007). In vivo studies of porosity gradient (80%-88%) poly(L-lactide-co-D,L-lactide)/β-tricalcium phosphate scaffolds showed similar results that more tissue growth occurred in the areas with higher porosity (Roy et al. 2003).

In addition to porosity, pore size of the scaffold is also an important issue that affects cellular interaction. If the pore sizes are too small, this will disturb cell migration, extracellular matrix production, and neovascularization. The minimum requirement for a pore size of 100 μm is suggested by Karageorgiou and Kaplan (2005). They also recommend that pore size larger than 300 μm is better for achieving a higher rate of bone regeneration and vascularization. A comparing study of hydroxyapatite scaffolds with 70% porosity and 800 μm pore size versus scaffolds with 60% porosity and 400 μm pore size, *in vitro* and *in vivo*, has been conducted (Kruyt et al. 2003). The scaffolds with 60% porosity and 400 μm pore size performed better in vitro while scaffolds with 70% porosity and 800 μm pore size showed more bone formation in vivo (Kruyt et al. 2003). Although the results are different from in vitro and in vivo studies, both the porosity and pore size affect cell proliferation and tissue regeneration.

Several methods have been used to measure the porosity and pore size of the scaffolds (Karageorgiou & Kaplan 2005). The simplest way to estimate the total porosity *(P_t)* is by using the Equation 2.1:

$$P_t = 1 - \rho_{\text{scaffold}}/\rho_{\text{material}} \qquad 2.1$$

where ρ_{material} is the density of the material and ρ_{scaffold} is the apparent density of the scaffold. Mercury intrusion porosimetry and the liquid displacement method are also available methods to measure the porosity of the scaffold (Maspero et al. 2002, Nazarov et al. 2004). Scanning electron microscopy (SEM) images can be analyzed by computer software to measure the porosity and pore size (Kim et al. 2002). In addition, microcomputed tomography (micro-CT) has been applied to determine the porosity and pore size of a 3D porous scaffold (Cartmell et al. 2004).

Mechanical properties of the scaffold play an important role in supporting the body, maintaining the spaces for cell in-growth and providing the correct physical stimuli to cells (Salgado et al. 2004, Agrawal & Ray 2001). They can be influenced by the porosity and pore size of the scaffolds. It is important to balance the porosity value and the mechanical needs for the target tissue. Moreover, the mechanical properties of the scaffold should better match those of surrounding bone tissues in case of early injury (Hutmacher 2000). Too low a mechanical strength is not suitable because it can not bear the in-situ load from the surrounding tissues while too a high mechanical strength is inappropriate since a stiff implant can stress shield the host tissues from the normal physiological loading, increase the pain, and consequently give rise to bone resorption and a depression of the osteoblastic activity (Iolascon et al. 2010).

Natural bone has been used as the template for bone scaffolds design and fabrication. Bone, as a composite material which consists of collagen and calcium phosphate, has been studied extensively (Currey 2002). The mechanical properties of bone (e.g. Young's modulus, shear modulus, strength, viscoelastic properties, and fracture mechanical properties) depend not only on the composition, but also on the structure of the bone (e.g. geometric shape of the components, bond between fibers and matrix, and bonds at points of contact of the fibers) (Fung 1993). Bone is slightly viscoelastic and its strain-displacement relationship is anisotropic. Moreover, bone can be organized into two different types: Compact bone (solid, only porous for canaliculi, osteocyte lacunae, blood channels and erosion cavities) and cancellous bone (porosity visible to the naked eye, rods and plates of bone are multiply-connected). So when we are discussing the

mechanical properties of bone, the specific type and part of the bone should be clarified. For example, the tensile strength of compact bone has a range from 50 to 300 MPa, and the modulus varies from 3 to more than 30 GPa (Cowins 1989, Rezwan et al. 2006). For cancellous bone, it has much lower strength and modulus than that of compact bone because of its high porosity. Normally, the modulus and tensile strength of human cancellous bone are in the range of 0.01 to 2 GPa, and 0.1 to 30 MPa, respectively (Black & Hastings 1998). The mechanical properties are not only different between various types but also within the same type. The mechanical properties of the femur, tibia, humerus and radius (human compact bones in different parts of the human body) are different.

Most scaffolds fabricated from polymer exhibits insufficient mechanical properties. Reinforcing with inorganic particles, fibers, and sheets have been used and dispersed in the polymer matrix to enhance the mechanical properties of the scaffolds (Xu et al. 2009, Swetha et al. 2010, Blaker et al. 2011). The architecture of the scaffold should be balanced with the mechanical properties. How to fabricate the polymer based scaffolds with high porosity and appropriate mechanical properties is still a challenge in bone tissue engineering.

2.2.4 Biodegradability

Great efforts have been made in developing biodegradable biomaterials for medical and related applications over last five decades (Shalaby & Karen 2003). Biodegradable materials are designed to overcome the side effects of permanent or non-degradable devices (generally metal-based), such as physical irritations, chronic inflammatory local

reactions, stress shielding, corrosion and repeat surgery. Since the 1960s, when the first biodegradable sutures were approved, a range of new generation biodegradable polymers has been developed and accepted for used in medical applications (Middleton & Tipton 2000).

Scaffolds with biodegradability can be gradually degraded or resorbed, and replaced by regenerated tissue after implantation. This avoids secondary surgery to remove the implants after tissue recovery. Degradation behavior of bone scaffolds is of crucial importance in tissue engineering, because the degradation rate is essentially linked to cell growth, host response and tissue regeneration (Babensee et al. 1998). The scaffold degradation rate needs to be controllable and match the rate of the bone regeneration (Nair & Laurencin 2007). In this way, the scaffold will completely degrade when the injury site is totally repaired. Several factors, such as scaffold composition, microstructure, chemical and physical properties, molecular weight as well as environmental conditions can affect the degradation kinetics of scaffolds (Wu & Ding 2004, Söntjens et al. 2012). Therefore, controlling and evaluation of the degradation behavior of composite scaffolds are of importance for the success of a biodegradable scaffold for bone tissue engineering. Current efforts have been focused on custom designing and synthesizing biodegradable polymers with tailored mechanical properties and controllable degradation rates (Nair & Laurencin 2007).

Synthesis of a copolymer is one of the common strategies to control the degradation rate of a polymer. Co-polyester, poly(lactide-co-glycolide) (PLGA) is a copolymer of glycolide with L- or DL-lactide PLGA. The degradability of PLGA can be controlled

with varied ratios of glycolide and lactide. The copolymer of 50% glycolide and 50% DL-lactide is very hydrolytically unstable and degrades faster than the copolymers at either end of the co-polymer composition range (Miller et al. 1977). Kim and his co-authors (2003) developed a composite scaffold consisting of poly(d,l-lactide) (PDLLA), PLGA (LA/GA=55/55), poly(lactide-b-ethylene glycol-b-lactide) (PLA-b-PEG-b-PLA) triblock copolymer and lactide. Its degradation rate can be tuned with different material compositions. More recently, a biomimetic approach using PLGA microspheres loaded with lysozyme (an antibacterial protein) as a filler material to control the degradation rate of a chitosan scaffold has been reported (Liu et al. 2012). How to precisely control the degradation rate of the scaffold matching the bone growth rate, and at the same time maintain adequate mechanical properties to support the body is another challenge in bone tissue engineering.

Scaffold degradation evaluation could be either tested *in vitro* or *in vivo*. For the *in vitro* studies, the scaffolds are immersed in a phosphate buffered saline (PBS, pH 7.4) at 37℃. For *in vivo* study, scaffolds are implanted into a suitable animal model and then retrieved at predetermined time points. The molecular weight loss and scaffold weight loss at different time intervals are measured to determine the degradation rate of the scaffold. Gel permeation chromatography (GPC) and viscometry are widely used to measure the molecular weight changes of the polymeric scaffolds.

2.3 Recent Development of Materials for Bone Tissue Engineering

Tissue engineering is defined as “an interdisciplinary field that applies the principles of engineering and life sciences toward the development of biological substitutes that

restore, maintain, or improve tissue function" (Langer & Vacanti 1993). More specifically, tissue engineering implies the combination of cells, scaffolds, and bioactive peptides used to guide the repair or formation of tissue. Bone tissue engineering potentially provides an alternative approach to treat the loss or malfunction of particular tissue. Bone tissue engineering requires a three-dimensional scaffold which serves as a 3D template for cell attachment, ingrowth, proliferation and bone-extracellular matrix formation to provide a structural support to a newly formed tissue (Chen et al. 2002, Liu et al. 2007). In recent years, there have been tremendous advances in the development of biomaterials for bone tissue engineering.

2.3.1 Biodegradable Oganic Polymers

Both synthetic polymers (e.g. poly(glycolic acid), poly(lactic acid), and polyurethane) and natural polymers (e.g. collagen, polysaccharides, and starches) have been extensively investigated in bone tissue engineering. Biodegradable polymers have become promising candidates for scaffold implants which can be gradually reabsorbed by regenerated tissue, avoid secondary surgery to remove the implants after tissue recovery or depletion of the drug supply and shorten the recovery time (Liu et al. 2008). Natural polymers can be considered as the first biodegradable biomaterials used clinically. They have some advantages such as bioactivity, natural remodeling, and ability to present receptor-binding ligands to cells (Nair & Laurencin 2007). Compared with the natural polymers, the synthetic polymers have more predictable properties and can be tailored for specific applications. In recent years, there have been tremendous advances in the development of synthetic biodegradable polymers used for bone scaffolds. These materials have been fabricated into three-dimensional porous scaffolds

which are conducive to various tissue regenerations (e.g. bone, cartilage, liver, and skin) because of their great biodegradation and biocompatibility (Peter et al. 1998, Kim & Mooney 1998, Zeltinger et al. 2001, Liu et al. 2007).

2.3.1.1 Poly(glycolic acid)

Poly(glycolic acid) (PGA) is one of the first biodegradable synthetic polymeric biomaterial used for biomedical application (Nair & Laurencin 2007). Synthesis of poly(grycolic acid) from the open ring polymerization of glycolic acid yield is shown in Figure 2.1. With high crystallinity (45-55%), PGA exhibits low solubility in most organic solvents and high tensile modulus. It is a rigid thermoplastic material, with high glass transition temperature (35-40 °C), and high melting point (>200 °C). PGA is the first DEXON® bioresorbable suture commercially used and approved by the US Food and Drug Administration (FDA) in 1969, because PGA possesses good compatibility, reproducible mechanical properties and predictable bioabsorption.

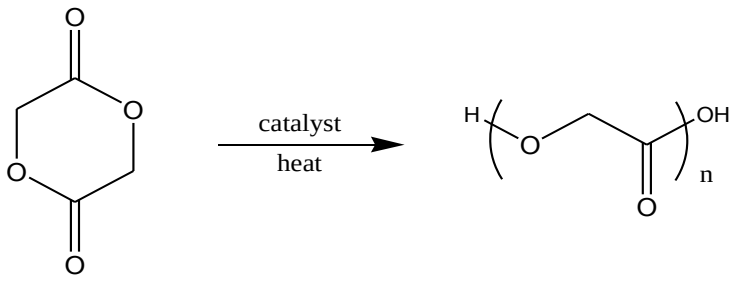

Glycolic acid Poly(glycolic acid)

Figure 2.1 Synthesis of poly(grycolic acid) from glycolic acid

PGA can be fabricated into a variety of structures by extrusion, injection, particulate leaching and solvent casting, and compression molding (Gunatillake et al. 2006). With excellent filament forming capacity, the current commercial process of producing PGA for medical applications is a braiding of multiple melt-spun fibers. Electrostatic

spinning is one of the promising fiber fabrication methods for PGA since it can achieve smaller fiber diameters than the traditional extrusion (Boland et al. 2001). A fiber with smaller diameter is of interest in tissue engineering scaffolds because it benefits cell culture and migration. These fabrics have been employed as scaffolding matrices in tissue engineering (Shum & Mak 2003). Since PGA has an excellent skin-closing ability without requiring sutures, a PGA non-woven fabric-fibrin glue composite matrix has been investigated as a dural substitute (Kawase et al. 2006, Terasaka et al. 2006). Furthermore, due to its good initial mechanical properties, PGA has been developed for bone internal fixation devices (Peltoniemi et al. 2002).

As a bulk degrading polymer, PGA would lose its strength in 1-2 months and mass within 6-12 months (Rezwan et al. 2006). The high degradation rate, low solubility and acidic degradation products limit the biomedical applications for PGA. Therefore, some more new biomaterials should be developed to meet the requirements of the biomedical field.

2.3.1.2 Poly(Lactic acid)

Another most widely investigated biodegradable polymer, poly(Lactic acid) (PLA), is attracting increasing interest in tissue engineering. It has gained approval by the FDA for use in many clinical applications, such as surgical sutures, staples, clips, screw, and pins (Mano et al. 2004, Gong et al. 2011). PLA is formed by the polymerization of lactide. Since lactide is a chiral molecule, it exists in two steroisomeric forms: L-lactide and D-lactide. There is also D-L-lactide which is formed with a 50/50 mixture of D- and L-lactide while meso-lactide is crystallized with two different amount of D- and L-

lactide. This gives rise to four different types of poly(Lactic acid): Poly(L-lactic acid) (PLLA), Poly(D-lactic acid) (PDLA), Poly(meso-lactic acid), and Poly(D-L-lactide) (PDLLA) (Figure 2.2).

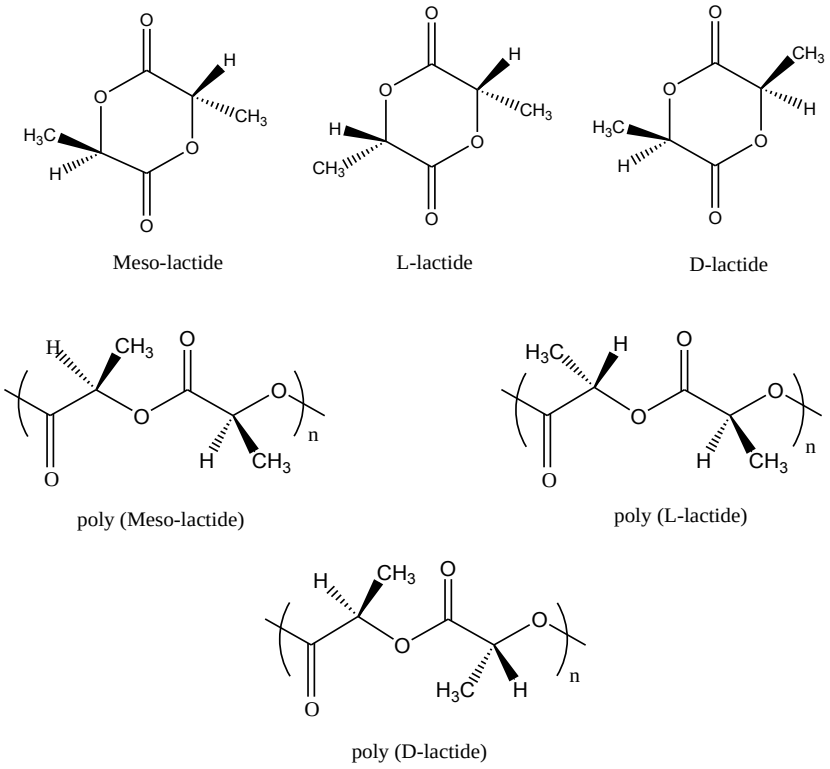

Figure 2.2 Types of lactide (meso-lactide, L-lactide and D-lactide) and their corresponding polymers (poly(meso-lactide), poly(L-lactide), and poly(D-lactide))

PLLA is a crystalline polymer with controllable crystallinity which depends on the molecular weight and polymer processing parameters. PLLA has good tensile strength (nearly 4.8 GPa), low extension and high modulus, and hence it has been considered as a fine biomaterial for load bearing applications, such as orthopedic fixation devices (Sabir et al. 2009). High strength fibers formed by PLLA have been developed in an improved suture over DEXON® and is FDA approved. PLLA has been investigated for use as a fiber-based scaffold for ligament replacement (Cooper et al. 2005). To improve

the mechanical properties of PLLA as a bone scaffold, researchers incorporated hydroxyapatite into the biopolymer (Hong et al. 2005, Uskokovic et al. 2007, Aleksendrić et al. 2010). PLLA has been fabricated into three-dimensional sponges and hybridized with collagen and hydroxyapatite. Furthermore, scaffolds with drug-release function have been developed using PLLA as the matrix (Huang et al. 2007, Uttarwar 2008).

PLA is much more hydrophobic than PGA due to the additional methyl group in the structure of PLA. Therefore, the degradation rate of PLLA is much slower, and needs more than 24 months to completely degrade (Middleton & Tipton 2000). The slow degradation also limits the application of PLLA. Some co-polymers are under investigation for improvement of their properties.

Poly(D-L-lactide) (PDLLA) is polymerized with random distributions of L- and D-lactide. It is an amorphous polymer and shows a lower strength (approximately 1.9 GPa) and faster degradation rate (12-16 months) compared to PLLA. It is therefore a good candidate for developing drug delivery vehicles and non-bearing or low-bearing scaffolds for tissue engineering. PDLLA has been widely used in the development of exogenous matrices suitable for facilitating tissue regeneration (Huang et al. 2005, Calandrelli et al. 2008, Wu et al. 2008b, Xu et al. 2009). It has been investigated as a biomedical orthopedic coating material because it can optimize interaction at the implant-tissue interface (Gollwitzer et al. 2005). In addition, different bioactive particles such as hydroxyapatite (Deng et al. 2008), bioglass (Blaker et al. 2011), wollastonite (Xu et al. 2009), $CaSiO_3$ (Zhang et al. 2009) have been incorporated into

the PDLLA matrix in order to enhance the mechanical properties and osteoconductive potential of the resulting composites. Combinations of drugs and PDLLA as a drug delivery system have been investigated. Since the growth factors have the ability to induce tissue regenerations, it is suggested by Schmidmaier (2001a, 2001b) that PDLLA coating osteosynthetic implants with growth factors (IGF-1 and TGF-β1) release will accelerate fracture healing significantly, without systemic side effects.

To fabricate a scaffold, one should note that the scaffold should have a controllable degradation rate which matches the tissue regeneration rate. In order to get a good control of the degradation rate, the degradation processes of PDLLA need to be considered. The depolymerization processes are crucial for the degradation of polymers, which are categorized into two classes: exogenous and endogenous. Exogenous degradation means that the polymers are depolymerized step-by-step by cleaving a small molecule from the terminus of the molecule. PLA is an example for the other degradation process, the endogenous mechanism, where it is depolymerizaed by hydrolysis at random. The degradation equations for poly (L-lactide) are shown below:

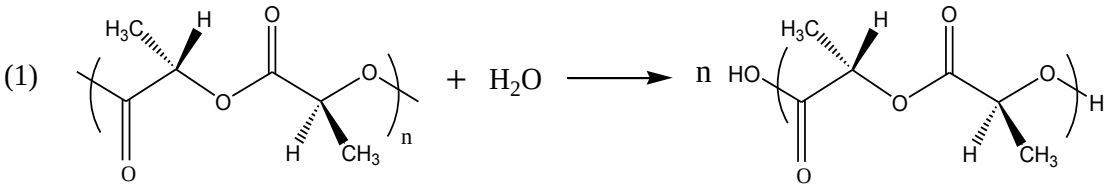

poly (L-lactide)

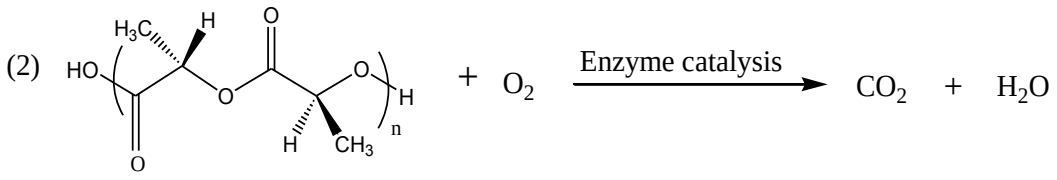

After the two-step reactions, the degradation products of PLA are CO_2 and H_2O which would be assimilated or removed by the human body. Therefore, biodegradable PLA is of value in short-term applications that require only temporary presence of a device such as drug-release scaffolds. When degradation occurs, the polymeric implant is associated with macroscopic changes in its appearance, physicomechanical properties and physical processes like swelling, deformation, or structural disintegration, weight loss, and the eventual depletion of drug or loss of function (Ratner et al. 2004). Due to the rapid penetration of water into the PLA matrix, the degradation takes place throughout the entire volume of the implant.

2.3.1.3 Poly(lactide-co-glycolide)

Co-polyester, poly(lactide-co-glycolide) (PLGA) has been investigated for a wide range of biomedical applications. It is the copolymer of glycolide with L- or DL-lactide (Figure 2.3). PLGA with varied compositions shows different properties (e.g. mechanical and degradation) and the relationship between them is not linear. Miller et al. (Miller et al. 1977) have shown that the copolymer of 50% glycolide and 50% DL-lactide is very hydrolytically unstable and degrades faster than the copolymers at either end of the co-polymer composition range. The degradation rates of intermediate co-polymers are faster than the homopolymers. Therefore, the degradation times of 50/50, 75/25, and 85/15 poly(DL-lactide-co-glycolide) are approximately 1-2 months, 4-5 months and 5-6 months, respectively (Middleton & Tipton 2000). It has shown that the properties of the PLGA, including degradability and the mechanical properties, depend on a variety of factors, including the LA/GA ratios, molecular weight, shape, and the

structure of the matrix. Moreover, their approval by the FDA for use in humans and good processibility pave the way for extensive use as a great biomaterial for tissue engineering and controlled drug delivery systems (Dorati et al. 2010, Zolnik 2008).

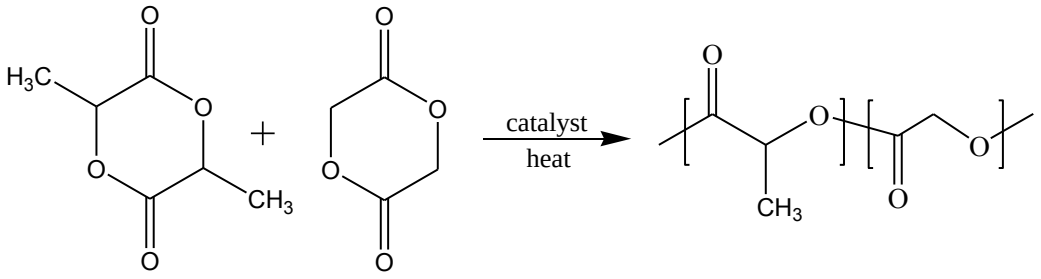

Lactide Glycolide Poly(lactide-co-glycolide)

Figure 2.3 Synthesis of poly(lactide-co-glycolide) from lactide and glycolide

PLGA with different ratios have been developed and applied to a wide range of biomedical applications. A commercially developed PURASORB® (Purac Biomaterialsis) PLGA has been used in vascular closure devices, coronary stents, drug delivery, wound management, and orthopedic devices. VICRYL™ (Ethicon Inc.) suture, another commercially available product, is a multifilament suture composed of a copolymer containing 90% glycolide and 10% L-lactide. PLGA fibrous scaffolds with different fiber diameters have been fabricated using the electrospinning method by controlling the polymer solution concentration and feed rate (Zhao et al. 2008b). The fibroblast attachment, proliferation, and migration showed a good cell response to the scaffolds (Zhao et al. 2008b). A porous PLGA microsphere sintered scaffold has been developed for bone tissue repair applications (Wang et al. 2009). However, PLGA chains lack functional groups, and have low mechanical strength. Inorganic fillers, such as hydroxyapatite have been introduced to improve these properties (Lee et al. 2008,

Wang et al. 2010). Moreover, PLGA has been used as a drug delivery vehicle for controlled release of drug or proteins. Sustained pDNA release for 2 months is achieved by a porous injectable PLGA scaffolds (Jeon et al. 2011). Drug-loaded PLGA microsphere has also been fabricated, acting as a coating material on porous hydroxyapatite scaffolds for controllable drug delivery (Son et al. 2011).

2.3.1.4 Poly(ε-caprolactone) (PCL)

The ring opening polymerization of caprolactone results in a semicrystalline polyester: poly(ε-caprolactone) (PCL) (Figure 2.4). The PCL is polyester with high processability, solubility in wide range of organic solvents, low melting point of 59-64 °C, and glass transition temperature (-60 °C). It can easily form miscible blends with other polymers. The presence of hydrolytically labile aliphatic ester linkages makes PCL a biodegradable polymer. However, compared to the polymers mentioned previously, PCL shows the longest degradation time of 2 to 3 years. The degradation rate of PCL can be increased by copolymerization of ε-caprolactone and other monomers, such as DL-lactide. Triblock copolymer of PCL and poly(ethylene glycol) (PEG) were synthesized and can be applied in injectable drug delivery system (Cai et al. 2008).

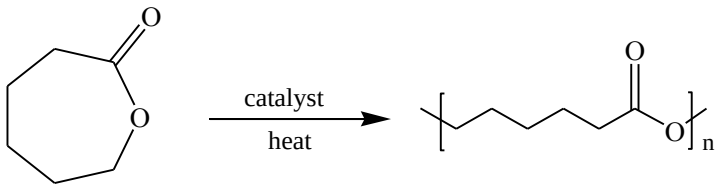

Figure 2.4 Synthesis of poly(ε-caprolactone) by ring opening polymerization of ε-caprolactone

With the slow degradability, permeability to wide range of drugs, and biocompatibility, PCL has been initially applied in a long term drug delivery system. One commercially developed long-term contraceptive device, Capronor®, that releases levonorgestrel over 12-18 months, has been investigated and evaluated in humans in early 1989 (Darney et al. 1989). Extensive research is ongoing to develop PCL drug carriers in the form of micro- and nanoshpheres (Sinha et al. 2004). Taxol-loaded PCL microspheres has been prepared and about 25% of the taxol were released from the microspheres by a 6 weeks drug release study (Dordunoo et al. 1995). To increase the drug release rate (or polymer degradation rate), PCL/PLGA (65:35) microsphere containing bovine serum albumin has been developed (Yang et al. 2001). Apart from the drug delivery system, PCL microspheres with bioactive apatite coated and macroporous morphology have been fabricated for the application in augmentation and bone tissue engineering (Hong et al. 2009). Biphasic calcium phosphate reinforced PCL composite microspheres with improved mechanical properties, good biocompatibility and the ability promoting cell adhesion, growth, and proliferation have been investigated as bone scaffolds (Bao et al. 2011).

2.3.2 Research Trends of Advanced Scaffold Materials

Materials used for bone scaffold fabrication should be designed to stimulate specific cell response at the molecular level. They should interact with cells and promote cell adhesion, growth, differentiation, and extracellular matrix formation and organization. The selection of biomaterials plays an important role in the success of bone tissue engineering. The primary requirements of the biomaterials used in tissue regeneration are biocompatibility, biodegradability and favorable mechanical properties.

Conventional single-phase materials cannot always provide all the necessary properties for the bone tissue engineering and the characteristics of a true human bone. Though a variety of biodegradable polymers have been developed and studied for tissue engineering, no single biodegradable polymer can meet all the requirements for biomedical scaffolds. For example, scaffolds derived from unmixed biodegradable polymers often lack osteoconducting properties and mechanical strength. Therefore, the design and fabrication of composite materials (a combination of two or more different materials) in order to develop a multifunctional bone scaffold is of great research interest. By incorporation of the bioactive particles to the polymers, it is possible to control the mechanical properties, such as strength and modulus of the composites, closer tonatural bone and improve the bioactivity of the composites. In particular, Section 2.3.4 deals with a comprehensive literature review of polymer/bioactive particles composites used in bone tissue engineering

2.3.3 Polymer/Bioactive Particles Composites

The use of particulate reinforcing fillers in biodegradable polymers is attracting increasing attention for researchers in tissue engineering. Hydroxyapatite (HAp) (Swetha et al. 2010), apatite-wollastonite (A/W) glass-ceramics (Xu et al. 2009), and bioglass® (Blaker et al. 2011) have been widely used as the bioactive phase in the biodegradable polymers reviewed previously for tissue engineering. The mechanical properties of commonly used bioactive filler materials and human bones, are listed in Table 2.1

Table 2.1 Mechanical property of HAp, (A/W) glass-ceramics, 45S5 Bioglass®, and human bones (Giesen et al. 2001, Rezwan et al. 2006, Sabir et al. 2009)

Materials	Compressive Strength (MPa)	Tensile Strength (MPa)	Elastic Modulus (GPa)	Fracture Toughness (MPa$\sqrt{m}$)
Hydroxyapatite (HAp)	>400	~40	~100	~1
(A/W) glass-ceramics	1080	215	118	2
45S5 Bioglass®	~500	42	35	0.5-1
Cortical bone	130-180	50-160	3-30	2-12
Cancellous bone	4-12	7.4	0.02-0.5	N/A

Hydroxyapatite (HAp), $Ca_{10}(PO_4)_6(OH)_2$, has been extensively investigated for a few decades. This is why HAp and related calcium phosphates (e.g. tricalcium phosphate, α-TCP/β-TCP) have been extensively investigated as substitute materials for bone grafts (Hench & Wilson 1999, Kim et al. 2005, Rezwan et al. 2006, Sopyan et al. 2007). Porous HAp exhibits a strong bonding to bone and lets the bone tissue grow well into the pores, leading to anincrease in the strength of the HAp implant (Sopyan et al. 2007). Therefore, particular attention has been paid to the preparation of porous HAp scaffolds for bone tissue engineering. This kind of scaffold could be applied for cell loading, drug-delivery agents, and artificial bone substitutes (Sopyan et al. 2007). However, the artificial porous HAp has lower mechanical strength of 0.21-0.41 MPa (Kim et al. 2005) as compared to natural bone (Table 2.1). The brittleness, slow biodegradation and difficulty in shape forming limits its application in bone tissue engineering. HAp alone cannot be used for load-bearing scaffolds. Considering the limitations of HAp, using HAp for both reinforcing and bioactivity in the polymer matrix is a promising solution to these problems (Kim et al. 2006).

In the HAp filled polymeric composites, HAp acts as a reinforcing material to enhance the mechanical properties, and meanwhile, it is also a bioactive component to improve the osteoconductivity and biocompatible properties of the scaffolds (Swetha et al. 2010, Zhao et al. 2008a). Therefore, development of composite scaffold is attractive. Furthermore, addition of a bioactive HAp phase in biodegradable polymers could alter the degradation rate by allowing rapid exchange of protons in alkaline water. It is suggested providing a pH buffering effect to the polymer and modifying the acidic polymer degradation (Li & Chang 2005). This would reduce the risk of inflammation. The water absorption and wettability of the scaffolds would be improved with the addition of HAp into the polymer matrix (Shikinami & Okuno 2001, Ren et al 2008). In addition to being reinforcing and bioactive fillers, HAp showed another advantage in the possibility of controling the biodegradation rate of the composite materials (Russias et al. 2006, Chen et al. 2013). With high degree of mechanical properties, bioactivity, and controllable degradability, polymer/HAp composites will be promising materials for bone scaffold fabrication.

Bioactive glasses are the widely used bioactive fillers in tissue engineering applications. In particular, 45S5 Bioglass® has drawn considerable interest because its dissolution products can upregulate the gene expression and control osteogenesis (Xynos et al. 2000). 45S5 Bioglasss contains 45% SiO_2, 24.5% Na_2O, 24.4% CaO and 6% P_2O_5, in weight percent. Among these constituents, SiO_2 plays an essential role in bone mineralization and gene activation. These commercial bioactive glasses have been reported as class “A” bioactive materials and found to support enzyme activity and

vascularization (Jones, Hench 2001). 45S5 Bioglass® has been successfully used in clinical treatments of periodontal disease and as a bone filler material (Hench 1998a).

The same as for HAp, bioglasses act as reinforcing fillers in the polymer matrix, extending their applications in bone tissue engineering. The mechanical properties of the porous poly(α-hydroxyacid)/Bioglass® have been improved; the water absorption and weight loss have been increased by the addition of Bioglass® (Maquet et al. 2004, Blaker et al. 2005). Moreover, the degradation kinetics of the composites can be controlled by Bioglass® incorporation. This is another key reason that makes bioglass a bioactive filler material for the bone scaffold. MG63 (human osteosarcoma cell line) and A549 cells (human lung carcinoma cell line) have been seeded on the porous PDLLA/Bioglass® composite scaffolds to investigate the effect of the Bioglass® content on the cell adhesion and growth (Verrier et al. 2004). The composite scaffolds show a good biocampatibility and the increasing amount of Bioglass® leads to enhanced MG63 cell attachment and proliferation. A549 cells grew better on PDLLA scaffold with 5 wt% Bioglass® when compared to the one with 40 wt% Bioglass® (Verrier et al. 2004). This implies that the appropriate concentration of Bioglass® particles in polymer-based scaffolds may be different from cell to cell. One of the disadvantages of bioglasses is that the crystallization of bioactive glasses decreases the level of bioactivity (Filho et al. 1996). This limits their application in bone tissue engineering since full crystallization occurs prior to the densification by glass sintering. So improved sintering processes need to be developed to prevent the full crystallization of bioglass and allow it achieve the required mechanical properties.

Glass-ceramic apatite-wollastonite (A-W) is a bioactive ceramic which has an ability to promote bone regeneration by providing strong interfacial bonding between the implant and host tissue (Hench & Wilson 1999, Xu et al. 2009). Glass-ceramic A-W is a ceramic containing crystalline apatite $Ca_{10}(PO_4)_6(O,F_2)$ and wollastonite ($CaO{\cdot}SiO_2$) in a $MgO\text{-}CaO\text{-}SiO_2$ glassy matrix. Compared with Bioglasss and HAp, glass-ceramic A-W shows a greater modulus, compression and tensile strength. It has been used for the fabrication of bone substitute because of its high bioactivity. The same as other ceramics, A-W glass-ceramic has a relatively low fracture toughness which limits its application in load-bearing applications. Therefore, it also becomes a filler material in the polymer matrix, with the dual roles of improving bioactivity and mechanical strength of the composite. A composite developed by A-W glass-ceramic incorporation in a polyethylene (PE) matrix showed a faster apatite formation after immersion in SBF as compared with that of HAPEX™ (a commercial available HAp/PE composite) (Juhasz et al. 2003). A-W glass-ceramic filled poly(methylmethacrylate) (PMMA) composites fabricated by Shinzati (2001) showed a higher osteoconductivity and better mechanical properties with larger amount of A-W glass-ceramic filler.

The basic functional subunits of cells and tissues are defined at the nanoscale, hence application of nanotechnology represents a new cutting edge in tissue engineering research (Armentano et al. 2010). Nanotechnology enables the development of new systems that mimic the complex, hierarchical structure of the native tissue. A nanocomposite is a composite material in which at least one component is on the nanometer-scale. It is considered as a new class of material because of its better properties than those in microscale counterparts. Compared to the HAp in micron range,

the nano-HAp has a larger surface area, so the nano-composites exhibit enhanced mechanical properties because of the strong interactions at the interface of the nano-HAp and polymer (Kothapalli et al. 2005). Moreover, it has been reported that nano-HAp could increase the initial calcium adsorption to the surface and hence enhance the binding of vitronectin that subsequently promotes osteoblast adhesion and shortens the bone regeneration rate (Webster et al. 2001). Three-dimensional biodegradable PLGA/nano-HAp composites microsphere-based scaffolds with high compressive strength, modulus and the appropriate pore structure for cell penetration have been fabricated (Lv et al. 2009). Biodegradable polyphosphazene/nano-HAp composite scaffolds for bone tissue engineering (Nukavarapu et al. 2008), biodegradable nano-HAp/PLA porous scaffolds for non-load bearing tissue engineering applications were also investigated (Kothapalli et al. 2005). Moreover, Yang and his coauthors (2004) have developed a biomimetic nano-HAp/type I collagen scaffold for bone tissue engineering. The results indicated the potential of this scaffold for exploitation of the extacellular matrix in bone regeneration. The processing of nanocomposites raises the possibility of realizing bone grafts with improved performance and is now a major research trend in bone tissue engineering.

2.3.4 Multifunctional Bone Scaffolds

A multifunctional bone scaffold is a scaffold system designed with a combination of different predefined functions, such as physical support, degradation, drug delivery function, and shape memory effect (SME), and is used in bone tissue engineering for assisting in bone regeneration. So far, the drug-eluting stent, including a shape memory metal stent platform, polymer drug carrier and drug, is an example of multifunctional

devices (Ma et al. 2012). However, the stent needs to be removed after the treatment by secondary surgery. A biodegradable composite with the SME and drug release function without adverse effect on other functionalities is a promising material for bone tissue engineering and involves minimally invasive surgery. Copolyester networks based on semi-crystalline oligo [ϵ -caprolactone)-*co*-glycolide] and amorphous oligo[(*rac*-lactide)-*co*-glycolide] precursors were developed as multifunctional materials with SME, degradability and drug release function (Neffe et al. 2009, Wischke et al. 2009). Independence of the functionalities can be proven. As biodegradability has been discussed in Section 2.2.4, a review on the shape memory polymers and drug delivery scaffolds are presented in the following paragraphs.

The ability to recover from a plastic deformation to its original shape when stimulated by a specific physical quantity is known as the shape memory effect (SME) (Huang et al. 2010). Shape memory materials (SMMs) are materials featured by the SME. Shape memory alloys (SMAs), shape memory ceramics (SMCs), and shape memory polymers (SMPs) have been utilized in many fields, such as aerospace engineering and medical devices. SMPs, a class of "actively moving" polymers, can recover from an initial temporary shape to their permanent shapes by an external stimulus such as temperature, light, pH, and magnetic field (Meng & Hu 2009). Compared to SMAs and SMCs, SMPs have higher recoverable strain of over 100% for 10% of SMAs and 1% of SMCs, respectively. Moreover, from the engineering aspect, polymers are cheaper and easier to process than metals and ceramics. The shape change, with a change of temperature, is called a thermally induced SME. This kind of polymer is an emerging class of smart materials with potential applications in many areas of our lives, such as high-

performance textiles (Mondal & Hu 2006), packaging materials (Charlesby 1960), intelligent medical devices (Small IV et al. 2009), and implants for minimally invasive surgery (Lendlein & Langer 2002).

Polyurethane-based SMPs have been fabricated as endovascular interventions for the treatment of vascular diseases (Langer & Tirrell 2004, Baer et al. 2007). A degradable SMP has been fabricated as a suture and showed a good shape memory effect and high potential in skin wound closure (Zheng et al. 2006). A degradable thermal SMP has been fabricated as a suture for wound closure and was tested in a rat model (Zheng et al. 2006). The SMP suture showed a good shape memory effect and high potential in skin wound closure. Moreover, the mechanical properties of shape memory polymer composites (SMPCs) have been improved by incorporating reinforcing fillers such as SiC particles (Liu et al. 2004), carbon powders (Yang et al. 2005), and hydroxyapatite (Zheng et al. 2006). SMPs and their composites can be fabricated into scaffolding devices with an interconnected porous structure, which is essential for cell growth, proliferation and tissue regeneration. Porous SMPs and SMPCs have been rapidly developed due to their advantages, e.g. greater volumetric expansion capabilities, wide range of mechanical and physical properties (Hearon et al. 2013). Biodegradable SMPs are considered as promising materials for designing multifunctional scaffolds for bone tissue engineering, mainly because of their SME, low-density, low-cost, flexibility, biodegradability, and biocompatibility.

In addition to the SME, creating a scaffold with a drug eluting function providing a local release of bioactive molecules to influence the healing of bone is one of the

important approaches of bone tissue engineering. Such delivery systems use biomaterials as drug carriers to deliver biologically active molecules at a desired rate for a desired period, so as to improve the effectiveness of drug therapy, reduce toxicity and promote cell proliferation (Langer 1998, Tessmar & Göpferich 2007). Degradable polymeric scaffolds are therefore becoming promising delivery vehicles to deliver drug or bone influencing proteins by covalently bonding the drug within the polymer and releasing with polymer degradation, or mixing between the polymer chains or coating on the polymer matrix to give an initial drug release. These drug delivery scaffolds for bone tissue engineering can reduce the amount of drug administration for shortening the therapeutic period and promoting cell adhesion, proliferation and tissue regeneration (Ratner 2002).

Biodegradable polymers have become attractive candidates for drug delivery applications. Among the biodegradable polymers for drug delivery systems, aliphatic polyesters such as PLA, PGA, and their copolymers PLGA have been extensively investigated due to their good biocompatibility and biodegradability (Olivier 2005, Hulse et al. 2005, Patel et al. 2008). Early growth factors such as bone morphogenetic proteins (BMP) were delivered by a semi-solid paste-like PLGA system (Smith et al. 1995). Such system used autologous blood or carboxymethylcelloulose (CMC) as the binding agent. PGA non-woven fabric, of the disk type, has been investigated as a BMP carrier for the ectopic bones (Yamamoto et al. 1996). A porous PLGA scaffold with continuously releasing ascorbate-2-phosphate (AsAP) and dexamethasone (Dex) was fabricated by the solvent casting/particulate leaching method (Kim et al. 2003). The amount of mineralization was higher than the control when mesenchymal stem cells

were cultured in the scaffold containing AsAP and Dex. PLLA scaffolds with Dex (Uttarwar 2008) and acetaminophen (Duarte et al. 2009) releasing functions have been fabricated by emulsion-freeze-drying and the supercritical-assisted phase inversion method, respectively. Moreover, some other degradable polymers such as poly(ε-caprolactone) (PCL) (Russo et al. 2010), poly(ethylene glycol) (PEG) (Otsuka et al. 2003), PLA-PEG block copolymers (Tessmar et al. 2003) have also been investigated as drug carriers.

Various methods have been used to fabricate drug/protein loaded polymeric scaffolds. The easiest way to add drugs to scaffolds is the direct mixing of the drug with the polymer matrix. This may lead to a drug loss or lower effectiveness of the drug during fabrication process, especially for a scaffold fabricated by a particular leaching method (Tessmar et al. 2006). In addition, if a high processing temperature is used, the drug may be decomposed. The electrospinning process with an additional coaxial spinneret was designed to provide a second channel for the protein solution and the incorporation of protein to the polymer fibers (Zhang et al. 2006). Surface coating is another easily achieved drug loading method by dipping the scaffolds in a protein solution (Sohier et al. 2003). These numerous biodegradable polymers, in combination with innovative processing methods, allow researchers to optimize controlled drug delivery systems for faster bone regeneration.

2.4 Fabrication Techniques of Polymer Based Bone Scaffold

A variety of fabrication technologies have been developed for processing biodegradable polymers into three-dimensional porous scaffolds. The conventional techniques include

fiber bonding, emulsion freeze drying, solvent casting/particulate leaching, gas foaming/particulate leaching, phase separation, and high-pressure processing (Hutmacher 2000, Liu et al. 2007). Latterly, solid freeform fabrication (SFF) has emerged as a novel technology that enables the fabrication of custom-made devices directly made from a computer aided design (CAD) data for developing a predefined structure (Hollister 2005).

2.4.1 Solvent Casting/Particulate Leaching

Solvent casting/particulate leaching has probably been the best known and most widely used method for the preparation of bone tissue engineering scaffolds. It involves the dissolution of the polymer in an organic solvent, mixing with salt particles (e.g. sodium chloride, sodium citrate, and saccharose), and casting the solution into a mould. After the evaporation of the solvent, the particulates are leached away using water to form the pores of the scaffold. This method has the advantages of independently controlling the porosity and pore size of the scaffold by varying the number and pore size of the leachable particles. The porosity of the scaffold can be adjusted from 30% to up to 90% and the pore size of the scaffold from around 50 μm-100 μm (Chen et al. 2001). Another advantage of this processing method is that only small amounts of polymers are needed for scaffold fabrication compared to other complex machinery (Tessmar et al. 2006). Therefore, such salt leaching technique is especially useful for biomaterials in the development stage, where only small quantities of polymers are available. Scaffolds produced by the technique based on the salt leaching method have been used in some studies for bone tissue engineering purpose, and have shown relatively good results (Xu et al. 2009, Ochi et al. 2003).

Although this method can be easily carried out, it presents some disadvantages, such as the possible retention of toxic solvent within the scaffold and the difficulty to leach out all the particulates (Mikos & Temenoff 2000). Therefore, this original method has been usually used for thin specimens or membranes. A modified method using lamination of several thin sheets was used to produce multi-layered structures (Mikos et al. 1993). The mechanical properties of the fabricated scaffolds are far from being ideal even when compared to those from trabecular bone (Gomes et al. 2002). The pore distribution within the scaffold is not uniform because the leachable solid particles with higher density compared to liquid polymer solution tend to deposit different densities of solid particles and liquid polymer solution during the salt leaching process (Guarino et al. 2008). Hou and his co-workers (2003) reported an improved technique, involving polymer coagulation, thermal compression molding and salt leaching, to better solve this distribution problem. This improved method has been successfully applied in the fabrication of three-dimensional porous scaffolds based on PDLLA, PCL, and 1000PEOT70PBT30, a segmented poly(ether ester) using polyethylene oxide (PEO) and polybutylene terephthalate (PBT). The obtained scaffolds have homogeneous pore morphologies.

2.4.2 Gas Foaming/Particulate Leaching

Gas foaming can be used to fabricate the highly porous polymer scaffolds without using organic solvent. It involves exposing the polymer to high-pressure (e.g. 5.5 MPa) carbon dioxide (CO_2) which can saturate the polymer with the gas (Mooney et al. 1996). The solubility of the gas in the polymer is rapidly decreased by reducing the CO_2 gas

pressure to atmospheric levels. This is induced in the nucleation and growth of gas cells within the polymer matrix. However, these gas foaming methods typically yielded a closed pore structure, which could hinder cell growth and migration (Harris et al. 1998). A novel technique combining high-pressure gas foaming and the particulate leaching technique was developed (Harris et al. 1998). Firstly, a solid mixture of PLGA and NaCl was fabricated through compression molding at 10 MPa, followed by exposure to high pressure CO_2 gas. After the gas foaming process, the NaCl particles were removed by leaching the scaffold in the water.

Moreover, a method combining gas foaming and the particulate leaching was reported by Nam (2000). Gas foaming/particulate leaching is another strategy for the fabrication of the porous scaffolds using an effervescent salt as a gas foaming agent (Yoon et al. 2001). A polymer/solvent gel containing well dispersed effervescent salt particles (e.g. ammonium bicarbonate) was firstly cast in a mold. Secondly, the molded mixture was immersed in hot water, and the ammonium bicarbonate particles leached out from the polymer matrix along with the evolution of ammonia and carbon dioxide gas. Afterward, a scaffold with open cellular structure and high levels of pore connectivity was obtained (Harris et al. 1998). This method can independently control the porosity and pore size of the scaffold by varying the amount and the pore size of leachable particles. Compared to the solvent casting/particulate leaching method, it can improve the interconnectivity of the pores in the scaffold.

2.4.3 Phase Separation and Freeze Drying

Thermal induced phase separation (TIPS) has become a popular technology to produce a high porosity scaffold due to the improved interconnectivity of the fabricated scaffold compared with the that fabricated from the solvent casting/particulate leaching method (Blaker et al. 2010, Mandoli et al. 2010). Briefly, a polymer solution is transferred to a freezer for crystallizing the solvent and inducing a solid-liquid phase separation. After freeze-drying the solvent, the resulting samples have a highly porous structure (porosity of 97%) with anisotropic tubular morphology and extensive pore interconnectivity. The structure of the scaffold is controlled by the quenching temperature, cooling method and time, presence of surfactant, and polymer concentration. In addition, TIPS can be used to create composite scaffolds by adding given amounts of bioactive powders into the polymer solution before phase separation (Blaker et al. 2010). The main advantage of TIPS is that a scaffold with larger thickness can be fabricated as compared to the solvent casting/salt leaching method. Hence, the scaffold with an improved interconnectivity and morphology similar to trabecular bone can be obtained by this method (Holly et al. 2000).

Highly porous PDLLA/Bioglass® composite scaffolds have been prepared by TIPS with macropores of 100 μm and micropores of 10-50 μm in diameter by Maquet (2004). Moreover, Ma and Zhang (2001) have reported an oriented microtubular scaffold fabricated by a modified phase separation method with a uniaxial temperature gradient. It is also reported that this technology may be used to generate porous scaffolds for fibrillar tissues. However, this technique using organic solvents may cause the problem of the solvent residual forming a potential source of toxicity for the cells.

2.4.4 Electrospinning

Electrospinning is a combination of electrospraying and spinning. A sufficiently high electric field is applied to the liquid droplet (one electrode) to make the droplet charged and come out from the tip of a die and be deposited onto a target substrate (the other electrode). The diameter of the fibers fabricated by this technique ranges from several microns to nanometers. Electrospinning has attracted great interest since it facilitates the large scale production of fibrous non-woven micro/nano fabrics and simplifies the fabrication process (Agarwal et al. 2008). The structural similarity to the tissue extracellar matrix (ECM) is another reason that makes eletrospinning widely used in the biomedical field (Bianco et al. 2009). Since the composition and structure of the ECM has been found to affect cell behavior (Causa et al. 2007), the electrospun scaffolds mimicking the architecture and biological function of ECM are considered as promising substrates for tissue engineering.

Electrospun PCL/Ca-deficient HAp nanocomposites have been fabricated and used to for embryonic stem cells culture and proliferation (Bianco et al. 2009). Aligning nanofibrous arrays has been reported with the benefits of guiding cellular growth (Cooper et al. 2011). Aligned chitosan/PCL fibers fabricated by electrospinning have been found to promote the attachment and proliferation of Schwann cells, which are important cells of the peripheral nervous system (Cooper et al. 2011). Aligned nanofibrous PLGA/nano-HAp scaffolds were also developed for bone tissue engineering (Jose et al. 2009). The fiber diameter and glass transition temperature of the composite increased with increasing amounts of nano-HAp. Although the

electrospinning technique using polymer solution has been successful in nano/micro-fibers fabrication, the potential clinical use of these fibers may be limited by the residual organic solvent (Zhmayev et al. 2010). Therefore, solvent-free, gas-assisted polymer melt electrospinning has been developed (Zhmayev et al. 2010). The limitation of this method is that the high temperature process may cause structure damage of the natural polymers or other bioactive inclusion (Li et al. 2012).

2.4.5 Solid Freeform Fabrication

With the rapid development of computer and materials processing technology, solid freeform fabrication (SFF), also commonly known as rapid prototyping (RP), has become available for scaffold fabrication in tissue engineering (Leong et al. 2003). Based on computer controlled layer-by-layer manufacturing, a data file describing the three-dimensional geometrical information of the target object is needed for SFF technologies. This data file can be created by computer aided design (CAD) software or converted from the images generated from computer tomography (CT) or magnetic resonance imaging (MRI). Such techniques make it possible to create scaffolds with precise porous architecture and allow the processing of a wide variety of powder materials including polymers, metals and ceramics. SFF can be generally classified into three-dimensional printing (3DP) (Sherwood et al. 2002a), fused deposition modeling (FDM) (Hutmacher 2001), 3D plotting (Landers et al. 2002a, Landers et al. 2002b), stereolithography (SLA) (Lee et al. 2007), and selective laser melting (SLM) (Lin et al. 2007)

3DP was developed at the Massachusetts Institute of Technology (MIT), and was the first SFF technique for tissue engineering and biomedical purposes (Sachs et al. 1992). There are also some commercially available 3DP machines (e.g. 3DP™, Therics, Inc., Princeton, NJ) (Koegler et al. 2004). The technology was based on the printing of a binder through a print head nozzle onto a powder bed. In contact with the binder, powders would bond together in the print path. After one layer was built, the platform moved downward a specific distance, and a fresh powder layer was coated onto it. The process was repeated until the entire object was made. To date, 3DP is possibly the most widely investigated SFF technique used for scaffold fabrication. Researchers have fabricated scaffolds from a variety of materials such as PLLA (Huang et al. 2007), PLGA (Sherwood et al. 2002), HAp (Ott & Irlinger 2009, Suwanprateeb et al. 2009), TCP (Warnke et al. 2010) and so on. Huang (2007) fabricated levofloxacin loaded PLLA implants with predefined microstructures. The drug-release profile implied that the 3DP technique had the potential to control the drug release rate. It should be noted that a drawback of SFF is the production of final scaffold products with low porosity (Ravichandran et al. 2012). Kim et al. (1998) suggested that incorporation of the particulate leaching technique in 3DP was an effective way to solve this problem. They fabricated PLGA scaffolds with the addition of the salt particles. The obtained scaffolds contained interconnected channels of size 800 μm and a total porosity of 60%. Large numbers of hepatocytes were successful attached on the outer surface and internal channels of the scaffolds. More recently, Inzana et al. (2014) utilized phosphoric acid as the base binder solution for 3DP the calcium phosphate/collagen scaffolds for non-loading bone defect regeneration. This method had high printing accuracy and it enabled the creation of composites with enhanced mechanical properties and improved

bone healing. However, the residual binder, phosphoric acid, could pose issues for biocampatibility.

For FDM, a moving heated nozzle was used to extrude a thermoplastic filament material in a layered fashion to build a 3D scaffold (Hutmacher 2001). This technique was successfully employed in the fabrication of honeycomb-like PCL scaffolds with well controlled pore size and porosity (Hutmacher et al. 2001). These PCL scaffolds showed good mechanical properties and excellent biocompatibility. Moreover, composite scaffolds, PCL/HAp, were also developed by FDM technology (Zein et al. 2002). Kim (1998) fabricated PCL/PLGA scaffolds through a multi-head deposition system (MHDS) based on FDM for tissue engineering (Kim & Cho 2009). The obtained scaffolds with controllable structure and good compatibility implied that MHDS was a good method for scaffold fabrication. A versatile system called 3D plotting was reported by Lander (2002a). This technique can be applied to fabricate hydrogel scaffolds with predefined internal and external structures. A number of factors, such as the liquid medium, temperature, nozzle type and the density of the plotting material as well as the rheological behavior, are of concern for 3D plotting. An agar scaffold with porosity of 35%-40% was fabricated by Landers (2002a). SLA is another well researched SFF technology, which uses a laser to crosslink photo-polymerizable polymer and fabricate precisely designed 3D scaffolds layer by layer (Cooke et al. 2003). Poly(propylene fumarate) (PPF) is one of the promising cross-linkable and degradable polymers that has been studied and fabricated into 3D scaffolds for critical-sized defect repair (Fisher et al. 2002). Optimal resin composition and laser parameters for constructing 3D scaffolds in a conventional SLA machine have been investigated by

Lee et al. (2007). They used PPF, diethyl fumarate (DEF), and bisacrylphpsphrine oxide (BAPO) as the row material, solvent and photoinitiator, respectively, for fabricating complex 3D scaffolds with controlled microstructures. SLA also shows the probability to control the surface feature of a 3D scaffold (Chen et al. 2006). The nanofibous PLLA scaffold with micropores on the struts mimicking the morphology of type I collagen have been created by using a SLA-fabricated negative mold and thermal phase separation of the PLLA solution. These micropores increased the surface area of the scaffolds and provided a favorable environment for bone tissue formation. However, there are some technical limitations of SLA, such as CT data imported error during image acquisition, irregular surface feature maybe found, and the low accuracy of the external geometry and inner pore structure of scaffolds (Kim et al. 2010). Moreover, there is limited number of reports on the surgery implantation of SLA-fabricated scaffolds.

"Organ printing" is defined as a biomedically relevant variant of rapid prototyping technology, which is based on tissue fluidity (Mironov et al. 2003). It has the potential to print biological tissues and organs in a layer-by-layer manner. Anthony Atala (2011), director of the Wake Forest Institute for Regenerative Medicine, demonstrated his progress in using 3DP to make a kidney during his TED Talk. However, it was not a functional human kidney, it was a scaffold made from a biocompatible and bioresorbable gel mixed with living cells. Printing an organ with its intricate inner structures, such as the fine networks of vessels and high cell density, are big challenges. Though far from perfect, 3D organ printing is a developing technology with great potential for tissue regeneration applications (Mironov et al. 2008). A liver tissue, built-

up in layers of thicknesses of 500 microns, has been printed by the bio-printing company *Organovo,* and the liver tissue can be maintained in a fully functional state with native phenotypic behavior for at least 40 days. The company *Organovo* now expects to unveil the world's first printed organ, "a human liver", next year.

Table 2.2 Summary of the methods used to process bone scaffolds (Liu et al. 2007, Hutmacher 2000)

Fabrication technique	Requirement of materials	Reproducibility	Pore size (μm)	Porosity range (%)	Problems
Solvent casting/ particulate leaching	Soluble in solvent	User, material and technique sensitive	30-1000	20-90	Solvent toxicity, particular remained, formation of a skin layer
Gas forming/ Particulate leaching	Soluble in solvent	User, material and technique sensitive	20-1000	<94	Solvent toxicity, difficult to control pore size
Phase separation and freeze drying	Soluble in solvent	User, material and technique sensitive	<200	70-95	Solvent toxicity, difficult to control pore size
Electrospinning	Soluble in solvent or thermalplastic	Machine control and solvent sensitive	20-100	<94	Solvent toxicity, difficult in shaping, insufficient mechanical properties
Solid freeform fabrication	Soluble in solvent or thermalplastic with low melting point	Machine and computer control	>150	<80	Limited resolution, costly

Table 2.2 summarizes the key characteristics of the above mentioned techniques commonly used in scaffold fabrication. Each of the above techniques has its advantages and disadvantages. Both electrospinning and phase separation have the advantages of easy processing and can fabricate scaffolds with high porosity and interconnectivity; nevertheless, they have the same problems with the residual solvent which may be harmful to human tissue. SFF can fabricate scaffolds with predefined porous architecture using a data file created by computer aided design software, however, the SFF facilities are expensive and have low resolution. The solvent casting/particulate leaching technique has the advantages of simplicity, efficiency and independently control of the porosity level and pore size of the scaffolds by varying the amount and size of the leachable particles. The problem with this method is that it is difficult to fabricate scaffolds with a uniform pore distribution because the leachable solid particles tend to deposit and form a skin layer of polymer. Furthermore, direct incorporation the drug with the polymer is a commonly used method to obtain drug delivery scaffolds, which is limited for water soluble drug loaded scaffolds fabricated by the particulate leaching method. Therefore, there still much room for improvement in scaffold fabrication methods. In this research, a modified solvent casting/particulate leaching technique, which applies polymer coagulation and uses cold compression molding and drug coating instead of conventional hot compression molding and direct drug mixing, has been developed and is presented in the next chapter.

Chapter 3. Development of PC-DC Scaffold Fabrication Technique and Characterization of Multifunctional Bone Scaffold

3.1 Overview of the Methodology

A PC-DC technique combining polymer coagulation, cold compression molding, particulate leaching, and drug coating methods has been developed for multifunctional scaffold fabrication. An overview of the methodology is illustrated in Figure 3.1.

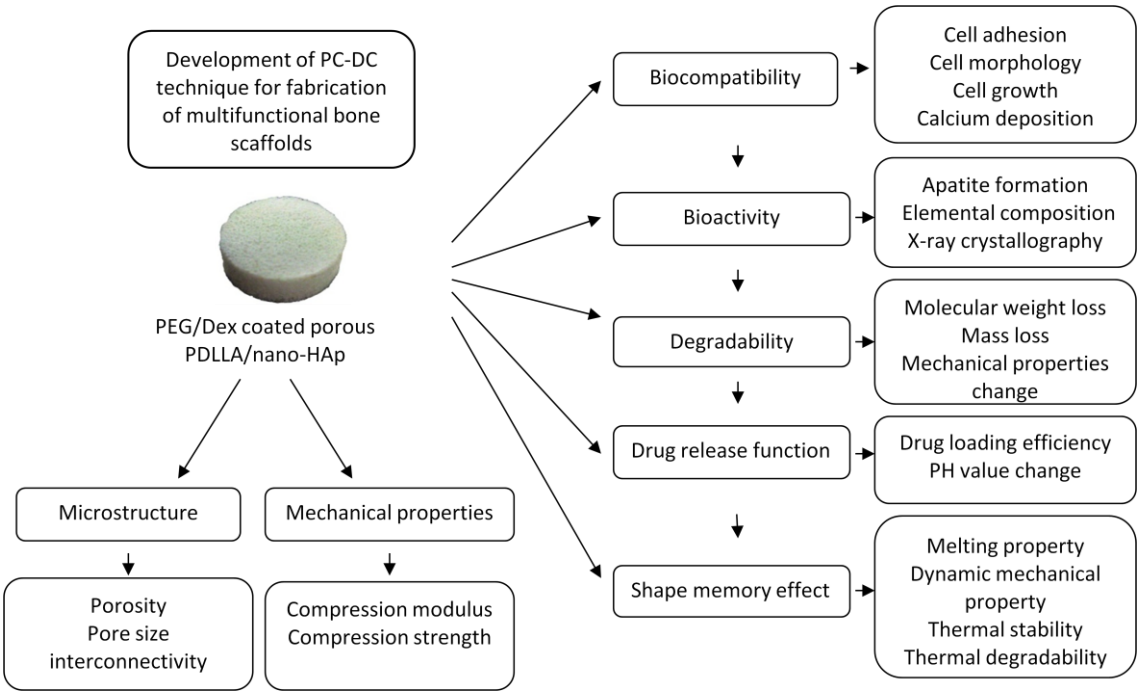

Figure 3.1 Overview of the methodology of this study

The porous Dex-releasing PDLLA/nano-HAp composite as a model system has been designed and prepared by this technique. The physical, chemical and biological properties of the multifunctional Dex-releasing were investigated. The microstructure, surface wettability, and mechanical properties of the scaffolds were characterized and are presented in Chapter 3. Biocompatibility is one of the most important requirements

for a scaffold. The ability of these scaffolds to support the osteoblast-like cell (MG63) adhesion, proliferation and phenotypic expression was evaluated and is described in Chapter 4. The bioactivity and degradability of these scaffolds were examined through assessment of apatite deposition, molecular weight change, mass loss, and mechanical properties change during incubation in simulated body fluids. Moreover, the drug release behavior of the scaffolds was also investigated as presented in Chapter 5. The shape memory effect was also studied and is described in Chapter 6. The effects of the fabrication conditions, nano-HAp fractions and porosity values of the composites on these properties were also investigated.

3.2 Introduction

Biodegradable polymers have been fabricated into scaffolds for various tissue regeneration because they can be gradually degraded and replaced by the newly regenerated tissues which can avoid secondary surgery to remove the implants after tissue recovery or when the drug supply is depleted (Liu et al. 2007, Biondi et al. 2008). Drug delivery technology has been attracting increasing interest in recent years for improving human lives. Such delivery systems utilize biodegradable materials as the drug vehicle to deliver biologically active molecules at a desired behavior, so as to improve the effectiveness of the drug therapy and to reduce toxicity (Langer 1998). Shape memory polymers (SMPs) have been considered as an intelligent material with potential applications in implants for minimally invasive surgery since they can be precisely positioned in the body in a temporary small shape and attain their application-relevant shape after implantation which can highly reduce the risk of surgery. Implantation of multifunctional porous scaffolds, with the function of biodegradability,

drug delivery capacity, and shape memory effect, may have high potential applications in treating bone damage. The scaffolds may not only act as a structural support but also provide the benefits of a fast recovery rate and high therapeutic efficacy to the diseased bone.

The scaffold fabrication condition and material selection greatly affect the structure and properties of the fabricated scaffold. As described in the literature review, one commonly used method, the solvent casting/particulate leaching technique has the advantages of simplicity, efficiency and independently controlling the porosity level and pore size of the scaffolds by varying the amount and size of the leachable particles (Douglas et al. 2009, Raucci et al. 2010). Nevertheless, it is difficult to fabricate a scaffolds with uniform pore distributed because the leachable solid particles with higher density compared to the liquid polymer solution tend to deposit and form a polymer skin layer (Guarino et al. 2008). Directly mixing the drug with the polymer to fabricate scaffolds with sustained drug release rate is a widely used method for drug loading into the scaffolds (Kim et al. 2003). However, this method cannot be applied when the scaffolds are prepared by the salt leaching method and loaded with water soluble drugs. In this part of the study, a novel technique which applies polymer coagulation to and solvent casting/particulate leaching method, and used cold compression molding and drug coating instead of conventional hot compression molding and direct drug mixing, has been developed. This technique can not only solve the distribution problem, but also avoids the decomposition of the polymer matrix and premature loss of the drugs. In this process, the rapid coagulation of the polymer, together with a bioactive inclusion and space holding agent, was the key step to ensure the scaffold had a uniform pore

distribution. Moreover, this step shortened the solvent evaporation time for the polymer deposition, turning into an easily-molded gel paste containing little solvent.

Biodegradable polymer, PDLLA, was chosen as the base material. To improve its mechanical properties and osteoconductivity, nano-HAp was chosen as the reinforcing and bioactive phase in the polymeric scaffold. Dex was chosen as the drug releasing model because of its great effect in inducing and maintaining the osteoblastic phenotype of exposing stem cells and its high anti-inflammatory capacity (Jaiswal et al. 1997, Yoon et al. 2003). PEG was used as a drug loading agent to assist drug loading and prolong the drug release. The PEG/Dex coated PDLLA/nano-HAp composite was studied as a model system to evaluate the PC-DC technique for scaffold fabrication. The surface wettability, morphology, and microstructure of the scaffolds were characterized by a contact angle meter, scanning electron microscopy (SEM), and micro-computed tomography (micro-CT), respectively. The effect of nano-HAp incorporation and porosity of the composite on the mechanical properties was also studied in this part of study, resulting in a paper published in the journal Composites Science and Technology (Chen et al 2011).

3.3 Fabrication of PDLLA/nano-HAp Scaffold with PEG/Dex Coating

3.3.1 Materials

Biodegradable polymer, PDLLA ($\overline{M}_{\eta}$ =75,000), purchased from the Jinan Daigang Bio-Technology Co., Ltd. (China), was selected as the matrix material. Commercially available nano-hydroxyapatite (nano-HAp) with a primary crystal size of 20-30 nm,

purchased from Berkeley Advanced Biomaterials, Inc (USA), was employed as the reinforcing phase in this study. The widely used sodium chloride (NaCl) crystals were chosen as the shape holding agent to become the pores in the scaffold. The NaCl crystals were milled and then sorted into a size range from 150 to 300 μm by sieving with standard testing sieves. After size separation, the sieved NaCl particles were stored in a cool, dry room prior to use. The NaCl crystals were purchased from Tianjin Hongyan Chemical Reagents Co., Ltd. (China). To enhance drug adhesion to the scaffold and to prolong the drug release in an aqueous environment, PEG with excellent hydrophilicity and biocompatibility was selected as the drug coating agent to assist Dex coating. PEG (M_w = 6000) was supplied by Tianjin Regent Chemical Co. Ltd (China). The drug model, Dex (CAS 50-02-2, 98% purity) was purchased from Sigma Aldrich Co., Ltd. Chloroform, purchased from the Shanghai Shenxiang Chemical Reagent Co., Ltd. (China), was chosen in this study as an organic solvent. All chemicals were of analytical grade and used without further purification.

3.3.2 PDLLA/nano-HAp Scaffold Preparation

Porous PDLLA/nano-HAp scaffolds were prepared by applying a salt particulate leaching method to polymer coagulation and using cold compression molding instead of conventional hot compression molding to avoid the decomposition of polymer matrix and bioactive inclusions. The pore size of the scaffolds was controlled by NaCl in the range of 150 to 300 μm. The porosity of the PDLLA scaffolds was controlled by the different PDLLA/NaCl weight ratios (1:7, 1:8 and 1:9). Nano-HAp (initial weight percentages of 10, 20, 30, 40, 50, and 60%), the reinforcing and bioactive phase, was mixed with the PDLLA scaffolds. For comparison, unfilled PDLLA scaffolds were also

prepared. The schematic representation of the steps in fabricating the porous PDLLA/nano-HAp scaffolds is shown in Figure 3.2 (a). The PDLLA was dissolved in chloroform at 40 °C and stirred by a homogenizer. Subsequently, nano-HAp and the sieved NaCl particles were dispersed in the PDLLA/chloroform solution under steering to obtain a well mixed PDLLA/NaCl/nano-HAp chloroform solution. After that, ethanol was added to the solution and the PDLLA/NaCl/nano-HAp mixture in the form of a gel paste (Figure 3.3) was then precipitated in ethanol. The gel paste mixture was then put into a cylindrical die of 10 mm diameter and compressed at a pressure of 10 MPa for 2 minutes at room temperature. After vacuum drying at 40 °C for 24 hours, the molded PDLLA/NaCl/nano-HAp composites were undergone a salt leaching process by being placed in the distilled water. Fresh distilled water was replaced every 2 hours for the first 10 hours, and then 2-3 times a day until there was no white precipitate detected after dripping silver nitrate solution into the water. After that, porous samples were then placed in a vacuum dryer at 40 °C for 24 hours.

3.3.3 PEG/Dex Coating

Figure 3.2(b) shows a schematic representation of the drug coating process. The PEG/Dex solution was prepared by dissolving a fixed amount of Dex (0.8%, w/v) and PEG (20%, w/v) into 50% ethanol, stirring for 1 hour. A vacuum was applied to the flask with the porous PDLLA/nano-HAp scaffolds in it, to increase the infiltration rate of the PEG/Dex solution into the scaffolds and improve the drug coating efficiency. The valve was closed and the PEG/Dex solution was then added into the flask by syringe. After 24 hours of immersion in the hydrophilic PEG/Dex solution under vacuum, a PEG/Dex film was coated onto the porous PDLLA/nano-HAp scaffolds. The scaffolds

were then removed and dried under vacuum for 24 hours at room temperature. Finally, fabrication of the PEG/Dex coated porous PDLLA/nano-HAp scaffolds was completed.

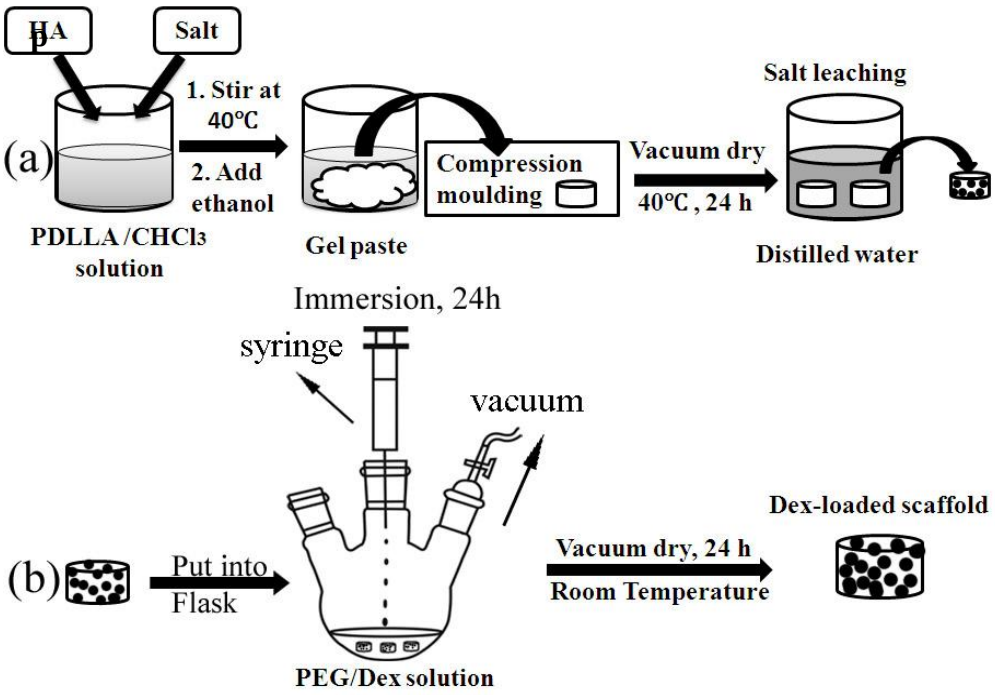

Figure 3.2 A schematic representation of (a) scaffold fabrication and (b) drug coating process

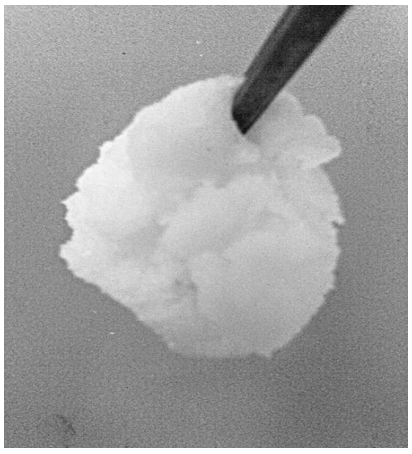

Figure 3.3 Photograph of the PDLLA/nano-HAp/NaCl mixture in a state of gel paste

3.4 Characterization of PDLLA/nano-HAp Scaffold with PEG/Dex Coating

3.4.1 Morphology of the Scaffold

Scanning electron microscopy (SEM, JEOL JSM-6490) was used for the morphology observation of the porous PDLLA/nano-HAp composites before and after the PEG/Dex coating. The samples were coated with gold to improve their conductivity. The dispersion of nano-HAp on the surface and inner side of the PDLLA composites was examined by an energy dispersive X-ray analysis detector (EDX, Oxford, INCA250 Energy System).

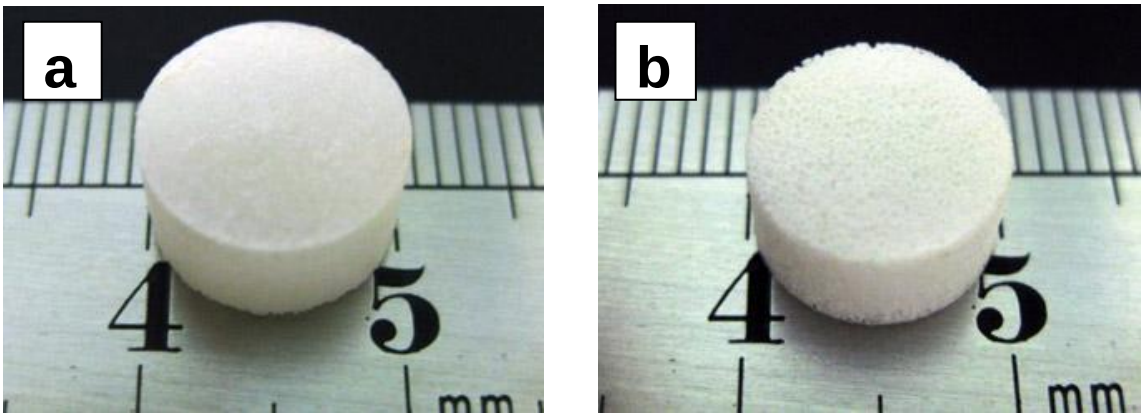

Figure 3.4 Photographs of the PDLLA/nano-HAp composites (cylinder: Ø10×5 mm) (a) material before salt leaching process, (b) material after salting process.

Photographs of the scaffolds before and after salt leaching are shown in Figure 3.4. It can be clearly observed that some pores exist on the porous scaffold after the salt leaching process while no apparent pore was observed on the pre-prepared scaffold before salt leaching. SEM images of the PDLLA/nano-HAp composites with and without the drug coating are shown in Figure 3.5.

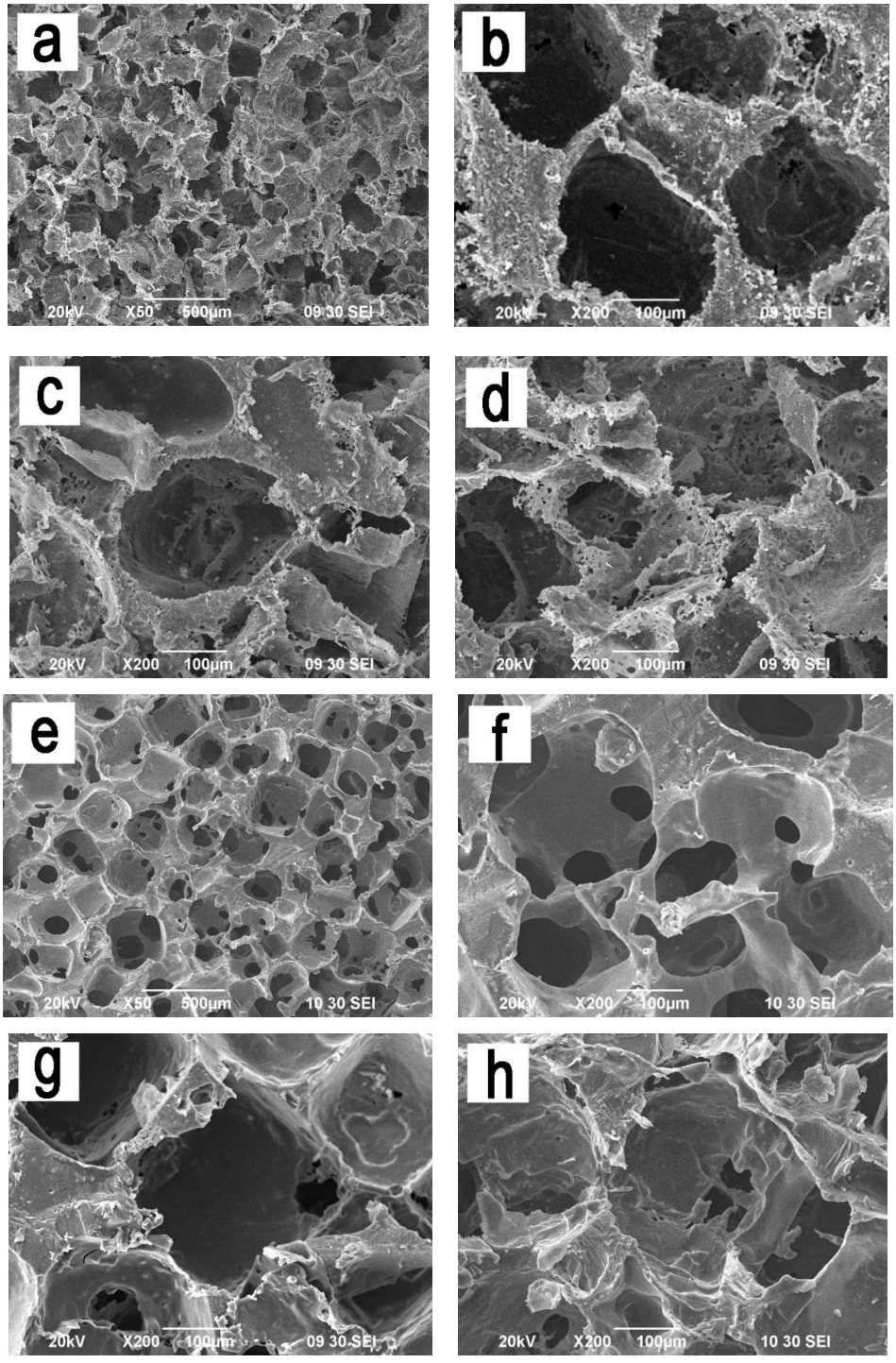

Figure 3.5 The SEM micrographs of PDLLA/nano-HAp composites without PEG/Dex coated: (a) Low magnification of 1:9; High magnification of (b) 1:7, (c) 1:8, (d) 1:9; PEG/Dex coated PDLLA/nano-HAp composites: (e) Low magnification of 1:7; High magnification of (f) 1:7, (g) 1:8; (h) 1:9.

It can be clearly seen from Figure 3.5, that the pores are homogeneously distributed throughout the composites and the pore walls of PEG/Dex coated samples are smoother than the uncoated ones. This indicates that the viscous PEG/Dex has successfully diffused into the porous samples and coated the pore walls. After the PEG/Dex coating, the initial interconnected porous structure was well maintained although some small pores in the PDLLA/nano-HAp composites were covered. Moreover, from Figure 3.4, it is observed that the pore sizes of the PDLLA/nano-HAp scaffolds ranged from 200 to 350 μm, which is close to those of the sieved NaCl particle sizes, meeting the minimum requirement of the pore size of 100 μm for a bone scaffold suggested by Karageorgiou and Kaplan (2005). Some pores larger than 300 μm can also be found, which may be beneficial to vascularization and new bone regeneration (Li et al. 2008).

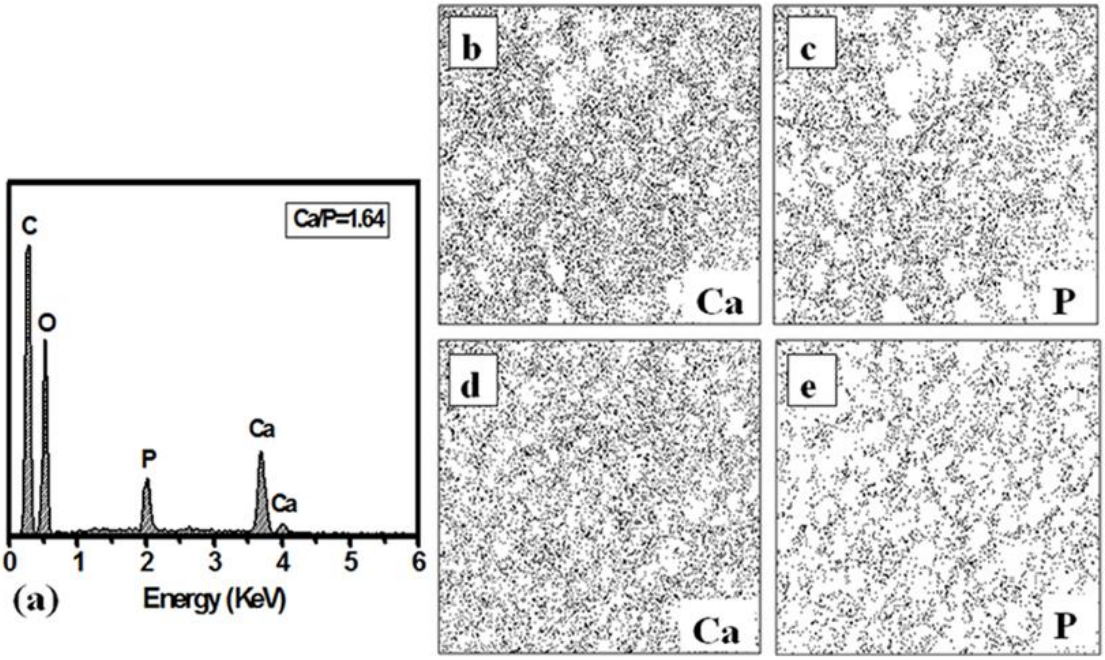

Figure 3.6 EDX analysis results: (a) EDX spectra of the PDLLA/nano-HAp composite, and Ca and P element distribution maps: (b), (c) on composite surface; (d), (e) in composite matrix.

From the EDX analysis results, the presence of Ca and P inside the PDLLA/nano-HAp matrix and on their surface can be demonstrated, as shown in Figure 3.6(a). The Ca/P ratio is 1.64, indicating that nano-HAp was successfully incorporated into the scaffold. In addition, the results of Ca and P element mapping are illustrated in Figures 3.6(b)-(e). The black dots represent the Ca and P elements inside the composites and on their surfaces. A homogenous dispersion of nano-HAp can be observed and it has the ability of improving the mechanical properties of the scaffold. A uniform pore distribution (white domain) in the scaffolds is also confirmed.

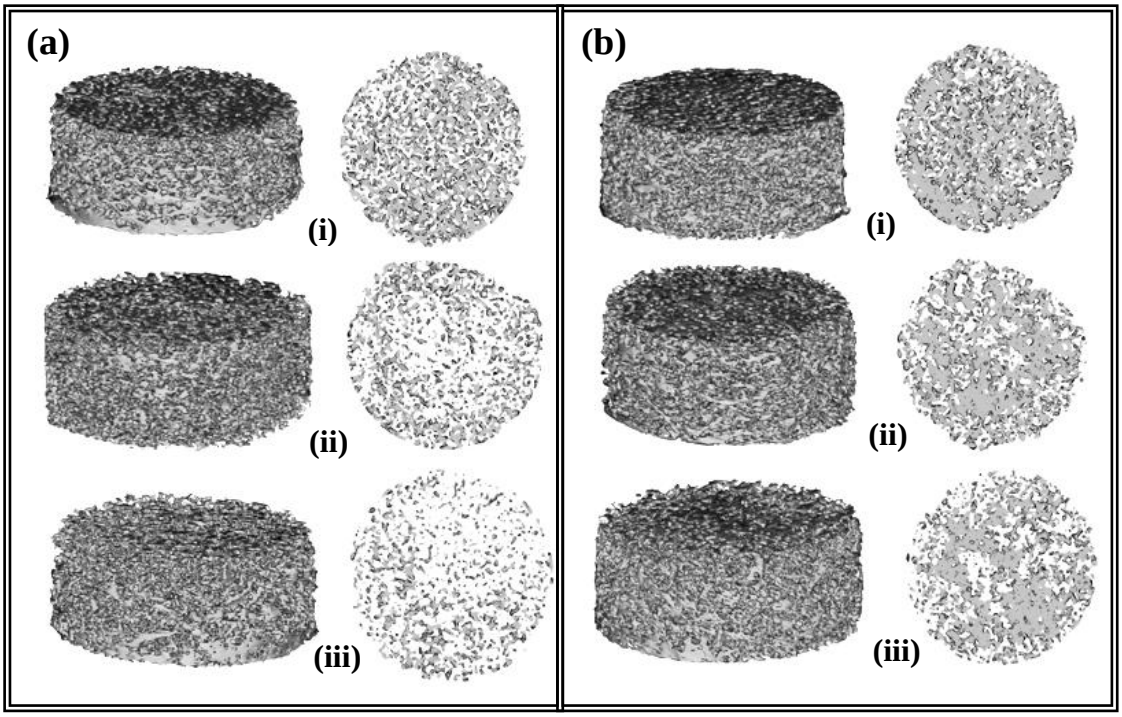

Figure 3.7 3D micro-CT reconstructed images of (a) PDLLA/nano-HAp composites and (b) PEG/Dex coated PDLLA/nano-HAp composites with different porosity (PDLLA/NaCl weight ratios of (i) 1:7, (ii) 1:8, and (iii) 1:9)

3.4.2 Microstructure of the Scaffold by Micro-computed Tomography

Porosity is an important parameter for bone tissue engineering scaffolds because it directly affects the diffusion of the physiological nutrients and gases in the scaffold. Micro-computed tomography (micro-CT, Skyscan1076) was carried out to obtain visualization of the entire miroctructure of the porous PDLLA/nano-HAp composites and to study the effect of the PEG/Dex coating on the porosity. The porous PDLLA/nano-HAp composites with and without the PEG/Dex coating, were scanned at 100 kV, 80 mA and 11.5 μm voxel resolutions to measure their open and total porosity. The open porosity, which took account of the open pores, was used to evaluate the interconnectivity of the scaffolds before and after coating.

The micro-CT 3D images of the PDLLA/nano-HAp composites before and after PEG/Dex coating, which were reconstructed from their corresponding cross-sectional segments (15 image slices each), are shown in Figure 3.7. The total and open porosity values of the PDLLA/nano-HAp composites, with and without the PEG/Dex coating, are listed in Table 3.1. The more the leachable salts were incorporated, the more pores would be left in the scaffold after salt leaching. The total porosity of the uncoated PDLLA/nano-HAp composite was only 66% when the weight ratio of PDLLA/NaCl was 1:7, while it reached 81.6% for a ratio of 1:9. Therefore, the porosity can be controlled by varying the amount of porogen. The values of the open and total porosities of each sample are very close, indicating high interconnectivity of the samples fabricated in this study. It can also be observed from Table 3.1 that the porosity and the interconnectivity of the PDLLA/nano-HAp composites decreased after the PEG/Dex coating, but the coated composites essentially retained their porous structures.

This implies that the porosity and pore size can be independently controlled by varying the amount and size of the NaCl particles when using the particulate leaching method. The microstructure of the scaffolds may promote cell growth, migration and the transport of nutrients and oxygen, as well as the removal of metabolic waste when implanted for bone regeneration (Hutmacher 2000).

Table 3.1 Total and open porosity of PDLLA/nano-HAp composites before and after PEG/Dex coating.

Porosity / Scaffolds	Before PEG/Dex coating		After PEG/Dex coating	
	Total porosity (%)	**Open porosity (%)**	**Total porosity (%)**	**Open porosity (%)**
1:7 + 20 wt% nano-HAp	66.01	66.00	51.48	51.21
1:8 + 20 wt% nano-HAp	77.02	77.01	58.04	57.94
1:9 + 20 wt% nano-HAp	81.58	81.57	61.51	61.44

3.4.3 Wettability of the Scaffold

Surface hydrophilicity is one of the important aspects that affect the biocompatibility of the materials in a biological environment (Xu & Wu 2009). Water contact angle measurement was conducted to evaluate the surface hydrophilicity of the unfilled PDLLA and the PDLLA/nano-HAp composites, with and without the PEG/Dex coating. The water-in-air contact angle of the samples was measured by a digital contact angle meter (Digidrop, Model R&D, GBX Company). The sample was placed onto the work stage of the meter. The contact angle was measured within 10 seconds after a droplet of distilled water (5μl) contacted the sample surface.

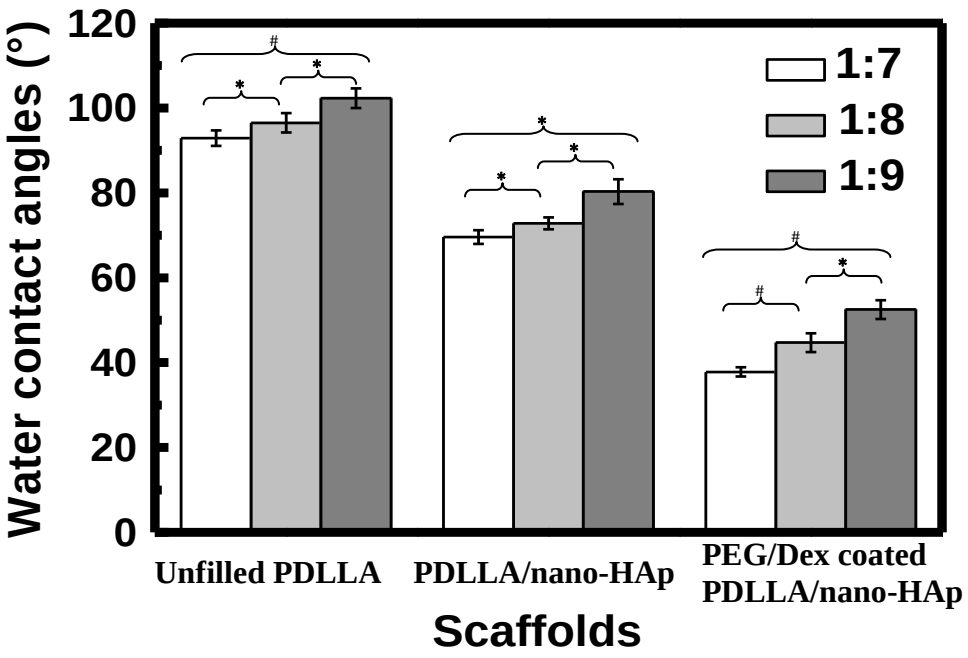

Figure 3.8 Water contact angles of the surface of unfilled PDLLA, PDLLA/nano-HAp composites and PEG/Dex coated PDLLA/nano-HAp composites with different porosities (PDLLA/NaCl weight ratios of 1:7, 1:8 and 1:9). (*indicates statistically significant difference for $p<0.05$; #indicates statistically significant difference for $p<0.01$, n=3).

Figure 3.8 shows the water contact angles of the unfilled PDLLA, the PDLLA/nano-HAp composites and the PEG/Dex coated PDLLA/nano-HAp composites with different porosities. With an increase in the porosity, the water contact angles of the composites increased. For each type of sample, the measured water contact angles of the samples with three different weight ratios were all statistically different. The PDLLA/nano-HAp composites had smaller contact angles than the unfilled ones. Furthermore, the water contact angles decreased significantly after the PEG/Dex coating. The reduction in the contact angles suggests that an improvement in surface hydrophilicity was achieved

with nano-HAp filling and hydrophilic PEG coating. The water contact angles decreased with nano-HAp which may benefit cell attachment and growth on the scaffolds.

3.4.4 Detection of Dex Loading

Fourier transform infrared spectroscopy (FT-IR, Nicolet Magna-IR 760) was adopted to validate the presence of Dex in the composites and the chemical interaction between the PDLLA and nano-HAp. The sample was mixed with a particular amount of KBr powder (sample/KBr=1/9, w/w), and pressed into a thin diaphanous film for measurement. The spectra of the PEG/Dex coated PDLLA/nano-HAp composite, unfilled PDLLA, nano-HAp, Dex, and PEG were determined in the measurement range of 400-4000 cm^{-1} at room temperature. Results from FTIR are shown in Figure 3.9. The characteristic peaks of Dex are observed in the spectra of the PEG/Dex coated PDLLA/nano-HAp composites at 1662.5 cm^{-1}, 1619.7 cm^{-1} and 1604.9 cm^{-1}. This indicates that Dex was successfully incorporated into the composite. A strong band at 1756.8 cm^{-1} can be observed in the spectra of the unfilled PDLLA, which is attributed to the carbonyl group (C=O). In the FTIR spectra of PEG/Dex coated PDLLA/nano-HAp composite, one peak at 1757.8 cm^{-1} is attributed to the original C=O vibration of PDLLA, while the peak at 1752.3 cm^{-1} corresponds to the interaction of PDLLA and nano-HAp, taking a blue-shift. The weak peaks in the range 3650 cm^{-1} to 3680 cm^{-1} are assignable to the vibration modes of the P–OH groups. This confirms that hydrogen bonding (namely, P–OH ··O=C bonding) was formed between the PDLLA and the nano-HAp (Zhou et al. 2007). This hydrogen bonding played an important role in mechanical properties improvement.

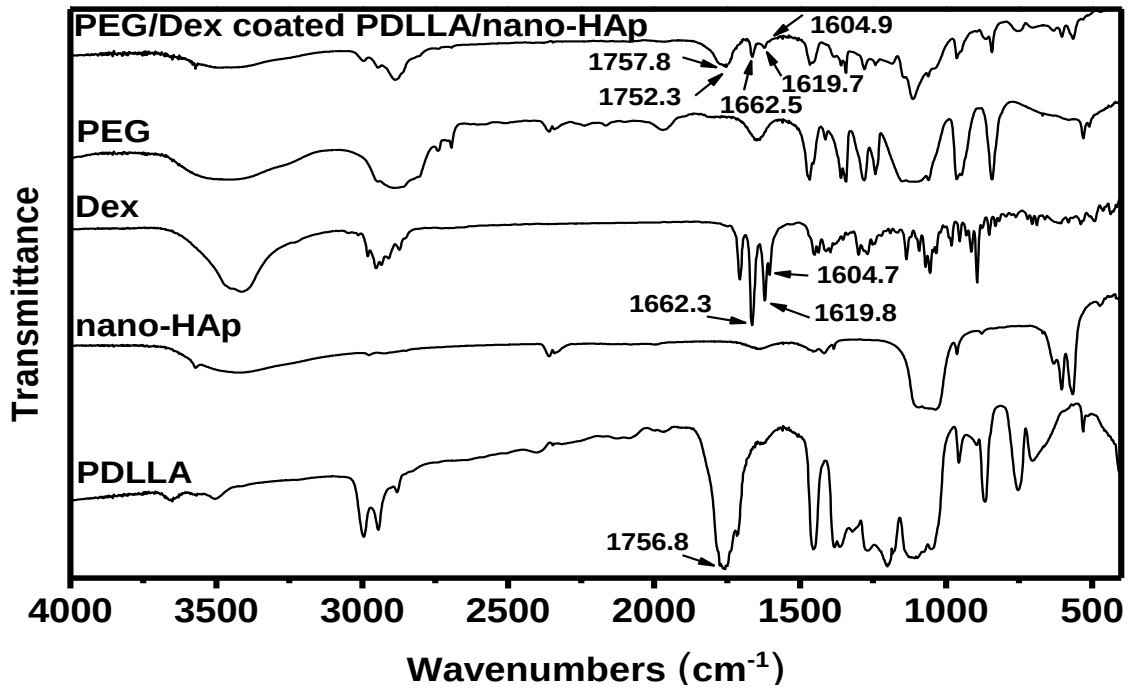

Figure 3.9 FTIR spectra of PEG/Dex coated PDLLA/nano-HAp composite, unfilled PDLLA, nano-HAp, Dex, and PEG.

3.4.5 Mechanical Properties

The compressive moduli and strengths of the porous PDLLA based samples with and without nano-HAp, were investigated by compression tests using a universal mechanical testing machine (MTS 810, Material Test System) at a crosshead speed of 2 mm/minute. Cold-molded cylindrical porous samples with a diameter of 10 mm and a height of 5 mm were employed as the test samples. The load was applied to the specimen until it was compressed to about 50% of its original height. According to the ASTM standard, D1621, the compressive strength (σ_{10}) was determined as the stress at which the strain reaches 10%. The compressive modulus (E) was calculated as the slope of the initial linear portion of the stress–strain curve. Five replicate measurements were conducted for each type of sample.

E and σ_{10} of the samples are listed in Table 3.2. For the unfilled PDLLA, the compressive modulus ranged from 25.3±1.2 MPa for a PDLLA/NaCl ratio of 1:9 to 64.8±2.7 MPa for a ratio of 1:7. The σ_{10} ranged from 1.5±0.1 MPa to 2.9±0.2 MPa. This is because the increase in the porosity of the unfilled PDLLA, which is associated with increasing amounts of porogen, led to a decrease of E and σ_{10}. A balance can be reached between porosity, pore size and mechanical properties. This phenomenon can be found in the PDLLA/nano-HAp composites as well.

Table 3.2 Compressive modulus (E) and the compressive strength (σ_{10}) of the PEG/Dex coated porous PDLLA/nano-HAp composites and unfilled PDLLA.

Samples (PDLLA/salt, w/w)	***E*** **(MPa)**	$\boldsymbol{\sigma_{10}}$ **(MPa)**
1:7	64.8±2.7	2.9±0.2
1:8	56.1±2.7	1.8±0.1
1:9	25.3±1.2	1.5±0.1
1:7 + 20 wt% nano-HAp	97.9±2.3	3.1±0.1
1:8 + 20 wt% nano-HAp	78.4±1.7	3.0±0.1
1:9 + 20 wt% nano-HAp	38.7±2.5	2.4±0.3

The compressive moduli and compressive strengths of the PDLLA composites with the addition of nano-HAp were increased by more than 50% and 20%, respectively, as compared with the unfilled ones. This is because a closer packing of polymer chains was formed when a high pressure applied to the PDLLA/nano-HAp composite in the compression molding process (Teng et al. 2007). The enhancement of the mechanical properties of the composite is likely due to the homogenous distribution of the nano-HAp in the PDLLA and the hydrogen bonding formed between the nano-HAp and PDLLA due to the high pressure during the compression molding (Zhou et al. 2007). The mechanical properties of the 1:7 and 1:8 nano-HAp filled PDLLA scaffolds fell

within the normal range of modulus (50-250 MPa) and strength (1-10 MPa) values for human cancellous bone (Lin et al. 2003). Therefore, the PEG/Dex coated PDLLA/nano-HAp composites fabricated in this study may have the potential to be used in trabecular bone regeneration.

3.5 Summary

Choosing an appropriate technique and biomaterials for scaffold fabrication is important for the control of pore size and structure, drug release capacity, shape memory effect, and mechanical properties of the scaffolds. In this part of study, a PC-DC technique was developed. Multifunctional PEG/Dex coated porous PDLLA/nano-HAp composites as a model system were successfully fabricated by this newly developed technique combining coagulation, cold compression molding, salt leaching and drug coating. This technique independently controlled the pore size and porosity of the scaffold by varying the amount and size of the leachable particles (NaCl). The cold compression moulding and drug coating method prevented decomposition of the polymer matrix and premature loss of the drug. This technique reduced solvent residual by the polymer coagulation, and particulate leaching/solvent casting steps. The gel-like polymer paste formed by coagulation of the PDLLA in the non-solvent proved easy to mold. Moreover, applying polymer coagulation to the solvent casting/particulate leaching method successfully solved the non-uniform distribution of the pores within the scaffolds. A layer of viscous PEG/Dex was observed on the pore walls of the scaffolds from the SEM images. The FT-IR spectroscopy suggested that Dex was effectively loaded into the matrix. PEG/Dex coating on the scaffold surface under vaccum is a promising way for drug

loading process. The technique is economical and can be applied to a wide range of polymers and inorganic fillers and drugs for scaffold fabrication.

The pores were distributed homogeneously throughout the scaffolds and the pore sizes were ranged from 200 to 350 μm. These pore sizes meet the requirement for a bone scaffold and the porosities of the scaffolds ranged from 66% to 81.6%. PDLLA/nano-HAp composite had higher compressive moduli and strengths than the unfilled ones. The significant improvement of the wettability of the PDLLA composites was achieved by the nano-HAp incorporating and the PEG/Dex film coating. The scaffolds may promote cell growth, migration and the transport of nutrients and oxygen, as well as the removal of metabolic waste when implanted for bone regeneration. In this chapter, the PC-DC technique and basic characteristics of the composites was presented. The biocompatibility is the most important requirement for a bone scaffold, the next step was to investigate the interaction between the cell and the fabricated scaffolds, and the results are presented in Chapter 4.

Chapter 4. *In Vitro* Human Osteoblast-like Cell Response to the PDLLA/nano-HAp Composites

4.1 Introduction

Autograft is considered as the golden standard treatment for large bone defects, which harvests the 'donor' bone from a non-load-bearing site in the patient's body. It can provide three essential element of bone regeneration: osteoconduction, osteoinduction, and osteogenic properties. Nevertheless, autologous transplantation is severely hampered by the limited amount of autograft and the associated complications at the donor site (Giannoudis et al. 2005). Implanting bone scaffolds made from biomaterials provides an alternative approach for bone defect repair and regeneration, avoiding the limitations of autologous bone graft (Chen et al. 2002). A multifunctional bone graft substitute/scaffold derived from biomedical materials with controllable structure, mechanical and bioactive drug release kinetic for cell growth and tissue regeneration is critical in bone tissue engineering. Design and fabrication of biocompatible scaffolds mimicking the structural and biological functions of the natural extracellular matrix (ECM) which provides cells with an optimized microenvironment is one of the major challenges (Ma 2008). Understanding the cell-ECM interaction mechanism becomes one of the focuses in the tissue engineering field, because it can provide valuable information including the effects of the surface composition, porosity, pore size, topography of the ECM on the cellular behavior, for fabricating a scaffold promoting the cell adhesion, growth, differentiation and later bone regeneration (Van Dijk et al. 2013, Dicesare et al. 2013).

The ability of the scaffold to support cell adhesion, growth and differentiation highly determines the degree of success of tissue engineering. Cultures of osteoblast-like cells in this scaffold in vitro is a promising approach to investigate the biological activity of a scaffold used as a cell carrier. In this part of the study, PDLLA/nano-HAp composites were fabricated using the recently developed PC-DC technique (Chen et al. 2011) for *in vitro* evaluation of osteoblast cellular responses. PDLLA/nano-HAp composites can be considered as one type of ECM which may have important influences on cell behavior. Therefore, in addition to the evaluation of microstructure, wettability, and mechanical properties of the composites, the *in vitro* cell interaction with composites was investigated and presented in this chapter. The potential application of the fabricated composite scaffolds is for bone tissue engineering, thus osteoblasts-like cells, MG63, was chosen in this research. MG63 is an osteosarcoma cell line with an osteoblastic phenotype and has been widely used in research in bone tissue engineering (Verrier et al. 2004, Liu et al. 2004, Wang et al. 2003). To the best of my knowledge, this was the first study of cellular response on PDLLA/nano-HAp composites using the MG63 cell model.

Four types of PDLLA/nano-HAp composites were fabricated: unfilled PDLLA with polymer/porogen ratios of 1:7 and 1:9 were used to study the effect of porosity on the cellular response; unfilled 1:9 PDLLA and PDLLA with 50 wt% nano-HAp were chosen to investigate the effect of nano-HAp incorporation; how the PEG/Dex coating affects the cell behavior was also explored. 3-(4,5-dimethylthiazol-2-yl)-2,5-diphenyltetrazolium bromide (MTT) assay, alkaline phosphatase activity (ALP) assay, scanning electron microscope (SEM), Alizarin Red staining (ARS) and fluorescence

staining were adopted to investigate the interactions between the MG63 cells and the samples. For comparison, unfilled PDLLA film fabricated by the solvent casting method was also investigated. The results showed that the PDLLA based scaffolds fabricated in this study are biocompatible and facilitate cell attachment and proliferation. The pore size of the fabricated scaffolds ranged from 200 to 350 μm and the high porosity of 60% to 80% allowed cells to host and penetrate inside the scaffolds. The whole scaffolds covered by the MG63 cells were observed after a 7-day culture, in which the number of cells on the PDLLA based substrates increased. Moreover, scaffolds with higher porosity values were beneficial for cell attachment, growth, migration and differentiation. Nano-HAp incorporation promoting calcium deposition (cell mineralization/osteoconduction) was also determined in this part of study.

4.2 Cell Culture

The human osteoblast-like cell, the MG63 cell, is an osteosarcoma cell isolated from a relative uncommon tumor. Though these cells possess abnormal growth characteristics, MG63 cells express typical osteoblast phenotypes, such as osteoblastic genes, synthesize bone matrix protein, and expression of ALP (Gartland et al. 2005). They became an extremely useful osteoblast cell model in bone regeneration research (Verrier et al. 2004, Srinivasan et al. 2012). In this study, MG63 cells (American Type Culture Collection, ATCC, USA) were chosen and seeded onto 3D porous PDLLA based scaffolds to study the effect of porosity, nano-HAp incorporation and PEG/Dex coating on the response of cultured cells. The MG63 cells were cultured in a tissue culture polystyrene (PS) flask (75 cm^2) at 37 °C in an incubator with 5% CO_2 in an air atmosphere. The optical microscope images of the MG63 cells well attached on the

culture flask are shown in Figure 4.1. From Figure 4.1 (a), MG63 cells with the size of about 80 μm are observed. The culture medium used for MG63 growth was Dulbecco's modified Eagle's medium (DMEM, Gibco, USA) with GlutaMAX™, supplemented with 10% fetal bovine serum (FBS, ATCC), and antibiotic-antimycotic (100u/ml penicillin, 100ug/ml streptomycin sulfate, Gibco). The medium was changed every third day. After the cells were near to cover the whole surface of the flask (about 5 days), the MG63 cells were trypsinized using 0.25% (w/v) Trypsin-EDTA (ATCC) for 3 minutes, centrifuged at 1200 rpm for 5 minutes, and resuspended in the medium to make a cell suspension. 4.3×10^6 cells were harvested from the 75 cm^2 culture flask after the cells reached subconfluence, as shown in Figure 4.1 (b) (cell counting by a hemacytometer).

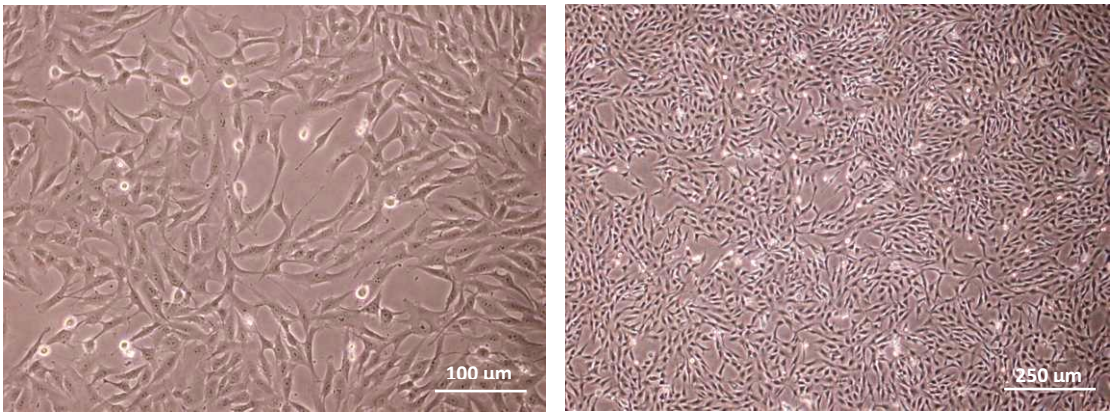

Figure 4.1 Optical microscope images of the MG63 cells grown on the culture flask at (a) magnification of ×10 and (b) magnification of ×4

Before cell seeding on the PDLLA based scaffolds, the 24-welled tissue culture plates were isolated with a 2% agarose gel layer in PBS to prevent non-specific cell adhesion. The scaffolds fabricated in this study, with diameter of 10 mm and thickness of 2 mm, were placed in 24-welled culture plates (SPL, Life Science Co., Ltd., Korea) and

sterilized by soaking in 70% ethanol for 4 hours and the scaffolds were left in PBS overnight, then exposed to ultraviolet (UV) radiation (2 hours for each side) for further sterilization and pre-wetting. After that, the scaffolds were presoaked in a complete cell culture medium for 1 day. A drop of 50 μl of the cell suspension containing certain cell numbers was added to the top of the scaffold and allowed to be absorbed by the porous scaffolds for 2 hours. The same number of cells were seeded on the unfilled PDLLA film as the control. Following a 2-hour cell absorption, 1 ml of additional complete medium was added to each well to cover the whole scaffold. Cells were further incubated at 37 °C in a humidified atmosphere with 5% CO_2 for various periods of time (1, 3, and 7 days) and the culture mediums were changed twice a week.

Experiments were run in triplicate for each sample and repeated three times. All data were expressed as mean ± standard deviation (SD). A one-way analysis of variance (ANOVA) and the Fisher LSD Test for means comparison were used to assess the significant differences. p values < 0.05 were considered statistically significant (n=3).

4.3 Characterization of the Scaffolds with Cells

4.3.1 Cell Adhesion

Cell adhesion is known as an important early cellular process which happens within 3 hours after cell seeding, and directly influences later cellular processes such as cell proliferation, migration and even tissue regeneration (Anselme 2000, Causa et al. 2006)). Although the same volumes of cell suspensions were injected onto the scaffolds surface and control films, only a fraction of the cells were left on the substrates while the remainder adhered to the cell culture plate. Fluorescence staining was conducted for

observation and evaluation of cell adhesion on the PDLLA based materials. A number of cells, about 10^4, were seeded on the specimens before staining. After a 4 hours culture, the cells were gently washed with PBS three times and fixed in 4% formaldehyde/PBS for 30 min, then permeabilized with 0.1% Triton X-100 in PBS for 5 min at room temperature. The scaffold with attached cells was incubated with 500 μm of 1μg/ml DAPI (Sigma) in PBS. The cell nuclei (DAPI, blue) of the cells were observed with a fluorescence microscope (Eclipse 80i, Nikon, Japan).

Figure 4.2 shows typical fluorescence microscopy images of the PDLLA based substrates and control film after a 4 hours culture. The cell nuclei (light blue dots) were stained with DAPI. The numbers of cells on the scaffold and film in the selected images were analyzed by a computer programme (*Image J*) and are shown in Figure 4.2. The MG63 cells attached to all the samples can be observed. Although good cell attachments were found on all the samples, more cells adhered to the 1:9 PDLLA scaffolds when compared to the 1:7 samples and the control films. This suggests that the higher porosity of the scaffold, the larger the space and surface area for cell migration and proliferation. For the PEG/Dex coated scaffold, the number of MG63 cells attached was the lowest. This is mainly due to the PEG coating having the ability of rejecting protein adsorption (Kingshott & Griesser 1999). Cell adhesion is highly dependent on the adsorption of adhesion proteins on the surface of the scaffolds that are recognized by the integrin receptors on the cells (Horbett 2004). Therefore, cell adhesion was disturbed by the less amount of protein adsorbed on the scaffold surface. This can be improved by incorporation or adsorption of RGD or fibronectin to the PEG/Dex coating (Jeschke et al. 2002).

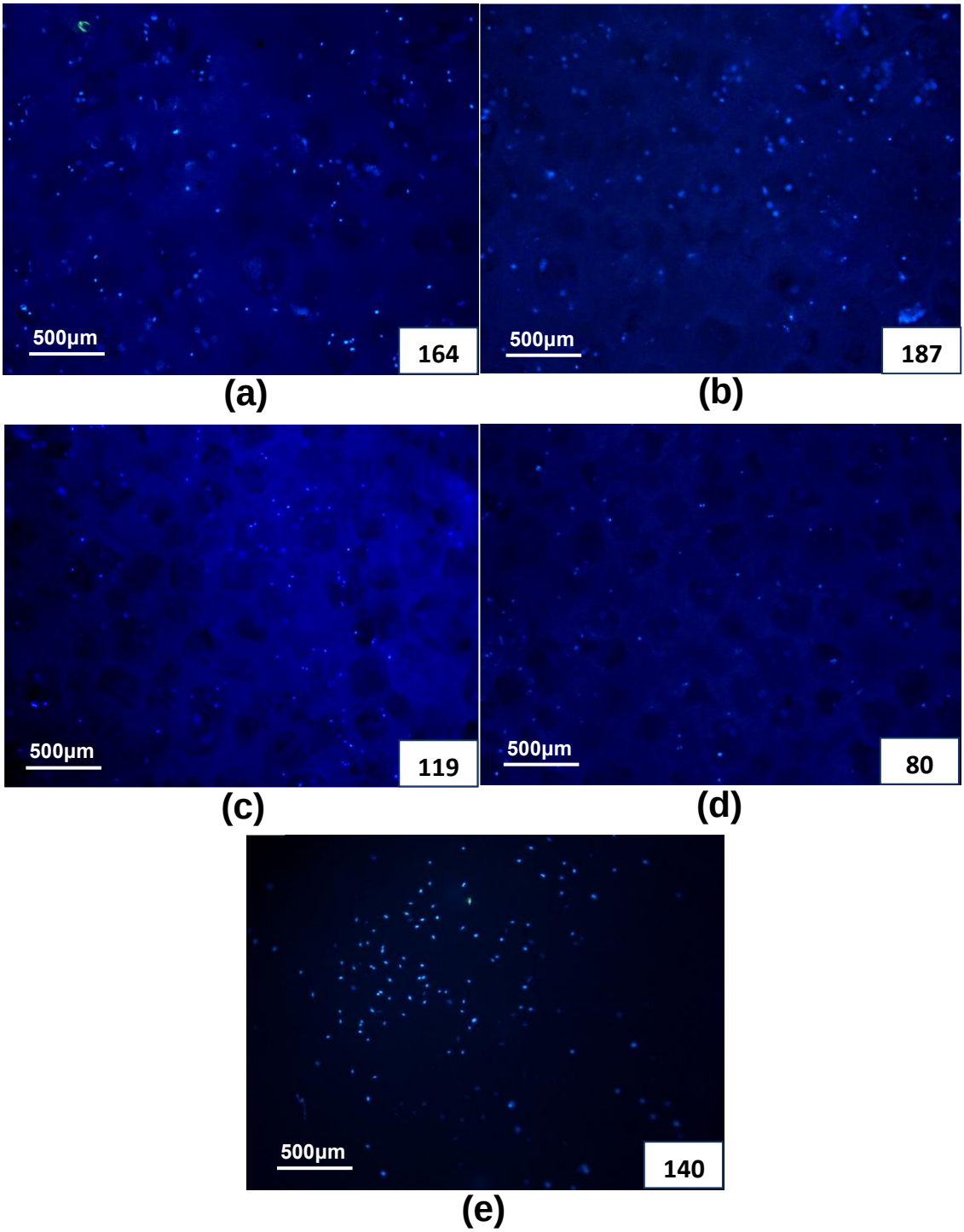

Figure 4.2 Fluorescence images of MG63 cells attached on the (a) 1:7 PDLLA scaffold, (b) 1:9 PDLLA scaffold, (c) 1:9 PDLLA/nano-HAp scaffold, (d) PEG/Dex coated PDLLA/nano-HAp scaffold and PDLLA control film after 4 hours culture. Cell nuclei were stained with DAPI. The cell numbers counted from the images by *Image J* are shown in the pictures accordingly.

4.3.2 MTT Test for Cell Proliferation

The proliferation of the cells was assessed quantitatively using the 3-(4,5-dimethylthiazol-2-yl)-2,5-diphenyltetrazolium bromide (MTT, Sigma) assay. The MTT assay relies on the ability of the viable cells to turn a yellow dye into a water-insoluble purple formazan product. The formazan product can be dissolved in dimethyl sulfoxide (DMSO) solution. The absorbance value of the DMSO solution in terms of optical density (OD) is proportional to the cell number on the substrate. The cell number was 2×10^4 for each sample. 5mg/ml of MTT in PBS solution was prepared and diluted by DMEM solution without FBS (1:10 v/v). For each time interval (1, 3 and 7 days), the cell seeded samples were washed by PBS twice. 1 ml of MTT DMEM solution was added to each culture well and incubated at 37 °C and 5% CO_2 for 4 hours. The supernatant of each well was then removed and 1ml of DMSO (Damao Chemical Reagents Co. Ltd., China) was added to dissolve the formazon. The absorbance value of the DMSO solution was measured at a wavelength of 570 nm with a microplate reader (Infinite F200, TECAN). Three samples of each kind were tested for each incubation period, and each test was performed three times. Background absorbance was obtained by incubation of the MTT substrate on the sample without cell seeded and subtracted from the results.

The results of MTT testing are shown in Figure 4.3. It is seen that the cell number on all the substrates and control film increased with culture time, suggesting good biocompatibility of PDLLA scaffolds fabricated in this study. Moreover, all the samples showed a higher cell activity than the control film. This is because the scaffolds can provide greater surface area for cell attachment and growth. More cells on the 1:9

scaffolds with higher porosity than the 1:7 ones after 7 days incubation. MTT results show that cells on the 1:9 PDLLA scaffold had fastest proliferation rate compared with cells on other scaffolds. This is because of the initial high number of cells attached to the scaffold which facilitated cell-cell communications to promote cell proliferation.

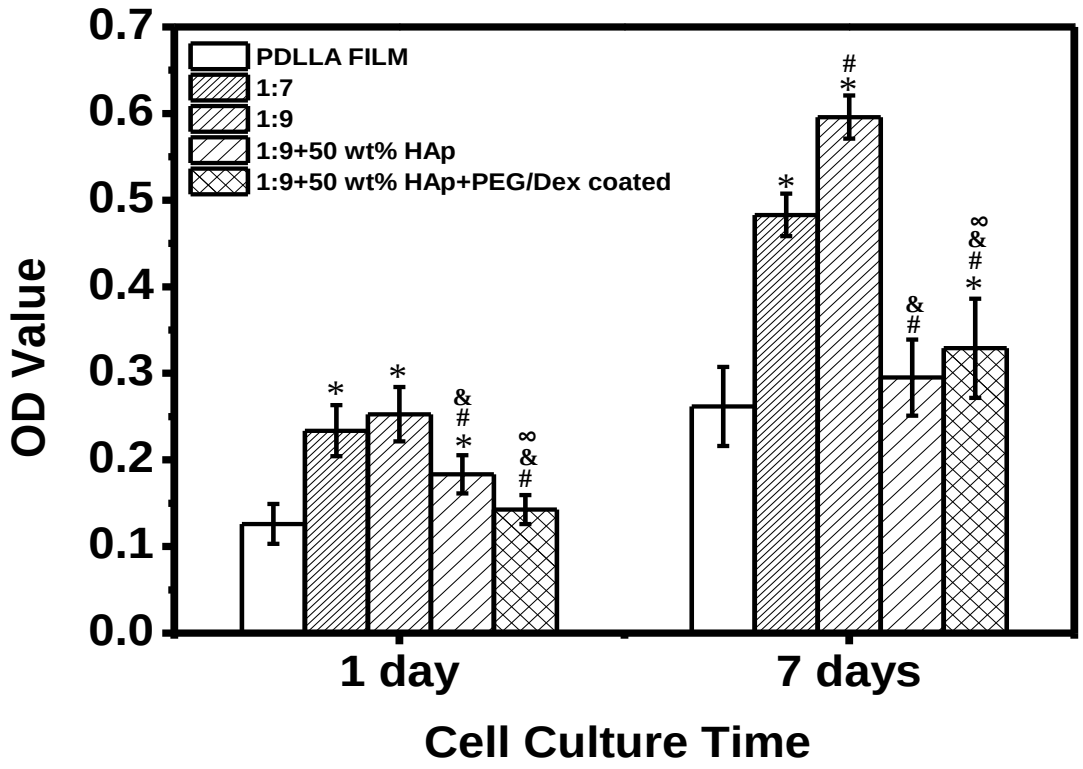

Figure 4.3 MTT assay on the PDLLA based scaffolds with same MG63 cell seeding density after 1 and 7 days culture. Results are mean ± SD. *, #, & and ∞ indicate the existence of statistically significant differences as compared with the results of unfilled PDLLA film, 1:7 PDLLA scaffold, 1:9 PDLLA scaffold, and 1:9 PDLLA scaffold with 50 wt.% of nano-HAp filled, respectively (n=3, p<0.05).

In addition, nano-HAp incorporation and the PEG/Dex coating played important roles in the cell proliferation. It should be noticed that the OD values of the PDLLA scaffolds

with 50 wt% of nano-HAp fill decreased when compared with the unfilled ones. One reason may be the lower number of initial cell adhering on the nanocomposites compared to the unfilled ones, leading to a lower cell proliferation rate (Causa et al. 2005). Another reason may be the excessive nano-HAp incorporation in the composites, causing a faster degradation and destruction of the composite which appears to damage the attached and proliferated cells (Lee et al. 2008). The cell activity of scaffolds with PEG/Dex coating was lower than the uncoated one after a 1 day culture, but increased after 7 days of culture. However, compared with the control, their OD values were higher, which indicated that the PEG/Dex coated PDLLA/nano-HAp scaffolds provided a biomimetic environment for cell attachment and growth.

4.3.3 Alkaline Phosphatase Assay

Alkaline phosphatase activity (ALP) is an important early osteogenic differentiation marker of osteoblasts (Robey 1989). The osteoblastic phenotype expression was measured by the ALP activity term. The specific activity of ALP was assayed in the cells as the release of *p*-nitophenol from *p*-nitophenolphosphate, indicating the osteoblast differentiation. The number of seeded cell was 2×10^4 for each sample. At the specified time scales (7 and 14 days), the cells attached to the PDLLA based samples were rinsed three times with PBS and lysed with 1% triton X-100 (Sigma, Inc., USA) for 15 minutes. The cell lysate was analyzed for alkaline phosphatase content using an alkaline phosphatase assay kit (Abcam®, UK). The amount of *p*-nitophenol released was determined by quantifying the optical density at 405 nm in a microplate reader (Infinite F200, TECAN).

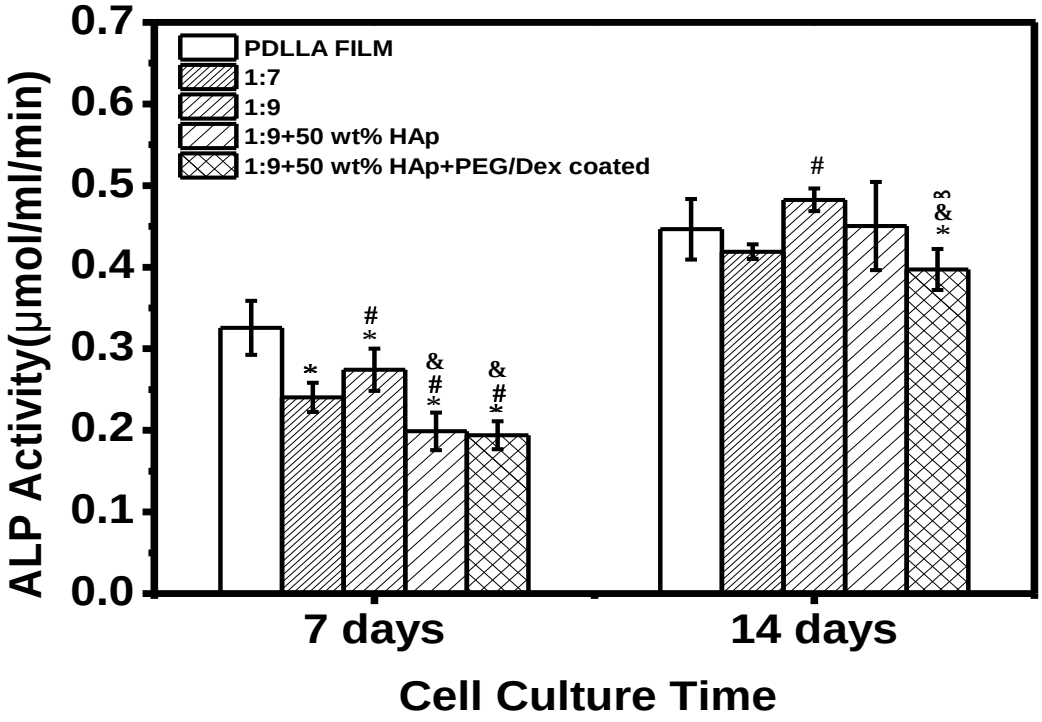

Figure 4.4 ALP activities of the MG63 cells on the PDLLA based scaffolds and control after 7 and 14 days culture. Results are mean ± SD. *, #, & and ∞ indicate the existence of statistically significant differences as compared with the results of unfilled PDLLA film, 1:7 PDLLA scaffold, 1:9 PDLLA scaffold, and 1:9 PDLLA scaffold with 50 wt.% of nano-HAp filled, respectively (n=3, p<0.05).

The results of the ALP activity assay are shown in Figure 4.4. The ALP activity of the MG63 cells cultured on the scaffolds and control film increased with culture time. At 7-day and 14-day culture times, the cells on the scaffold with higher porosity value, showing a higher ALP activity, could be found, as seen in Figure 4.4. The release of ALP from MG63 cells on the nano-HAp filled and PEG/Dex coated composite scaffolds are lower than those of the unfilled scaffolds, as ALP is secreted by osteoblasts only when proliferation has stopped and the mineralization step is abount to start. Nano-HAp filled and PEG/Dex coated composite scaffolds showed slower cell

proliferation rates as suggested by the MTT test. Therefore, cells on unfilled PDLLA reached confluence earlier than on the nano-HAp filled and PEG/Dex coated composite scaffolds which were kept their differentiated state. So the metabolic activity of the cells may reach a higher level with a longer culture time (Causa et al. 2005). No significant difference between the nano-HAp filled and PEG/Dex coated scaffolds could be found after 7 days of culture. The ALP activities of the cells on porous scaffolds were lower than those of the control film at 7 days. However, they had a faster rate of increase than the cells on the control film during the following 7 days of culture. In fact, the sustained release of ALP over time, even with low values, indicated the maintenance of osteoblastic phenotype for human osteoblast attached to the composites.

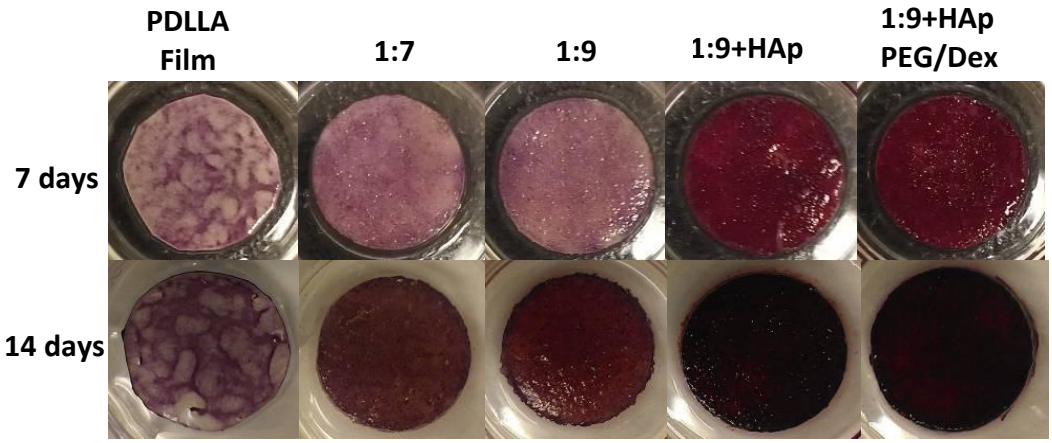

Figure 4.5 Alizarin Red staining of PDLLA based scaffolds and control film after 7 days and 14 days culture. With increasing culture time, all the samples exhibited darker red color.

4.3.4 Mineralization of MG63

Visualization of the mineralization of MG63 cells on the PDLLA based scaffolds was measured by Alizarin Red staining (ARS, Damao Chemical Reagents Co. Ltd., China).

The cell seeding density was 2×10^4/sample. After 7, and 14 days cell culture on the scaffolds, the cells on the scaffolds were rinsed with d-H_2O and then fixed for 1 hour using 70% ethanol at 4 °C. Ethanol was removed and cell/scaffold constructs were washed with d-H_2O and stained with ARS (40mM) for 20 min at room temperature. After rinsing 5 times with d-H_2O to remove any residual stain, the stain was desorbed with 10% cetylpyridinium (CPC, Aladdin Industrial Coporation, China) for 1 hour. CPC was collected and analyzed for optical density using a microplate reader at 540 nm.

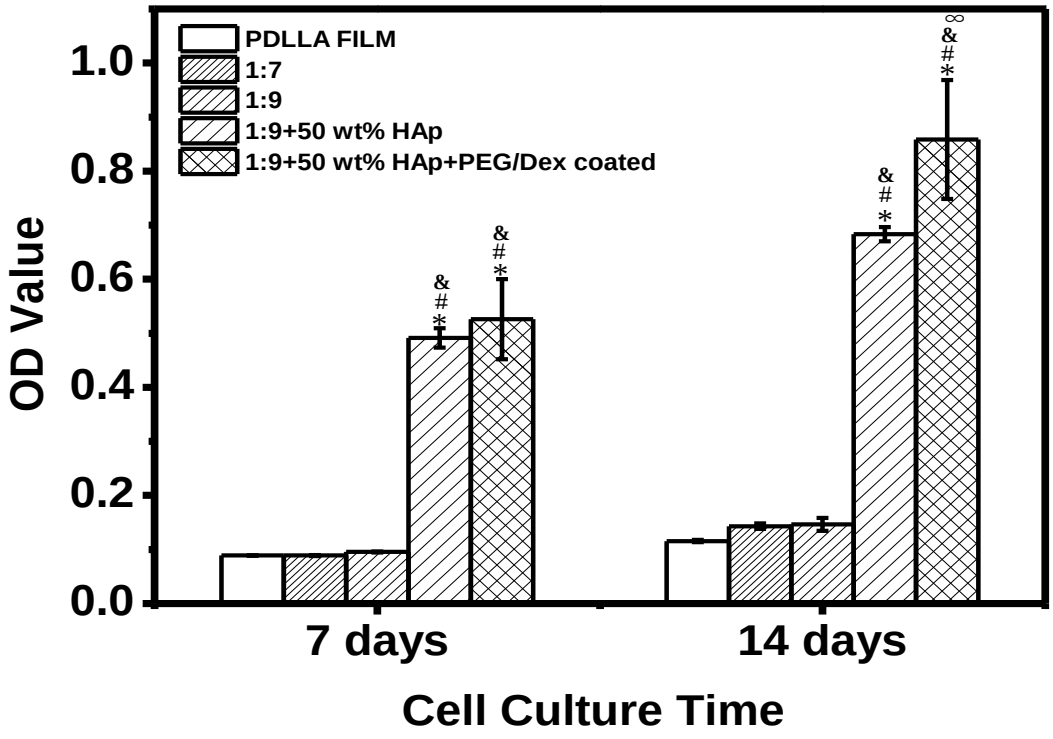

Figure 4.6 Alizarin Red staining for mineralization in the MG63 cells on the PDLLA based scaffolds and control after 7 and 14 days culture. Results are mean ± SD. *, #, & and ∞ indicate the existence of statistically significant differences as compared with the results of unfilled PDLLA film, 1:7 PDLLA scaffold, 1:9 PDLLA scaffold, and 1:9 PDLLA scaffold with 50 wt.% of nano-HAp filled, respectively (n=3, p<0.05).

The images of the ARS stained PDLLA scaffolds and control films after 7 and 14 days of culture are shown in Figure 4.5. The calcium salts could be stained into red by ARS for detection of the mineralization of the cell. From Figure 4.5, scaffolds with nano-HAp showed darker color compared to the unfilled ones and control film at the two different time points. This is an indication of larger calcium deposition amounts on the HAp filled composite. Moreover, the ARS staining proved the increasing mineralization of the MG63 cells with the culture time (darker color). These results could be further confirmed by the OD value of the cetylpyridinium solution which desorbed the ARS from the samples (Figure 4.6). Nano-HAp filled scaffolds showed higher OD value than the unfilled ones and the film and the OD value of all the scaffolds increased with time. Additionally, the highest degree of mineralization was achieved by the MG63 cells on PEG/Dex coated PDLLA/nano-HAp scaffold after 14 days. This suggested that PEG/Dex coating and nano-HAp incorporation could promote bone formation, which is of great importance for a scaffold in bone tissue applications.

4.3.5 Cell Morphology

Scanning electron microscopy (SEM) was used for cell morphology observation on the scaffolds. The cell seeding density was 10^4/well for the SEM. the culture medium after the samples had been cultured for a predetermined period (4 hours, 3 and 7 days) was removed and discarded. The samples were washed with PBS three times and the cells adhering to the samples were then fixed with 2.5% glutaraldehyde in PBS for 24 hours at 4 °C. After thorough washing with PBS, the cells on the samples were dehydrated sequentially in an ethanol graded series (30%, 50%, 70%, 80%, 90%, and 100%) for 15

min each, 100% twice and allowed to dry in a clean fume hood at room temperature for 4 hours. The cell-attached samples were sputter-coated with gold and examined by a scanning electron microscope (SEM, JEOL JSM-6490).

Fluorescence staining was also conducted for cell morphology observation and growth evaluation. A number of cells about 10^4 were seeded on the scaffolds before staining. After periods of 4 hours, 3, and 7 days culture, the cells were gentle washed with PBS three times and fixed in 4% formaldehyde/PBS for 30 min then permeabilized with 0.1% Triton X-100 in PBS for 5 min at room temperature. The scaffold with cells was incubated with 500μm of 10 μg/ml TRICT-phalloidin (Sigma) in a dark room for 30 min. After rinsing, 500 μm of 1μg/ml DAPI (Sigma) in PBS was added to each well. The cytoskeleton (phalloidin, red) and the nuclei (DAPI, blue) of the cells were observed with a fluorescence microscope (Eclipse 80i, Nikon, Japan).

The cell morphologies always change after the cells contact the ECM, in order to stabilize the cell-ECM interface. The SEM and the fluorescence images of the MG63 cells on the unfilled PDLLA film and the PDLLA based scaffolds after 4 hours, 3 days and 7 days culture are shown in Figures 4.7-4.11. It can be observed that the cells were well attached on all the PDLLA based scaffolds and control film after 4 hours of culture, with spherical shape, as seen in the SEM images [Figures 4.7 (a), 4.8 (a), 4.9 (a), 4.10 (a) and 4.11 (a)]. Their filopodia began to extend which is a sign of cell spreading and migration. Most of the cells after a 3 days culture were spread out, progressively flattened and the neighbor cells began to connect with each other by cytoplastic webbing. Moreover, the cells could even grow into the pores of the scaffolds. Figure

4.10 (c) shows a bridge crossing a pore formed by an MG63 cell on a 50 wt% nano-HAp filled PDLLA scaffold (PDLLA/NaCl=1:9) after a 3 day culture. After 7 days of culture, all the samples were covered by the satisfactorily spreading cells [Figures 4.7 (e, f), 4.8 (f), 4.9 (f), 4.10 (f), 4.11 (f)]. One pore of the scaffold covered by the cell after 7 days of culture is shown in Figure 4.10 (e). The increase of cell number with increasing culture time is clearly observed in Figures 4.7 to 4.11. The cells cultured on different kinds of scaffolds showed similar behavior using SEM and fluorescence observation. No deleterious or cytotoxic responses were observed from all the images. These suggest that the PDLLA based scaffolds fabricated by the proposed method are good substrates for osteoblast-like cell attachment, growth and proliferation. The MG63 cell division was also determined as shown in Figure 4.7 (g) after 3 days of culture.

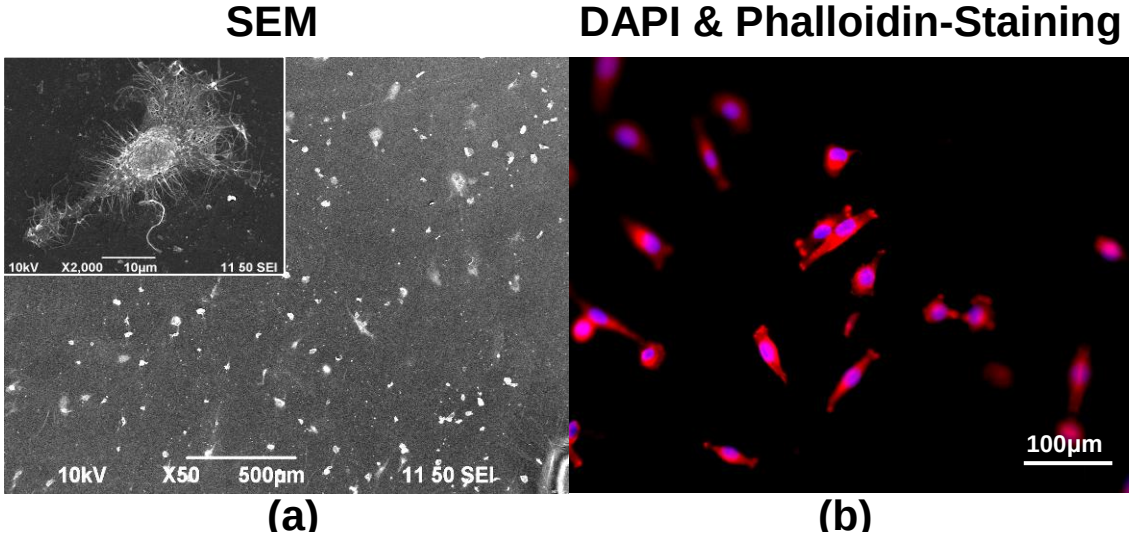

Figure 4.7 SEM (a,c,e,g) and fluorescence (b,d,f,h) micrographs of MG63 cells after (a,b) 4 hours, (c,d) 3 days, (e,f) 7 days culture on the unfilled PDLLA film at low and high magnification (insert), (g) MG63 cells division and (h) cytoplastic webbing of MG63 cells.

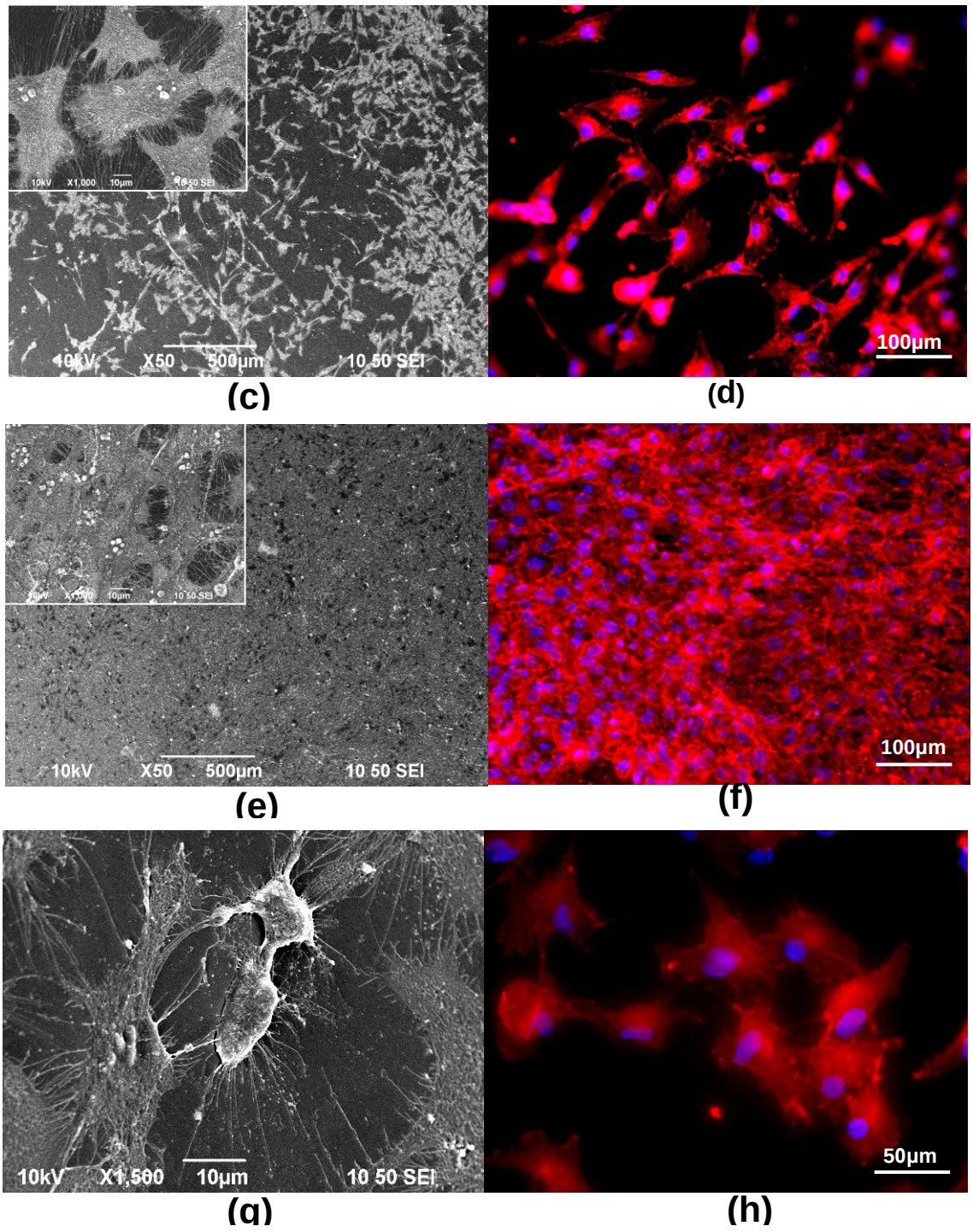

Figure 4.7 (Continued) SEM (a,c,e,g) and fluorescence (b,d,f,h) micrographs of MG63 cells after (a,b) 4 hours, (c,d) 3 days, (e,f) 7 days culture on the unfilled PDLLA film at low and high magnification (insert), (g) MG63 cells division and (h) cytoplastic webbing of MG63 cells.

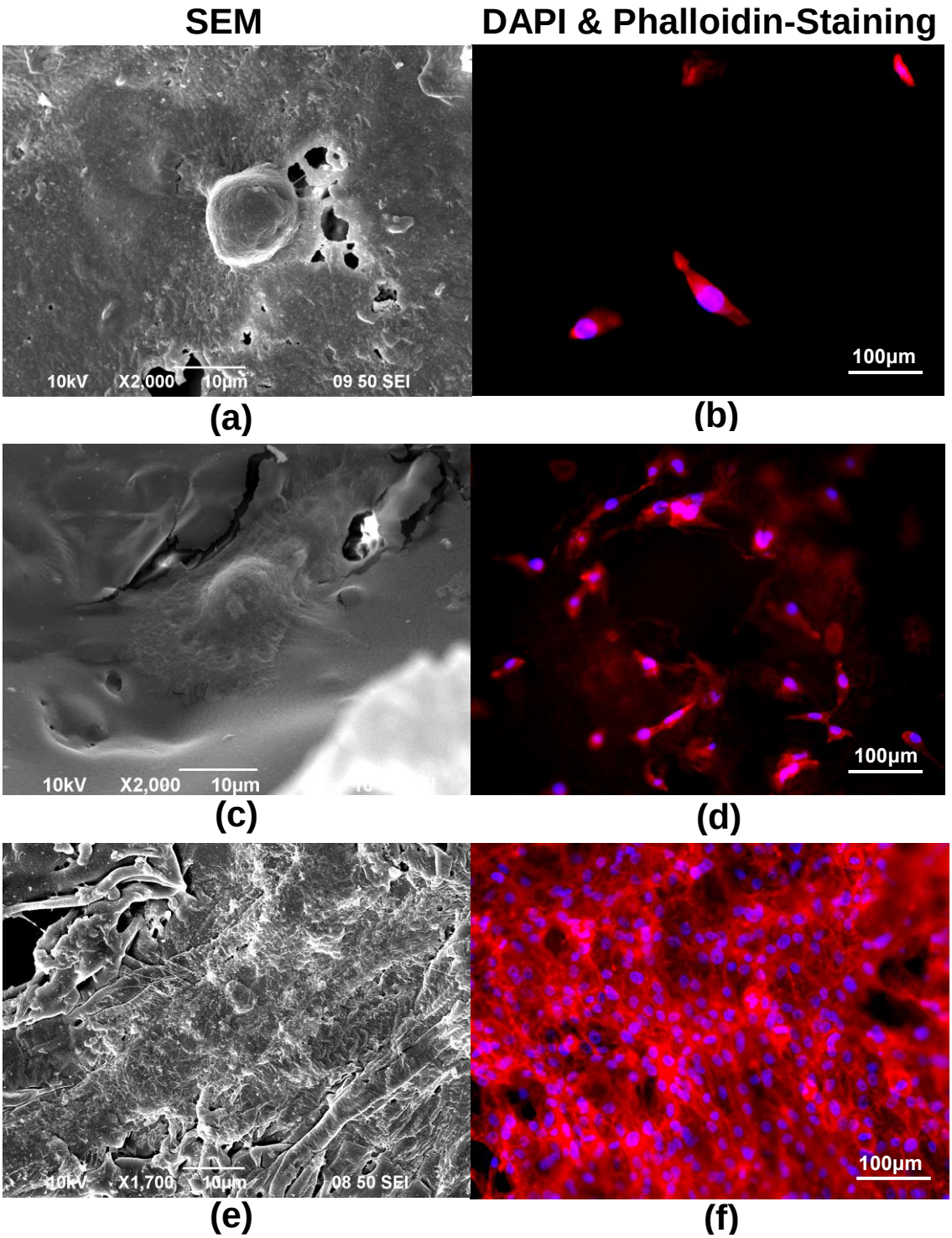

Figure 4.8 SEM (a,c,e) and fluorescence (b,d,f) images of MG63 cells after 4 hours (a,b), 3 days (c,d), and 7 days (e,f) culture on the unfilled PDLLA with polymer/porogen ratio of 1:7.

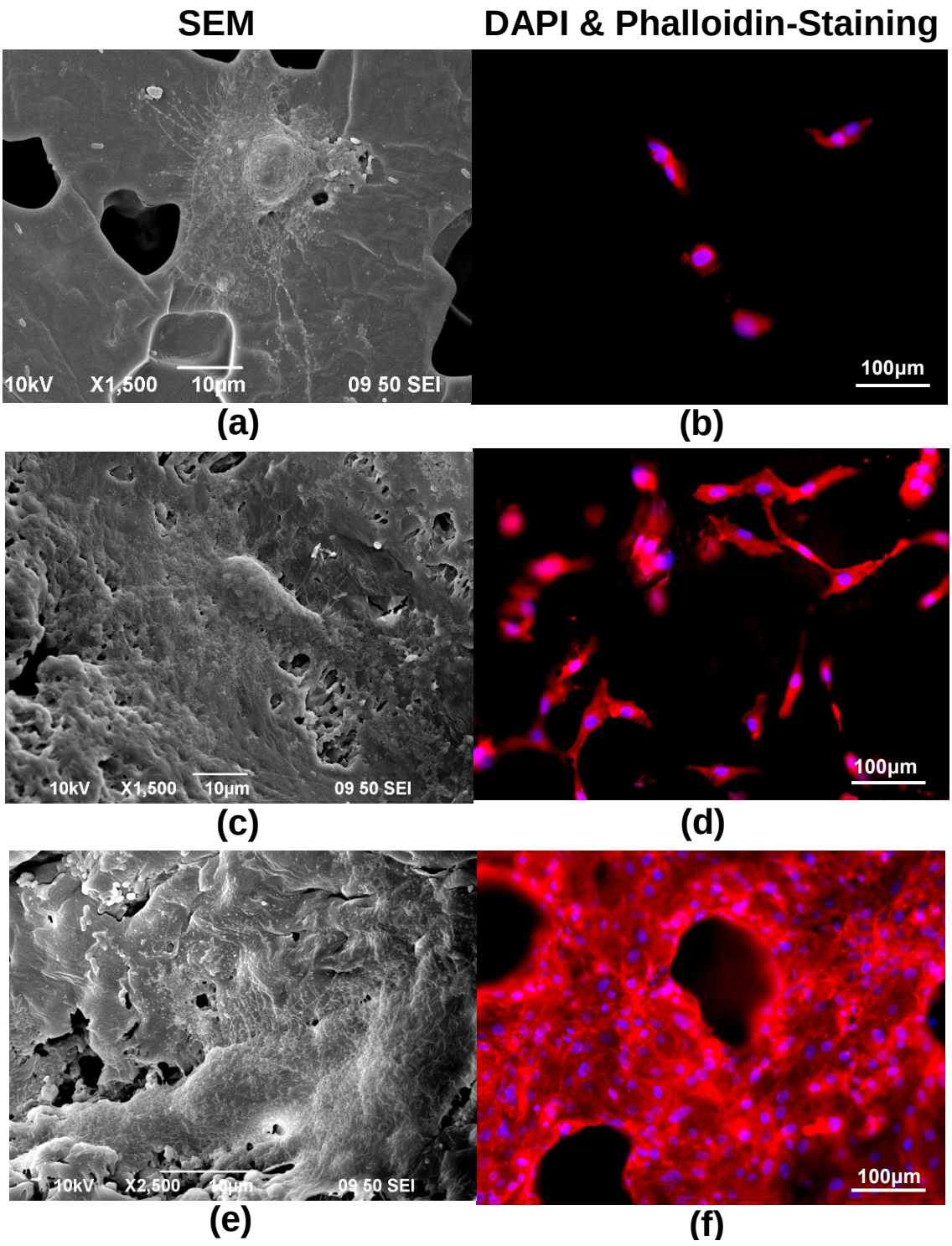

Figure 4.9 SEM (a,c,e) and fluorescence (b,d,f) images of MG63 cells after 4 hours (a,b), 3 days (c,d), and 7 days (e,f) culture on the unfilled PDLLA with polymer/porogen ratio of 1:9.

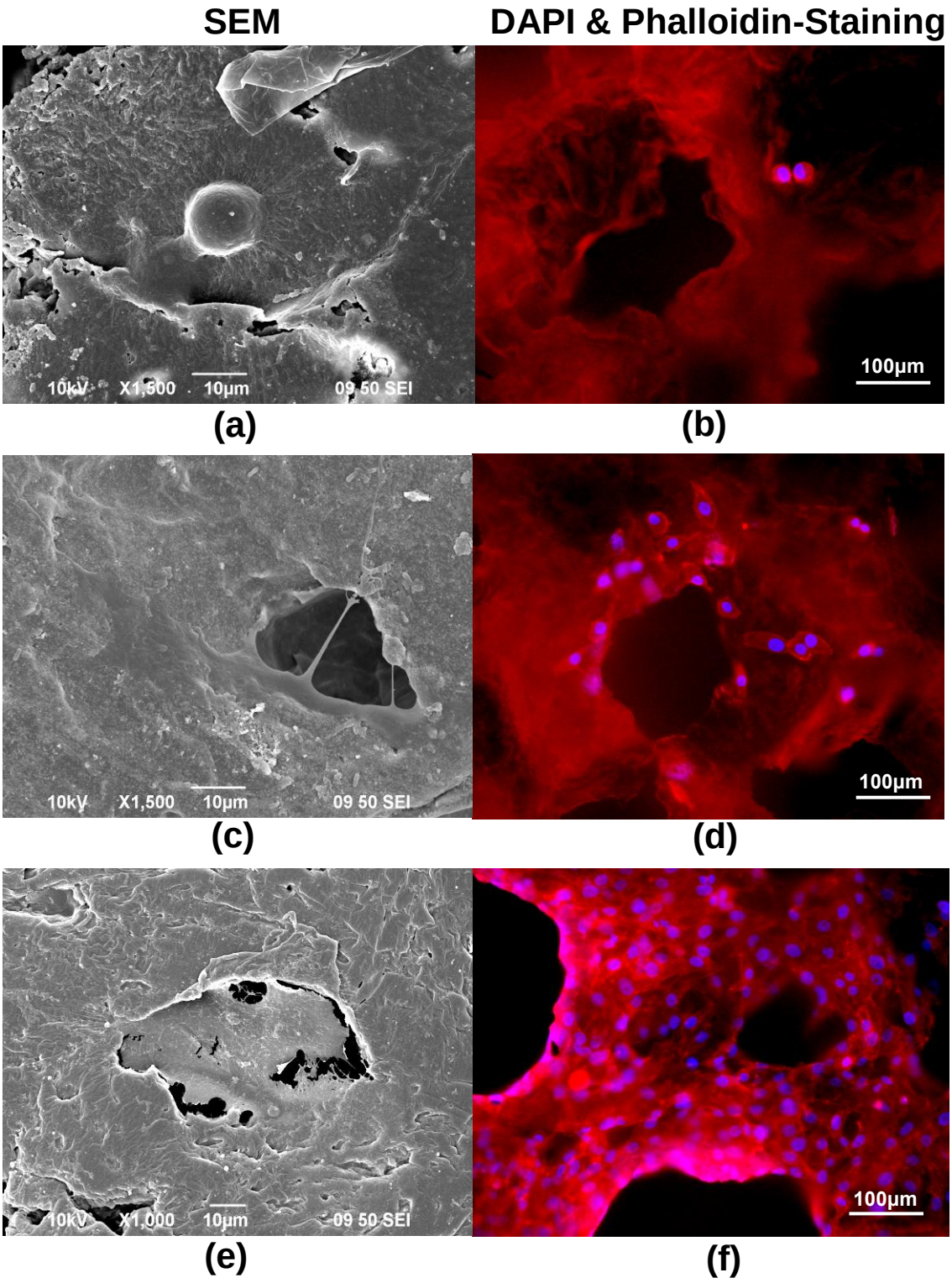

Figure 4.10 SEM (a,c,e) and fluorescence (b,d,f) images of MG63 cells after 4 hours (a,b), 3 days (c,d), and 7 days (e,f) culture on the PDLLA/50 wt% nano-HAp composite with polymer/porogen ratio of 1:9.

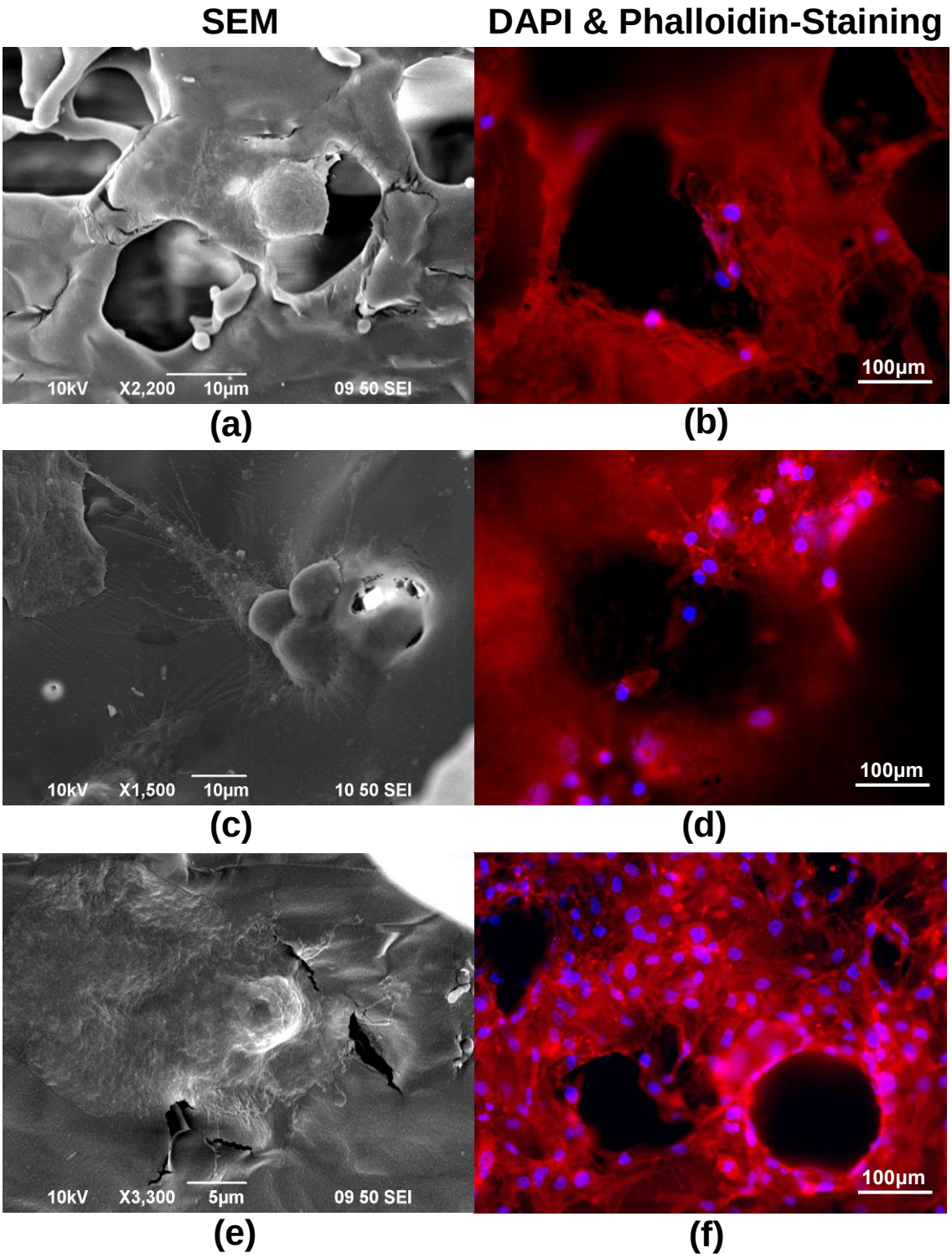

Figure 4.11 SEM (a,c,e) and fluorescence (b,d,f) images of MG63 cells after 4 hours (a,b), 3 days (c,d), and 7 days (e,f) culture on the PDLLA/50 wt% nano-HAp composite with polymer/porogen ratio of 1:9 and PEG/Dex coating.

4.4 Summary

In this part of the study, human osteoblast-like cells, MG63, cultured on the PDLLA based composites shows that the cell adhesion, proliferation and differentiation were highly influenced by the chemical composition and microstructure including porosity and pore size of the scaffolds. The SEM and fluorescence images show that the pore size of the fabricated scaffolds ranged from 200 to 350 μm, and high porosity of 60% to 80% allow not only the fluid passage through the scaffolds structure, but also the cells hosting and penetrating inside the scaffolds. The whole scaffolds covered by the MG63 cells were observed from the fluorescence images after 7 days culture. The cell morphology changed from spherical shape to a well spread-out flat shape with time, and no deleterious or cytotoxic responses were observed. MTT results showed that the higher the porosity of the scaffold, the more cell adhesion and the faster proliferation rate of cells on the scaffold. The results from the ARS and ALP assay prove that the scaffold with higher porosity and the addition of nano-HAp facilitated osteogenic differentiation of the osteoblast progenitor MG63 cells. All these confirm that the PDLLA based scaffolds fabricated in this study are biocompatible, osteoconductive and facilitate cell attachment and proliferation. After confirming the biocompatibility of the PDG/Dex coated PDLLA/nano-HAp composites, the other important properties of a bone scaffolds, such as, bioactivity, degradability, and drug release capacity are discussed in the following chapter.

Chapter 5. *In Vitro* Bioactivity, Degradation and Drug Release Capacity of PDLLA/nano-HAp Composites

5.1 Introduction

Degradation behavior of composite bone scaffolds is of crucial importance in tissue engineering, because the degradation rate is essentially linked to cell growth, host response and tissue regeneration (Babensee et al. 1998). The scaffolds should have a controllable degradation rate that matches the regeneration rate of new bone tissue. The degradation kinetics of composite scaffolds can be affected by their composition, microstructure, chemical and physical properties, and molecular weight, as well as the environmental conditions (Wu & Ding 2004, Söntjens et al. 2012). Therefore, controlling and evaluating the degradation behavior of composite scaffolds are of great importance for the success of a biodegradable scaffold for bone tissue engineering. In previous chapters, a novel PC-DC technique was developed for fabrication of PEG/Dex coated PDLLA/nano-HAp composites, with independently controllable pore size and porosity. The improved wettability, compressive moduli and strengths of the PDLLA/nano-HAp composites, without incubation in simulated body fluids (SBF), were well confirmed. The degradability of the PDLLA/nano-HAp composite was investigated by measuring their mass and molecular weight changes during incubation in a SBF in this part of study. An interesting phenomenon in which that nano-HAp has a great effect of increasing the degradation rate of the composites in the first 7 days incubation, but little effect for the following 21 days was found. Therefore, nano-HAp could be used to control the degradation rate of composites to enable the applications in bone tissue engineering.

The formation of a biomimetic apatite layer on the surface of a bone scaffold after being implanted in the body is the critical requirement for bonding to living bone. It was reported by Oyane (2003) that apatite formation in a SBF could be reproduced when the artificial biomaterial was implanted in a living body. Therefore, the SBF can be applied to estimate *in vitro* bioactivity of the artificial biomaterial by the apatite deposition on the implant. The bonelike apatite coated on artificial biomaterials has been confirmed with an improvement in the biological properties of these materials (Song et al. 2004). Since the deposition of bonelike apatite on an implant material surface has been confirmed as beneficial for cell adhesion and proliferation, a large amount of research studies have focused on the mechanism and time requirement for apatite formation in the SBF, as well as modification to the formulation or pH value of the SBF for accelerating apatite formation (Chou et al. 2004, Chen et al. 2005). The question of how the SBF incubation (e.g. incubation time and apatite formation) affects the mechanical properties and the degradability of the bioactive scaffold may be raised. So far, very limited studies have been reported on the changes of the mechanical properties of biodegradable porous PDLLA/nano-HAp composites during incubation in a SBF. In this chapter, *in vitro* evaluation of the bioactivity, degradability, and change of mechanical properties of porous Dex-releasing PDLLA based scaffold materials, with different amounts of nano-HAp, was undertaken. The bioactivity of the samples was validated from the biomimetic apatite formation on the surface of the samples after incubation in a SBF. The relationship between the SBF immersion time and the compressive modulus and strength of the PDLLA/nano-HAp composites was monitored in detail. An improvement in bioactivity (apatite formation ability) through the addition

of the nano-HAp content in the composites was found. Nano-HAp incorporation and apatite formation made a positive impact on the mechanical properties of the composites; however, plasticization and degradation of PDLLA had a negative impact. Moreover, the PDLLA/nano-HAp composite with pH-compensation effect of reducing the risk of chronic inflammation complications was confirmed.

Drug delivery technology, utilizing biodegradable materials as the drug vehicle to deliver biologically active molecules at a desired behavior, is attracting increasing interest in recent years for improving human live (Langer 1998). Such delivery systems can improve the effectiveness of the drug therapy and to reduce toxicity. The PEG/Dex coated PDLLA/nano-HAp composites fabricated in this study were equipped with a drug release function. In this part of study, an *in vitro* drug release study was carried out to investigate the drug release behavior. The influences of porosity and nano-HAp fraction on the Dex release behavior of the PDLLA based scaffold materials were also investigated. Some results from this part of study have been published in the *Journal of the Mechanical Behavior of Biomedical Materials* (Chen et al. 2013).

5.2 Preparation of SBF

The SBF was prepared by dissolving reagent grade sodium chloride (NaCl), sodium hydrogen carbonate ($NaHCO_3$), potassium chloride (KCl), di-potassium hydrogen phosphate trihydrate ($K_2HPO_4\ 3H_2O$), magnesium chloride hexahydrate ($MgCl{\cdot}6H_2O$), calcium chloride ($CaCl_2$), sodium sulfate (Na_2SO_4), and tris-hydroxymethyl aminomethane (Tris, $(CH_2OH)_3CNH_2$) into deionized water (Kokubo & Takadama 2006). To prepare 1000 ml of SBF, a beaker with 700 ml of deionized water was heated

to 36.5±1.5 °C in a water bath. All the reagents were dissolved in the sequence given in Table 5.1, making sure to initiate dissolution of one reagent after the previous one was completely dissolved, and that the solution was clear without precipitation generated during the preparation process. The pH value of the solution was adjusted with 1 M hydrochloric acid (HCl) to pH 7.40 at 36.5 °C. After the temperature of the solution cooled down to room temperature, the deionized water was added up to the marked line (1000 ml). The prepared SBF was kept at 5-10 °C. Finally, the ion concentration in SBF prepared by this method closely resembled with that of human blood plasma, as listed in Table 5.2.

Table 5.1 Order, amounts and purities of the reagents used in preparation of 1000 ml of SBF

Order	Reagent	Amount	Purity (%)
1	NaCl	8.035 g	99.5
2	$NaHCO_3$	0.355 g	99.5
3	KCl	0.225 g	99.5
4	K_2HPO_4 $3H_2O$	0.231 g	99.0
5	$MgCl{\cdot}6H_2O$	0.311 g	98
6	1.0 M HCl	39 ml	–
7	$CaCl_2$	0.292 g	95
8	Na_2SO_4	0.072 g	99.0
9	Tris	6.118 g	99.0
10	1.0 M HCl	0-5 ml	–

Table 5.2 Ion concentration of SBF in comparison with human blood plasma

Ion	Ion concentration (mmol/l)	
	SBF solution	**Human blood plasma**
Na^+	142.0	142.0
K^+	5.0	5.0
Mg^{2+}	1.5	1.5
Ca^{2+}	2.5	2.5
Cl^-	147.8	103.0
HCO_3^-	4.2	24.0
HPO_4^{2-}	1.0	1.0
SO_4^{2-}	0.2	0.5

5.3 Sample Preparation and Incubation Process

The PEG/Dex coated porous PDLLA scaffolds filled with different amounts of nano-HAp (0, 20, 40 and 60 wt%) were fabricated using the PC-DC technique described in Chapter 3 (Chen et al., 2011). The PDLLA/nano-HAp composites with a porosity of around 80% were produced by controlling the weight ratio of PDLLA and NaCl to 1:8. The PDLLA was firstly dissolved in chloroform, and nano-HAp and sieved NaCl particles (150-300 μm) were subsequently dispersed in the PDLLA/chloroform solution by a homogenizer. PDLLA/NaCl/nano-HAp gel paste was precipitated by dripping ethanol into the solution. This gel paste was then compression molded into a specimen with dimensions of 10 mm in diameter and 5 mm in height using a powder compressing machine (Model 769YP-15A) under 10 MPa at room temperature. After salt leaching and drying of the molded composites, porous PDLLA/nano-HAp composites were prepared. Finally, PEG/Dex coated porous composites were fabricated by immersing the pre-prepared PDLLA/nano-HAp porous composites in a hydrophilic PEG/Dex (20/0.8, w/w) solution (10 ml) under vacuum for 24 hours.

The unfilled PDLLA and the composites with different amounts of nano-HAp were immersed separately in a clean 50 ml plastic centrifugal tube with the SBF. Lids were placed on the tubes to form an airtight seal for preventing contamination. To ensure the sample was fully immersed in the SBF, the centrifugal tube with SBF and sample was placed in a water bath at 37 °C, as shown in Figure 5.1. The scaffolds were soaked in the SBF at 37 °C without vibration for 7 days, 14 days, and 28 days. The mediums were refreshed every 7 days. After the various soaking periods, the samples were then taken out from the flasks, washed gently with deionized water and then vacuum dried overnight at 40 °C.

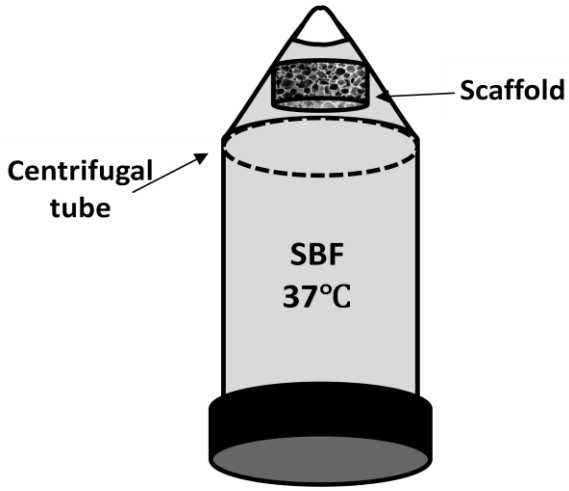

Figure 5.1 Schematic diagram of the scaffold fully immersed in the SBF

One-way analysis of the variance (ANOVA) was performed for every assay and the results were expressed as mean ± standard deviation. A Fisher's least significant difference (LSD) test was used for comparison between the sample means, and to determine the statistical significance of the data for $p<0.05$.

5.4 *In Vitro* Bioactivity: Apatite Formation

5.4.1 Morphology Observation

The microstructure changes and the morphology of the deposited biomimetic apatite layer on the PDLLA/nano-HAp composite surfaces after incubation in the SBF were characterized using scanning electron microscopy (SEM, JEOL JSM-6490). The samples were coated with gold to improve their conductivity.

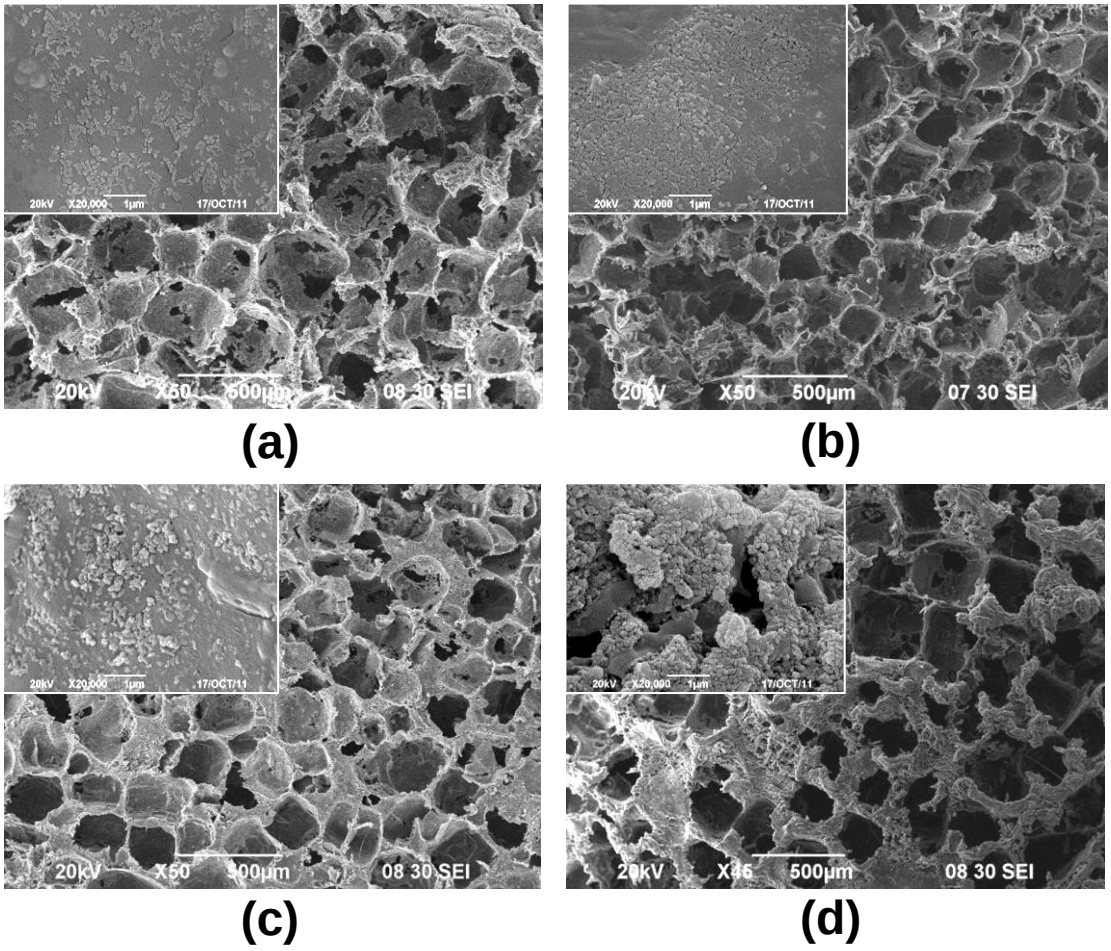

Figure 5.2 SEM micrographs of the porous scaffolds after (a, b, c, d) 7 days and (e, f, g, h) 28 days incubation in SBF at low and high magnification (inset): (a, e) unfilled PDLLA, PDLLA filled with (b, f) 20 wt%, (c, g) 40 wt%, (d, h) 60 wt% of nano-HAp.

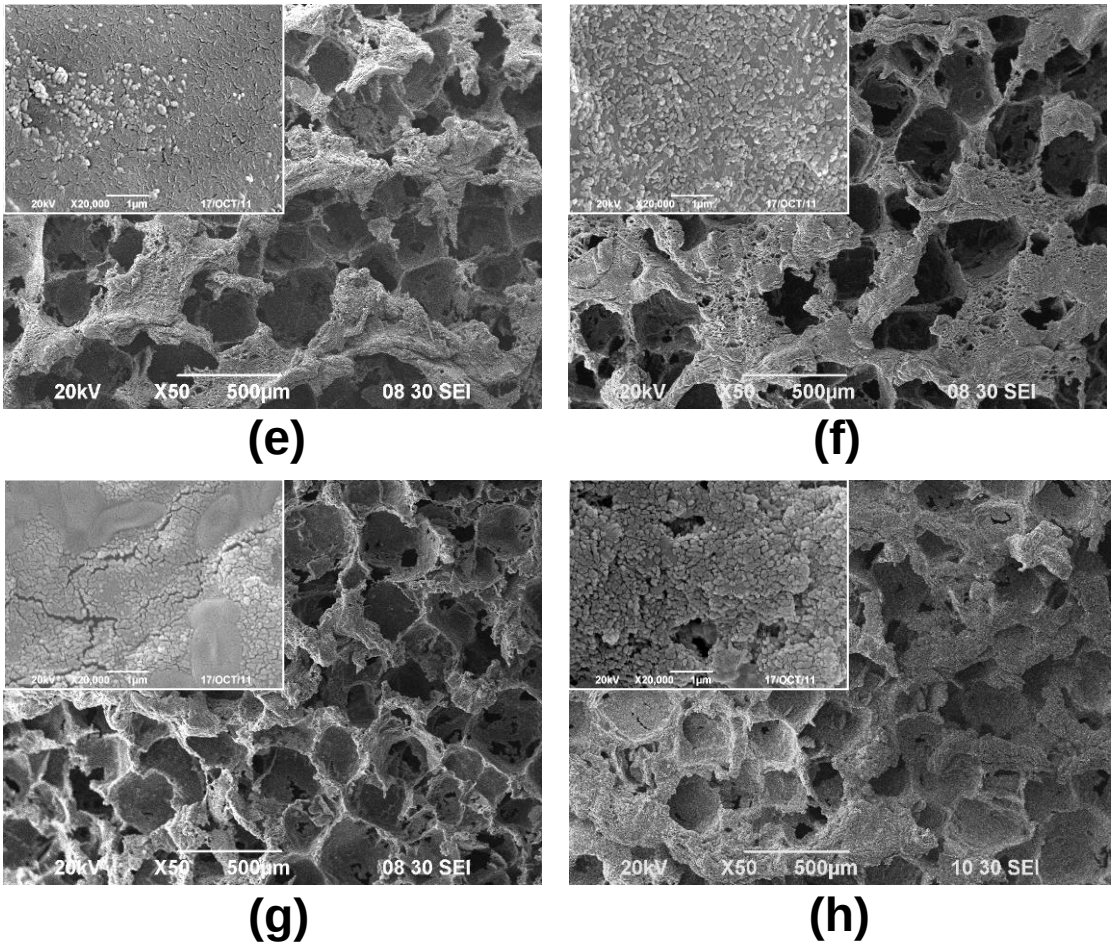

Figure 5.2 (Continued) SEM micrographs of the porous scaffolds after (a, b, c, d) 7 days and (e, f, g, h) 28 days incubation in SBF at low and high magnification (inset): (a, e) unfilled PDLLA, PDLLA filled with (b, f) 20 wt%, (c, g) 40 wt%, (d, h) 60 wt% of nano-HAp.

The microstructure changes of the porous PDLLA composites (filled with 0 wt%, 20 wt%, 40 wt% and 60 wt% of nano-HAp) after incubation in the SBF for 7 and 28 days are shown in Figure 5.2. For the unfilled PDLLA samples after 7-day incubation, as shown in Figure 5.2(a), the pore walls became thinner and the pore sizes clearly increased, as compared with Figure 5.2(a). For the nano-HAp filled samples, Figures 5.2(b, c, d) show a relatively smaller increase in pore sizes compared with the unfilled

ones after 7-day incubation, as shown in Figure 5.2(a). Moreover, from the high-magnification SEM images of the PDLLA composites after a 7-day incubation [Figures 5.2(a, b, c, d)], apparently some apatite crystals were deposited on all types of samples and the amount of the deposited apatite increases with increasing nano-HAp amount in the composites. Moreover, more apatite could be observed on the surface of the PDLLA/nano-HAp composites than the unfilled ones for the same incubation time. After 28-day immersion in the SBF, all the PDLLA based composites showed larger pore sizes and their pore surfaces were covered with a layer of apatite, as shown in Figures 5.2(e, f, g, j). The amount of the apatite deposition increased with the incubation time. A few flake-like apatite particles were formed on the surface of the samples after incubation for 7 days, while more and bigger apatite particles were formed and joined together on the samples after 28-day incubation. The deposited apatite particles almost formed a continuous layer on the PDLLA composite with 40 wt% of nano-HAp as shown in Figure 5.2(g), and some additional particles were deposited on the former apatite layer on the composite filled with 60 wt% of nano-HAp after 28 days of incubation, as shown in Figure 5.2(h). The results suggest that PDLLA composites, containing more nano-HAp, can facilitate the formation of biological apatite. This finding is in agreement with some previous studies where the addition of nano-HAp not only acted as reinforcing filler, but also provided a bioactive property to the composites (Chen et al. 2007, Deng et al. 2008).

5.4.2 Characterizations of the Bioactive Layer Formed on the Composites

The element composition of the bioactive layer formed on the scaffold surface was examined by an energy dispersive X-ray analysis detector (EDX, Oxford, INCA 250 Energy System). EDX can be used to quantify the elements by calculating the area

under the peak of each identified element and after taking account of the accelerating voltage of the beam to produce the spectrum, perform calculations to create sensitivity factors that will convert the area under the peak into a weight or atomic percentage. As the filled weight fraction of the nano-HAp does not significantly affect the atomic components of the calcium phosphate (Deplaine et al. 2010), and the surface of the PDLLA composite scaffold with 60 wt% of nano-HAp was fully covered with apatite after a 28-day incubation in the SBF, as shown in Figure 5.2(h), this sample was therefore chosen as the representative sample for the EDX test.

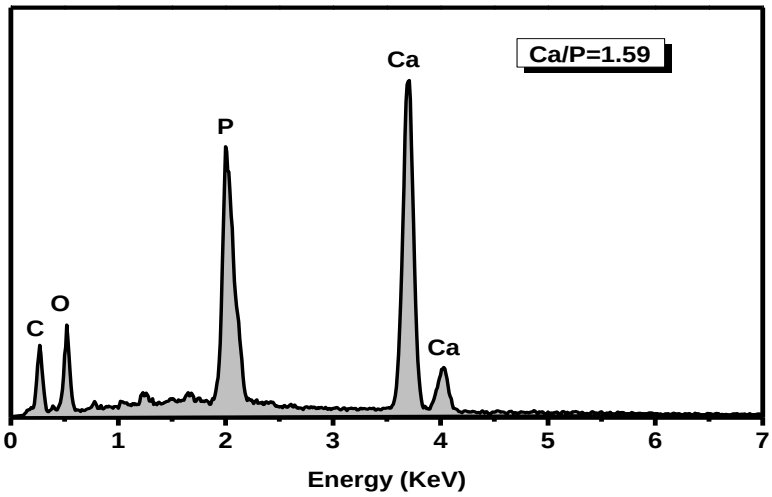

Figure 5.3 EDX spectrum to confirm the presence of apatite formation on the surface of the PDLLA/60 wt% nano-HAp composite after incubation in SBF at 37 °C for 28 days.

An EDX spectrum of the apatite grown on the surface of the PDLLA/60 wt% nano-HAp composite (as the result of the representative volume) is illustrated in Figure 5.3. The atomic percentages of the main elements C, O, P, and Ca were 5.27%, 7.23%, 33.72% and 53.78%, respectively, and thus the Ca/P ratio was calculated as 1.59 (by 53.78/33.72), confirming the presence of calcium-deficient and non-stoichiometric

apatite on the surface of the sample after incubation. It is known that the Ca/P ratio of apatite in natural bone is lower than 1.67 when compared to stoichiometric apatite, therefore, the apatite formed on the composites is of greater biological interest than the stoichiometric apatite, from the view point of biomemetics (Deng et al. 2001).

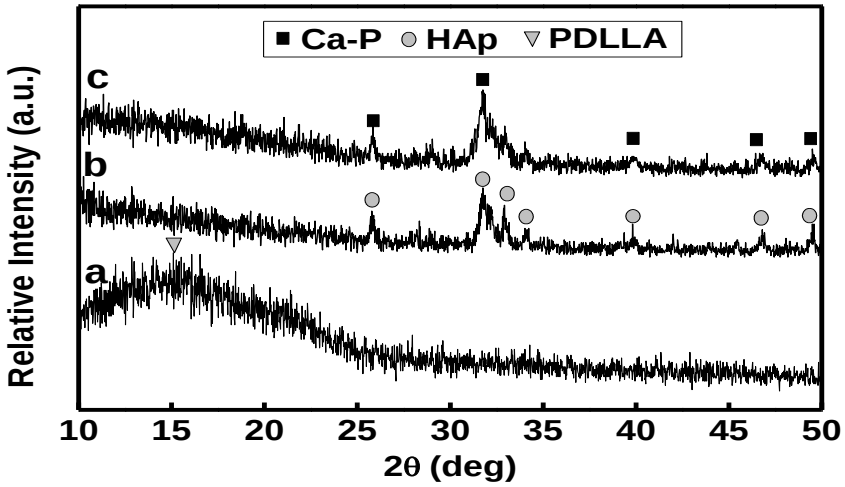

Figure 5.4 TF-XRD graphs of (a) unfilled PDLLA before immersion in SBF; (b) PDLLA/60 wt% nano-HAp composite before immersion in SBF; and (c) PDLLA/60 wt% nano-HAp composite after immersion in SBF for 28 days

The phase structure of the unfilled PDLLA, PDLLA/nano-HAp and the PDLLA/nano-HAp composites after soaking in SBF for 28 days were characterized by an X-ray diffractometer (XRD, Bruker D8 Discover) with Cu K_α radiation. The samples were scanned at 2θ angles, ranging from 10 ° to 50 °, at a scanning rate of 0.02 °/s. The thin-film X-ray diffraction (TF-XRD) patterns of the PDLLA sample, with and without nano-HAp, before and after incubation in the SBF for 28 days, are shown in Figure 5.4. The unfilled amorphous PDLLA matrix was characterized by the broad 2θ peaks between 10 ° and 25 °, as shown in Figure 5.4(a). The characteristic peaks of HAp observed in Figure 5.4(b) confirm the successful incorporation of the nano-HAp into the

PDLLA matrix. After 28-day immersion in the SBF, the PDLLA/nano-HAp composites showed characteristic peaks at 2θ=25.8°, 31.7°, 32.9° and 46.7°, which correspond to the formed Ca-P crystal layer shown in Figure 5.4(c). The peaks for the samples after incubation in the SBF were stronger and broader than those prior to incubation. This further confirms the formation of the Ca-P crystal layer on the PDLLA/nano-HAp composites after incubation in the SBF.

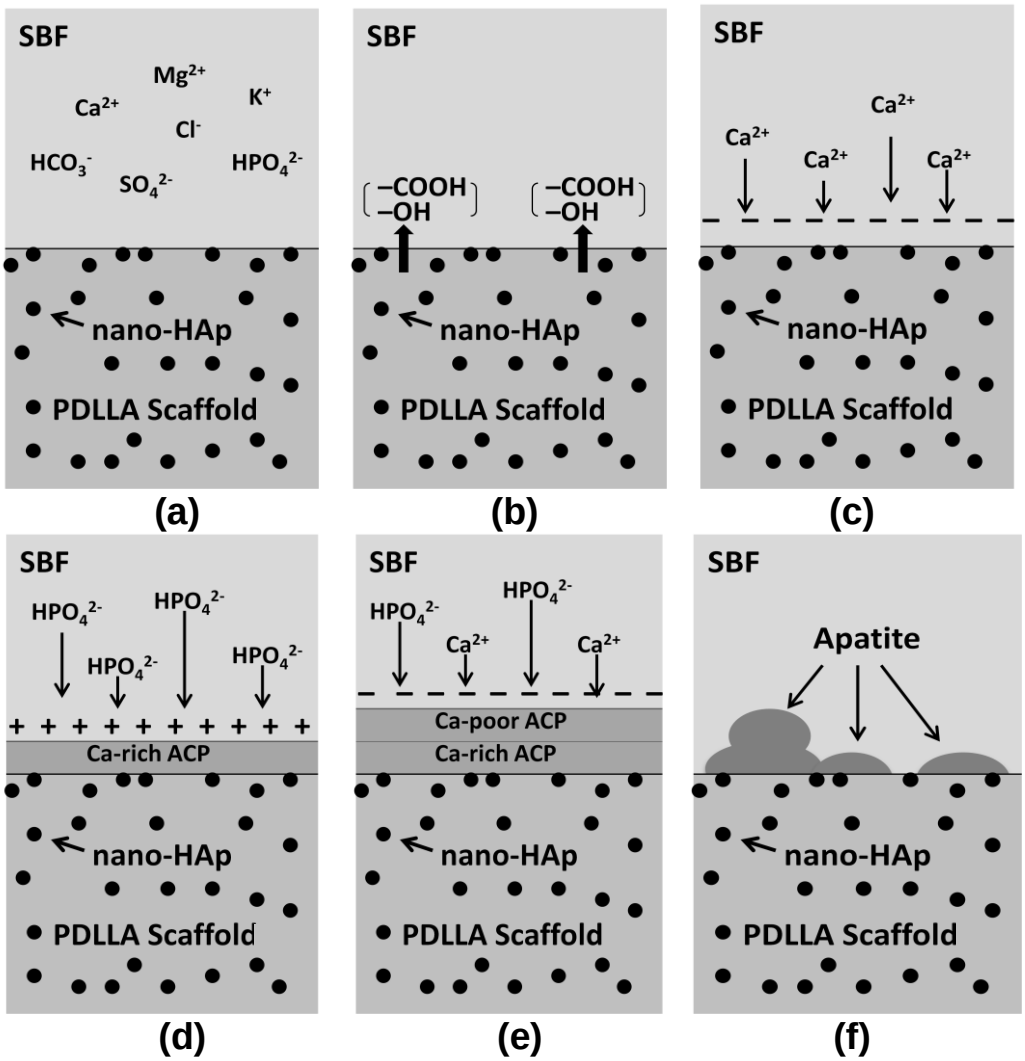

Figure 5.5 Schematic diagram of the mechanism of bonelike apatite formation on the PDLLA/nano-HAp composite scaffold in SBF (formation sequence is from (a) to (f))

The process and kinetics of apatite formation on the scaffolds can be affected by the surface composition and structure of the scaffolds (Kim et al. 2005). The hydrolysis of PDLLA and the nano-HAp filling place an important role in apatite forming (Zhang & Ma 1999). The mechanism of bonelike apatite formation on the PDLLA/nano-HAp scaffolds is schematically illustrated in Figure 5.5. In the SBF, –COOH, and –OH groups can be generated from the hydrolysis of PDLLA [Figures 5.5(a-b)]. The weak acidic group –COOH may dissociate in SBF and further change to $–COO^-$, which leads to the PDLLA surface being negatively charged. Moreover, the nano-HAp revealed negative surface potential (Kim et al. 2005). The –COOH, $–COO^-$, –OH groups and nano-HAp located at the surface of PDLLA scaffolds may interact with positive Ca^{2+} in the SBF to form a Ca-rich amorphous calcium phosphate (ACP) [Figure 5.5(c)]. The surface potential can increase and gain positive charge. The Ca-rich ACP on the PDLLA then interacts with the negative HPO_4^{2-} in the fluid to form the Ca-poor ACP [Figure 5.5(d)]. The Ca-poor ACP appears to be stable by gradually crystallizing into bonelike apatite with a low solubility in the SBF [Figures 5.5(e-f)]. Therefore, increasing the nano-HAp fraction gives way to the increasing nano-HAp to the SBF, which helps to provide a more negatively charged surface on the scaffold that attracts positive Ca^{2+} and stimulates apatite nucleation. The bonelike apatite formed on the scaffold can provide better cell interaction and osteoconductivity, and is the reason why scaffolds with higher fractions of nano-HAp show better bioactivity.

5.5 Degradation of the Composites

5.5.1 Molecular Weight Change

The degradability of the PDLLA/nano-HAp composites with different nano-HAp amounts was investigated by a gel permeation chromatography (GPC, Waters Associates, Inc.) system to determine their molecular weight loss. The measurements were carried out at 30 °C at a flow rate of 1ml/min using tetrahydrofuran (THF) as an eluent. A set of monodisperse linear polystyrene standards (Polysciences, Inc.) were used to obtain a calibration curve. The weight average ($\overline{M_w}$) molecular weights of the samples were estimated. Three replicate measurements were conducted for each type of sample.

The results of GPC are shown in Figure 5.6. The $\overline{M_w}$ of all the samples decreased with time after incubation in the SBF, resulting from the degradation of the PDLLA. After a 28-day incubation, the unfilled PDLLA had the lowest $\overline{M_w}$ compared to the filled ones. However, for the first 7 days of incubation, the degradation rate increased when the PDLLA were filled with larger amounts of nano-HAp, because the PDLLA with higher nano-HAp content could increase the hydrophilicity of the composite and hence promote the penetration rate of the SBF. Therefore, the $\overline{M_w}$ of the PDLLA with 60 wt % of nano-HAp decreased faster than the other filled samples, as shown in Figure 5.6. In all, incorporation of the nano-HAp can be used to control the degradation rate of the PDLLA/nano-HAp composites.

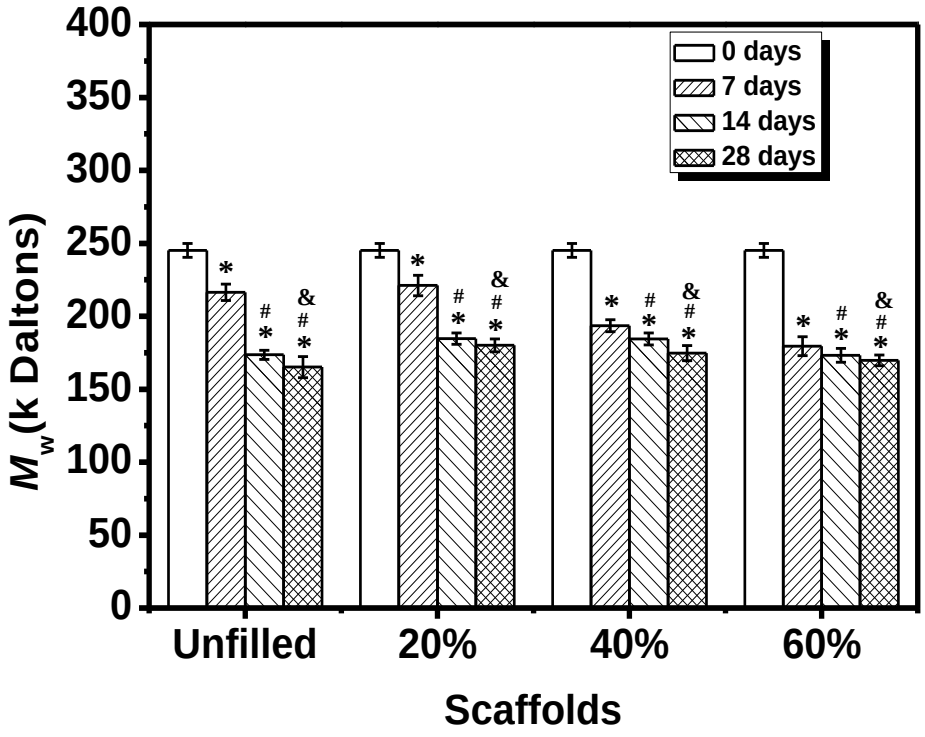

Figure 5.6 Weight average molecular weight ($\overline{M_W}$) changes of PDLLA scaffolds with 0, 20, 40, 60 wt% of nano-HAp after incubation in SBF for different time periods. Results are mean ± SD. *, #, and & indicate the existence of statistically significant differences as compared with the results of 0 day, 7 days, and 14 days, respectively (n=3, p<0.05).

5.5.2 Mass Loss

The mass loss, another result of degradation, was investigated. The original mass of the unfilled PDLLA and PDLLA/nano-HAp composites were measured prior to incubation in the SBF. After the samples had been soaked in the SBF for different time periods, they were dried for 24 hours in a vacuum oven at room temperature, and weighed again. The weight loss (W_L) of each sample was obtained from Equation 5.1.

$$W_L = (W_O - W_D)/W_O \times 100\% \quad 5.1$$

where W_O is the original mass of the sample, W_D is the dry weight of the sample measured after each incubation period. Three specimens were measured for each type of sample.

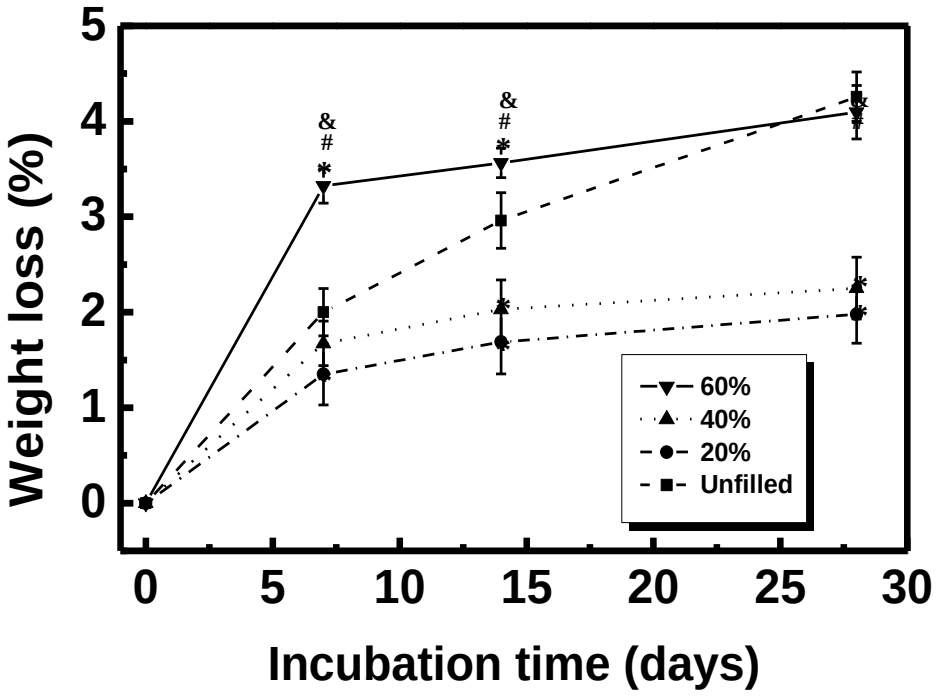

Figure 5.7 Weight losses of the PDLLA composites filled with different amounts of nano-HAp (0, 20, 40, and 60 wt%) after incubation in SBF for different time. Results are mean ± SD. *, # and & indicate the existence of statistically significant differences as compared with the results of unfilled PDLLA, 20 wt% and 40 wt% nano-HAp filled PDLLA composites, respectively (n=3, $p<0.05$).

Figure 5.7 shows the weight losses of the scaffolds during the first 28-day incubation period in the SBF. The weight losses of all the specimens immersed in SBF increased with time. It can be observed from Fig.6 that the weight losses of the samples with 20 wt%, 40 wt% and 60 wt% of nano-HAp after 28 days of incubation were 1.9%, 2.2%

and 4.2%, respectively. This suggests that the PDLLA/60 wt % nano-HAp have the highest weight losses during their 28 days of incubation in the SBF as compared with the others. However, there is no statistically significant difference in the weight losses between the composites with 20 wt% and 40 wt% of nano-HAp during the incubation period. The reason of the rapid weight losses of the composites are the dissolution of the nano-HAp particles, and degradation and fragmentation of the polymer matrices in the composites. In addition, incorporation of nano-HAp increases the overall hydrophilicity of the composites which resulted in increasing their hydrolysis rates. Therefore, the composites with large amounts of nano-HAp, for example, 60 wt%, had a faster weight loss rate especially during the first 7-day incubation (Ang et al. 2007). However, the weight loss of the unfilled PDLLA was higher than that of the composites with 20 wt% and 40 wt% of nano-HAp but lower than that of the composite with 60 wt% after 7 days. It is because the higher amounts of bonelike apatite deposition on the samples with 20 wt% and 40 wt% of nano-HAp than on the unfilled one, and can retard the weight loss of the composites. As the apatite formation rates of the unfilled PDLLA was slower than that of the nano-HAp filled composites during incubation in the SBF, the unfilled PDLLA had a higher weight loss of nearly 4.4% after 28 days of immersion, as compared with the composites. However, there are no statistically significant differences between the unfilled PDLLA and the PDLLA/60 wt% nano-HAp composite after a 28-day immersion.

5.6 Mechanical Properties Evaluation after Incubation in SBF

In order to investigate the effects of apatite deposition and polymer degradation on the mechanical properties of the porous multifunctional PDLLA based composites, uniaxial

compression tests were conducted at room temperature using a mechanical universal testing machine (MTS 810, Material Test System) to determine the compressive moduli (E) and strengths (σ_{10}) of the cylindrical samples, before and after incubation for different periods in the SBF (i.e. 0 day, 7 days, 14 days and 28 days). A crosshead speed of 2 mm/min and a load cell of 500 N were adopted for the tests. The E and σ_{10} of each sample were determined by calculating the slope of the initial linear portion of the stress-strain curve and the stress at which the strain reached 10%, respectively (ASTM standard, D1621). Five specimens were examined for each type of sample.

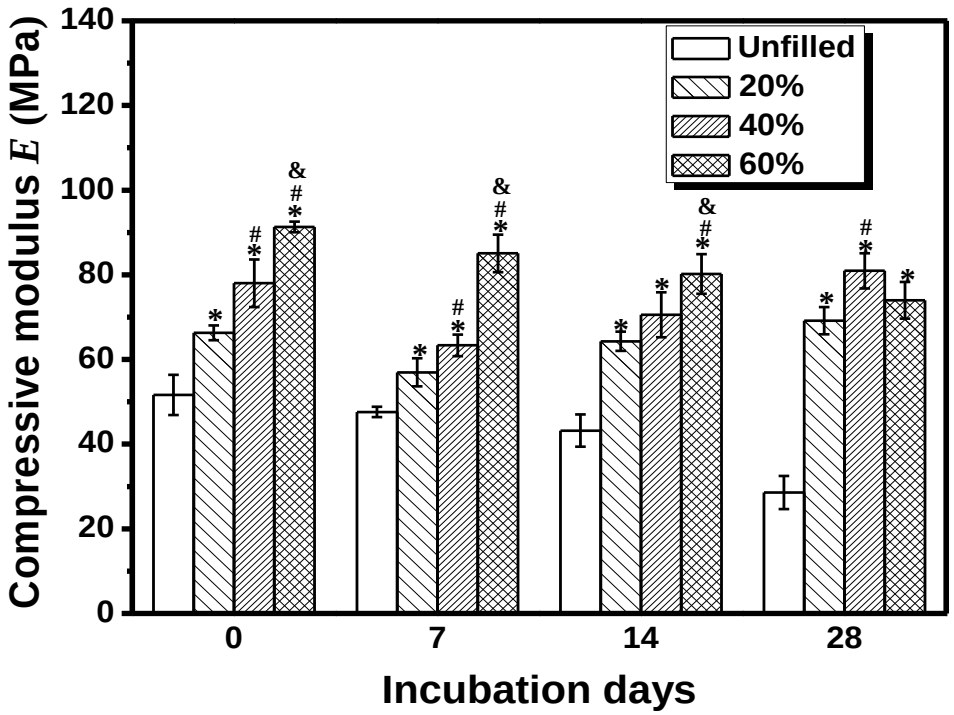

Figure 5.8 Changes in compressive moduli (E) of the PDLLA composites with different amounts of nano-HAp after incubation in SBF for different time. Results are mean ± SD. *, #, and & indicate the existence of statistically significant differences as compared with the results of unfilled PDLLA, PDLLA with 20 wt% and 40 wt% of nano-HAp, respectively (n=5, p<0.05).

The E and σ_{10} of the PDLLA composites with different amounts of nano-HAp before incubation in the SBF are shown in Figures 5.8 and 5.9, noted as 0-day incubation. Before incubation, PDLLA/nano-HAp composites had higher E and σ_{10} than the unfilled PDLLA ones. E and σ_{10} of the PDLLA with 60 wt% of nano-HAp increased to 91.3 ± 1.2 MPa and 2.5 ± 0.2 MPa, respectively, which were close to the data for human cancellous bone (Rezwan et al. 2006). The increase in E for the PDLLA/nano-HAp composites is mainly attributed to the addition of the rigid nano-HAp filler (Thomas et al. 2006). Nano-sized HAp with a high total surface area can enhance stress transfer between the matrix and the fillers. Therefore, the addition of nano-HAp led to the increase in σ_{10} through an efficient stress transfer mechanism (Fu et al. 2008). In addition to the high surface area of the nano-HAp, the interfacial adhesion between the fillers and the polymer matrix is of great importance for σ_{10} (Kovačević et al. 2008). The hydrogen bonding formed between the uniformly distributed nano-HAp and the PDLLA matrix under compression molding also increased the interfacial adhesion and hence the enhancement of the σ_{10} of the PDLLA/nano-HAp composites is due to the better load transfer (Zhou et al. 2007, Fu et al. 2008).

The changes in the E and σ_{10} of the porous PDLLA based nanocomposites after incubation in the SBF for different times are shown in Figures 5.8 and 5.9. After soaking in the SBF for 7 days, the E value of all the PDLLA based samples decreased, as shown in Figure 5.8. The main reasons for this decrease are the pore size increase of the samples, the decrease in the molecular weight of the PDLLA, and the loss of the

nano-HAp particles. In addition, the reduction of *E* can also be attributed to the plasticizing effect because the terminal carboxylic acid functional group on the PDLLA chains facilitates water penetration (Blaker et al. 2011). From the 7-day to the 28-day incubation, it could be observed that the *E* value of the PDLLA composites with 20 wt% and 40 wt% of nano-HAp increased with incubation time. The increase of *E* can be mainly attributed to the apatite deposition on the composites and the improvement of the interfacial adhesion between the deposited apatite and the PDLLA matrix. From Figure 5.8, the *E* values of the unfilled PDLLA reduced from 51.6±4.7 MPa to 28.6±3.9 MPa after a 28-day incubation, because of the continuous degradation of the PDLLA and relatively little apatite being deposited during the incubation. Nano-HAp particles filled in the PDLLA composite tended to fall off and interact with the SBF because of their good hydrophilicity. The loss of nano-HAp particles led to the formation of some voids within the PDLLA matrix, and hence more surfaces of the PDLLA were exposed to hydrolytic attack, accelerating the degradation of the PDLLA and weakening its overall structure. Therefore, when the PDLLA composite was filled with a higher content of hydrophilic nano-HAp, this phenomenon was more obvious and resulted in the *E* reduction of the scaffolds with 60 wt% of nano-HAp, within the 28-day incubation. However, the scaffolds with 40 wt% nano-HAp after a 28-day incubation could reach an *E* value of 80.9±4.1 MPa, which was much larger than that of an unfilled PDLLA. In general, the incorporation of the nano-HAp into the PDLLA can promote apatite deposition on the composites and enhance their compressive moduli.

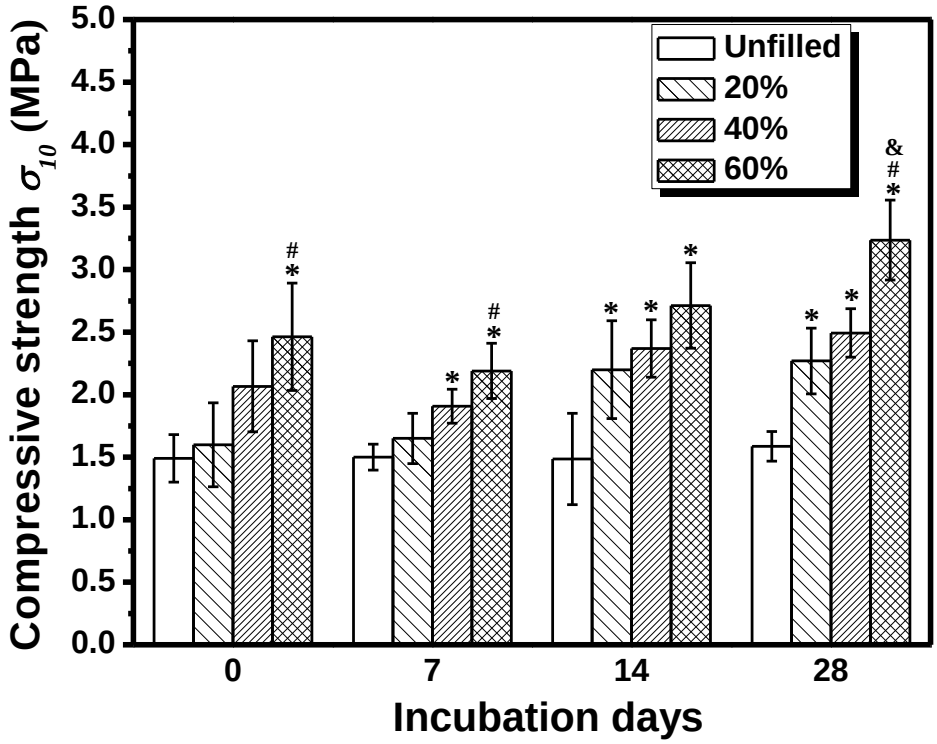

Figure 5.9 Changes in compressive strength (σ_{10}) of the PDLLA composite s with different amounts of nano-HAp after incubation in SBF for different time. Results are mean ± SD. *, #, and & indicate the existence of statistically significant differences as compared with the results of unfilled PDLLA, PDLLA with 20 wt% and 40 wt% of nano-HAp, respectively (n=5, p<0.05).

On the other hand, the compressive strengths of the PDLLA based samples after incubation exhibited different trends, as shown in Figure 5.9. For the unfilled PDLLA samples, σ_{10} almost maintains the same value during the incubation. σ_{10} of the PDLLA/nano-HAp composites slightly decreased after a 7-day incubation, increased in the following two weeks, and reached the highest values after a 28-day incubation. In addition to the plasticization of the PDLLA matrix and the loss of the nano-HAp particles, the initial reduction of σ_{10} is mainly due to the degradation of PDLLA which

increased the pore size in the composites, as shown in Figure 5.2. With increasing incubation time, more apatite mineral could be deposited onto the sample surface, leading to higher σ_{10} values for the samples, especially those with high nano-HAp content. This trend is similar to that of *E*. These results show that the mechanical properties of PDLLA/nano-HAp composites *in vitro* are affected by the properties of the filler, incubation time, plasticization and degradation of the polymer matrix.

5.7 *In vitro* Drug Release Study

5.7.1 Dex Loading Capacity

The initial drug loading amounts of the PDLLA based composites were determined by analyzing the Dex released mediums of the composites using a UV/vis spectrophotometer (UV1102, Techcomp Ltd.). Weight gains of the samples after drug coating were also measured to estimate the initial amount of the Dex loading. The weight gain and initial drug loading amount in the composites after the PEG/Dex coating are illustrated in Table 5.3. Samples with larger porosity gained more weight than the smaller ones since larger surface areas, were exposed to the PEG/Dex solution. Weight gains of the PDLLA/nano-HAp composites after drug coating were greater than those of the unfilled ones. The initial drug loading amount generally increased with the presence of nano-HAp in the composites for different PDLLA/NaCl ratios. The weight gain and initial drug loading amount increased with increasing fraction of hydrophilic nano-HAp. Therefore, the incorporation of the hydrophilic nano-HAp is shown to be an alternative method to increase the initial drug loading amount.

Table 5.3 Weight gains after drug coating and initial drug loading amounts of the PEG/Dex coated porous PDLLA/nano-HAp composites and unfilled PDLLA.

Samples (PDLLA/salt, w/w)	Weight gains (mg)	Drug loading amounts (mg)
1:7	48.2 ±1.2	1.62 ±0.10
1:8	48.8 ±1.7	1.67 ±0.06
1:9	49.6 ±2.7	1.90 ±0.12
1:7 + 20 wt% nano-HAp	57.2 ±4.5	2.06 ±0.06
1:8 + 20 wt% nano-HAp	58.0 ±2.3	2.22 ±0.08
1:9 + 20 wt% nano-HAp	65.4 ±4.6	2.33 ±0.12
1:8 + 40 wt% nano-HAp	61.2 ±3.4	2.28 ±0.06
1:8 + 60 wt% nano-HAp	67.5 ±2.6	2.39 ±0.14

5.7.2 Drug Release Behavior

The PEG/Dex coated porous PDLLA/nano-HAp composite was placed in a closed vial containing 10 ml of 10 mM phosphate buffered saline solution (PBS, pH=7.4), and kept in a water bath at 37 °C for 30 days. The medium with released Dex from the composite was collected at predetermined time intervals and replaced with the same volume of fresh PBS. The mediums were analyzed by a UV/vis spectrophotometer at a wavelength of 242.5 nm, while the pH values of the PBS mediums were recorded using a pH meter (SevenGo™ pH-SG2, Mettler Toledo). For comparison, the unfilled PDLLA were also studied. The Dex-releasing profiles of the PDLLA based composites are shown in Figure 5.10. Figure 5.10 shows that all the PDLLA samples has a similar drug releasing profile, which involved a sustained release of Dex after an initial burst. Nearly 50% of the drug was released within one day and the rest was sustainably diffused out of the samples over the following 34 days. The main reason for this release behavior may be due to the subsequent drug coating, which produced some free drugs located near the surface of the coated layer (Uttarwar 2008, Zhang et al. 2008).

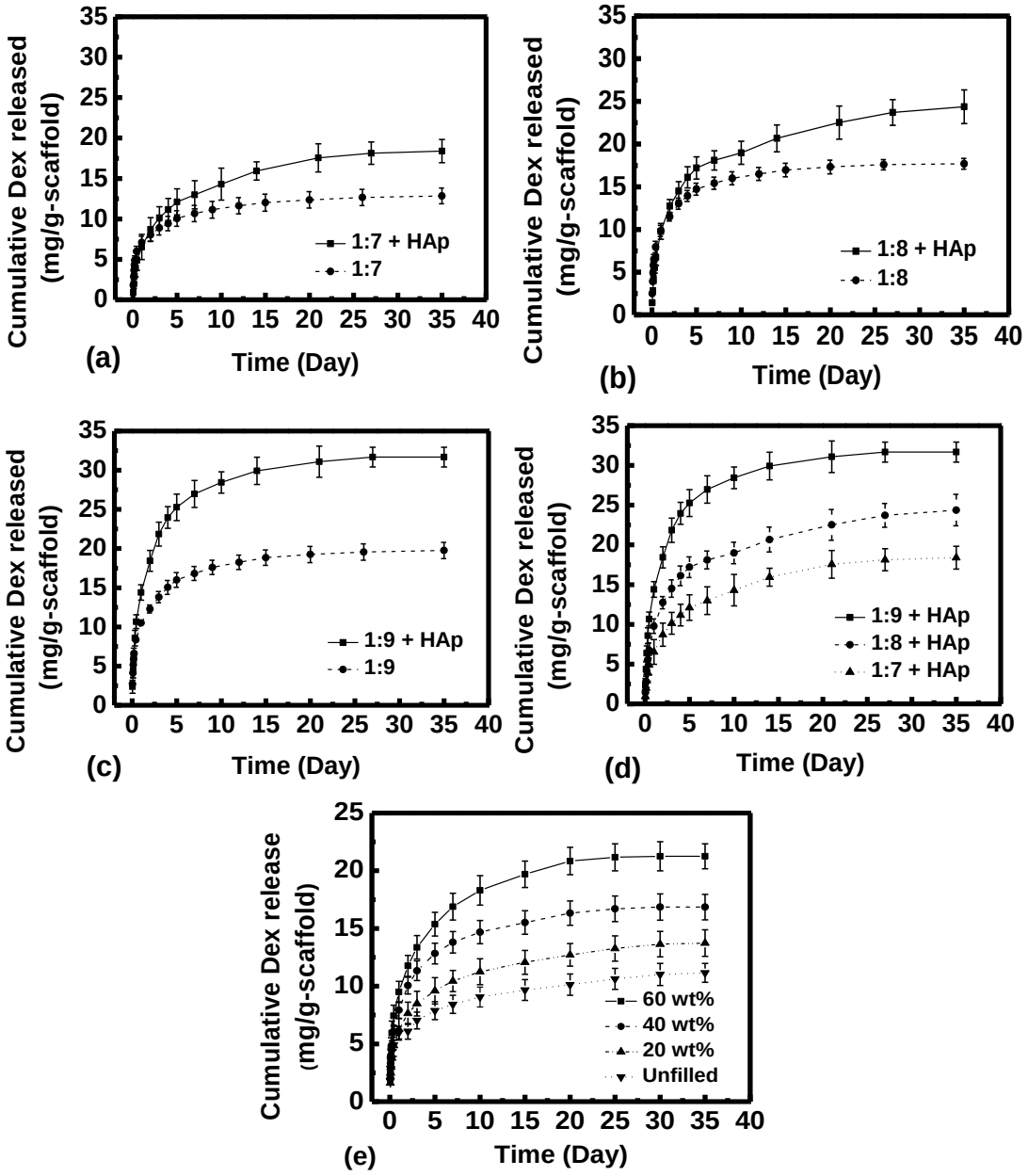

Figure 5.10 The cumulative release of Dex from the PDLLA/nano-HAp composites as a function of time (a) 1:7 PDLLA composites with and without nano-HAp fillers; (b) 1:8 PDLLA composites with and without nano-HAp fillers; (c) 1:9 PDLLA composites with and without nano-HAp fillers; (d) 1:7, 1:8 and 1:9 PDLLA/nano-HAp composites; (e) 1:8 PDLLA based composites with different amounts of nano-HAp (0, 20, 40, and 60 wt.%). Results are mean ± SD, n=3.

A comparison was made between the PDLLA based samples, with and without nano-HAp filling. From Figures 5.10 (a-c), the Dex-coated PDLLA/nano-HAp composites show greater cumulative drug release amounts of 40%, 40% and 60% than for the unfilled ones for three different PDLLA/NaCl ratios of 1:7, 1:8 and 1:9, respectively. As the incorporation of the hydrophilic nano-HAp (20 wt%) improved the drug loading capacity of the composites, thicker PEG/Dex films were coated on the PDLLA/nano-HAp composites than the unfilled ones, as the adhesive force of the thick PEG/Dex films may be weaker than for the thin ones. The Dex release from the thick PEG/Dex films of the PDLLA/nano-HAp composites was relatively easier, leading to a larger total drug release amount. Therefore, the nano-HAp filler was one of the factors that influenced the drug release behavior, particularly the total drug release amount.

Figure 5.10(d) illustrates the effect of the porosity of the PDLLA/nano-HAp composites on the drug releasing behavior. Among these three different samples, the 1:9 PDLLA sample showed the largest total Dex release amount. This may be attributed to the larger surface area of the 1:9 PDLLA sample (porosity=81.6%) with a greater initial drug loading amount as compared with that of the 1:8 (porosity=77%) and 1:7 (porosity=66%) samples. The results indicate that adjustment of the porosity level can control the drug release behavior to a certain degree.

The effects of the nano-HAp fractions on the drug release behavior were investigated and the cumulative Dex-release curves of the PDLLA composites with 0, 20, 40, and 60 wt% of nano-HAp are shown in Figure 5.10(e). PDLLA composites with a higher content of nano-HAp were found to have a faster Dex release rate during the first 30

hours. Afterwards, all the composites had nearly the same release rates. This can be attributed to hydrophilic nano-HAp incorporation which improves the drug loading capacity of the composites, as shown in Table 5.3. The more the nano-HAp is filled, the thicker the PEG/Dex layer coated on the composites, with more Dex being loaded into the composites. It is reasonable to conclude that the drug release amounts of the composites with higher concentration of the nano-HAp are larger.

5.7.3 pH Value Change

The pH value of most body fluids ranges from 7.35 to 7.45 (Razaq 2003), in which proteins and many other biological molecules can function properly. Deviations in the pH value, for example unusual decrease and increase in blood pH, named acidosis and alkalosis, respectively, can lead to death if untreated (Starr & McMillan 2012). Therefore, for bone tissue regeneration, it is important to evaluate the pH value change of the aqueous medium when biodegradable scaffolds are used. Figure 5.11(a) shows the pH evolution of PBS, for PDLLA composites incorporated with different amounts of nano-HAp being immersed for 35 days. There is a decrease in the pH of the PBS after 35-day immersion of all the PDLLA samples prepared in this study. Such decrease in the pH is due to the carboxylic acid produced from the degradation of the PDLLA via hydrolysis (Hile et al. 2004). The pH of the PBS containing unfilled PDLLA samples decreases from the initial value of 7.4 to 6.6 after 35 days of incubation. Different from the unfilled PDLLA, the pH value changes of the PBS containing PDLLA/nano-HAp composites show different patterns and become stable during the incubation period from the 5th to the 20th days. Moreover, the pH values of the PBS containing different kinds of samples fit the Weibull distribution, as shown in Figure 5.11(b). Figure 5.11(b)

shows decreasing trends in the pH value of all PDLLA samples, and PDLLA/nano-HAp composites show a slower decreasing rate in the pH value than unfilled ones. This suggests that the nano-HAp has the effect of reducing the acidity of the medium and serves as a buffer system (Bucholz 2002, Schiller & Epple 2003). Moreover, the more the nano-HAp is filled, the less the pH of the neighboring environment decreases.

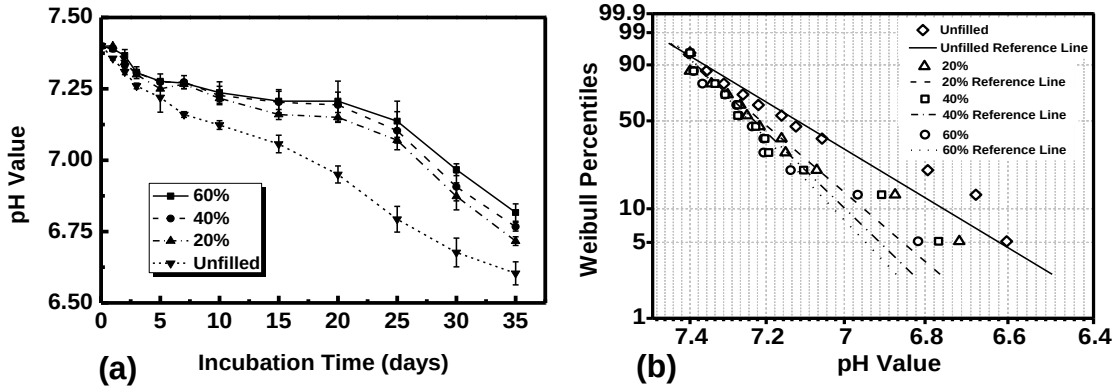

Figure 5.11 The pH changes of PBS after immersion of porous PDLLA with 0, 20, 40, 60 wt.% of nano-HAp, (a) pH versus incubation time and (b) The Weibull probability plot of pH value data.

5.8 Summary

PEG/Dex coated porous PDLLA/nano-HAp composites, fabricated by the PC-DC technique showed improved bioactivity, due to apatite formation, and enhanced mechanical properties close to human cancellous bone. The effects of the nano-HAp fillers on the molecular weight, mass loss and drug release behavior of the PDLLA composites, as well as the pH value changes of PBS, were thoroughly investigated *in vitro*. The PDLLA/nano-HAp composites had a fast degradation rate during the first 7 days incubation and the degradation rate slowed down in the following 21 days.

Mechanical properties of the PDLLA/nano-HAp composites after incubation in the SBF can be greatly affected by the weight loss, degradation and apatite formation of the samples. Results from the mechanical properties investigation show that the weight loss, polymer plasticization, and degradation of the PDLLA/nano-HAp composites resulted in a reduction of their compressive moduli and strengths. On the other hand, compressive moduli and strengths of the scaffolds were improved due to the rigid apatite formation on them after the SBF incubation. 35-day Dex-releasing was observed from the drug release study. The initial drug loading amounts and total drug release amounts increased with the fraction of nano-HAp and porosity of the scaffolds. A larger total drug release amount of scaffold provides with longer drug release times and higher drug concentration around the damaged bone tissue, which may improve the efficiency of treatment. Moreover, the PDLLA/nano-HAp composites had a pH buffering effect during a 35-day incubation in the PBS, so that the risk of chronic inflammation complications can be reduced. The PDLLA/nano-HAp scaffolds fabricated in this study have been confirmed with great biocompatibility, interconnected porous structure, similar mechanical properties as human cancellous bone, drug delivery ability and degradability. The shape memory effects, as well as their thermal mechanical properties are described in the next chapter.

Chapter 6. Shape Memory Effect of the PDLLA/nano-HAp Scaffolds

6.1 Introduction

With the development of surgical techniques, such as minimally invasive surgery, smart materials are required to fulfill the requirements for the functionality of implants. Smart materials with shape memory effect (SME) enable the insertion of a temporary compressed bulk device in the body through a small incision and the implants can attain their required shape by a stimulus. The intravascular stent is a good example for the application of minimally invasive surgery. Shape memory polymers (SMPs) have the capability of recovery from an initial temporary shape to permanent shapes by an external stimulus such as temperature, light, pH, or magnetic field (Meng & Hu 2009). These kinds of polymer form an emerging class of smart materials in many areas of our lives, such as high-performance textiles, packaging materials, intelligent medical device (Biological MicroElectroMechanical system, Bio-MEM), and there is high potential in minimally invasive surgery. In the field of bone tissue engineering, multifunctional porous scaffold fabricated by degradable SMPs may not only relieve pain by the small incision from the minimally invasive surgery, but also promote tissue regeneration by the drug release function. However, unreinforced SMPs show low stiffness which results in a small recovery force. Porous shape memory polymer composites (SMPCs) were rapidly developed due to their advantages, e.g. greater volumetric expansion capabilities, wider range of mechanical and physical properties compared to the unfilled SMPs (Hearon et al. 2013). As the reinforcing phase has great effect on the SME of the composites, to understand the relationship between the incorporators and SME is

important for fabricating a bone composite with controllable shape fixation and recovery rate.

Multifunctional porous PDLLA/nano-HAp composites were prepared by a technique involving polymer coagulation, particulate leaching, and cold compression moulding developed in this study. The microstructure, mechanical properties, cellular response, bioactivity, degradability, and drug release behavior of the porous PDLLA/nano-HAp composites were investigated and the results are presented in the Chapter 3 to 5. So far, study on the shape memory behavior of porous PDLLA/nano-HAp scaffolds has hardly been addressed. In this part of the study, shape memory behavior of the composites was evaluated by a physical bending test and a cyclic thermomechanical compression test. Thermal properties such as thermal degradability, stability, and dynamic mechanical properties are of importance for study of the SME of the composites. Before the evaluation of SME, thermal characterization, thermogravimetric analysis (TGA), differential scanning calorimeter (DSC), and dynamic mechanical analysis (DMA) were carried out to characterize the polymeric thermal transitions and to determine the shape transition temperature of the SMPCs. The shape recovery time, shape fixation ratio and shape recovery ratios of the porous PDLLA composites with different nano-HAp fractions were quantitatively investigated. The results from these tests showed that the relationship between the SME and the nano-HAp fraction were nonlinear. PDLLA with 10 wt% nano-HAp showed the best fixity and recoverability when compared with those filled with 30 and 50 wt% nano-HAp. Moreover, the larger the maximum strain applied to the test sample, the lower the shape recovery ratios.

6.2 Preparation of Samples

Porous PDLLA/nano-HAp scaffolds were fabricated by the polymer coagulation, cold compression molding and particulate leaching method described in chapter 3 (Chen et al. 2011). The general fabrication procedure for PDLLA/nano-HAp scaffolds was as follows: PDLLA ($M\eta$=75,000) was dissolved in chloroform. Nano-HAp with crystal size of 20-30 nm (10, 30, 50 wt %) and sieved NaCl particles (particle size: 150-300 μm, PDLLA/salt =1:8 w/w) were subsequently added to the PDLLA/chloroform solution with a vigorous stirring until a homogeneous dispersion was obtained. An excess volume of cold ethanol was dripped into the solution to form a PDLLA/NaCl/nano-HAp gel paste. This gel paste was then compression molded into cylinders and rectangular plates using a compressing machine (Model 769YP-15A) under 10 MPa at room temperature. After salt leaching in the DI water and vacuum drying, porous PDLLA/nano-HAp scaffolds were prepared.

6.3 Thermal Analyses

6.3.1 Thermal Degradation Properties

The thermal degradation properties and stability of the scaffolds were evaluated from 30 to 500 °C at a heating rate of 10 °C/min using a thermogravimetric analyzer (TGA, TA Instruments Q500). Nitrogen protection with a volume flow rate of 40 ml/min was used for the tests.

The thermal degradation properties of PDLLA and their nanocomposites are shown in Figure 6.1. The DTG and TGA thermograms show that the incorporation of nano-HAp increased the onset degradation temperature (T_i) from 278 °C for unfilled PDLLA to 310 °C of PDLLA/50 wt% nano-HAp, and the thermal degradation process was delayed. Moreover, the end degradation temperature (T_f) and the maximum degradation temperature (T_{max}) showed an increase trend with the addition of nano-HAp. This is known as a barrier effect which is caused by the hindrance of nano-HAp to the diffusion of the degradation products from the polymer to the gas phase (Chen et al. 2007). TGA thermograms show mass residuum of the PDLLA scaffolds with nano-HAp and they increase with nano-HAp content. The mass residuum is mainly attributed to the non-decomposition of nano-HAp at the test temperature. This is further evidence of the successful incorporation of different amounts of nano-HAp. The actual nano-HAp loading amounts can be observed from the mass residuum in the TGA thermograms. The actual nano-HAp loading ratios in the PDLLA/nano-HAp composites reduced to 10, 23, and 37 wt% when 10, 30, and 50 wt% of nano-HAp was added to the PDLLA/chloroform solution, respectively, during the scaffold fabrication. This shows a similar result to that reported by Qing et al. (2008). Though the actual loading ratios decreased compared with the initial nano-HAp loading ratios, they still maintained a relative high nano-HAp amount. This is because the polymer coagulation which can make the polymer, nano-HAp and salt rapidly deposit at the same time. This prevents an excessive loss of nano-HAp in the composites and suggests that the PC-DC technique developed in this study can control the nano-HAp loading amount.

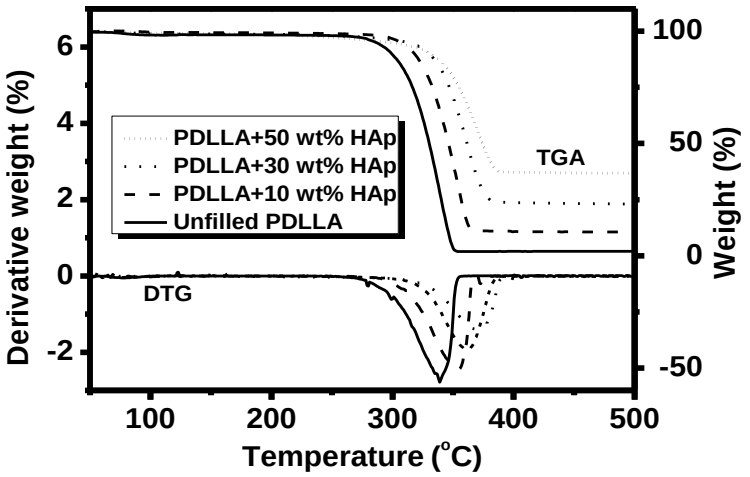

Figure 6.1 TGA and DTG thermograms for PDLLA scaffolds with different amounts of nano-HAp filled

6.3.2 Melting Properties

Melting properties and T_g of the PDLLA/nano-HAp composite scaffolds were determined by a differential scanning calorimeter (DSC, Perkin Elmer DSC7). The samples were heated from 30 to 200 °C at a heating rate of 10 °C/min. Nitrogen with a volume flow rate of 20 ml/min was used for all the thermal tests. The weights of the samples were in the range 4 to 6 mg.

The DSC thermogram curves of the PDLLA based composites are shown in Figure 6.2. The glass transition temperature (T_g) of the samples was defined as the extrapolated onset of the DSC curve. T_g of the PDLLA scaffolds with 0, 10, 30 and 50 wt% of nano-HAp were 50.3, 51.7, 52.7 and 54.5 °C, respectively. The slightly increase of T_g with the addition of nano-HAp is due to (i) the interfacial interaction of polymer matrix and

the nano-HAp phase, and (ii) micro-Brownian thermal motion of PDLLA chain segments being constricted by the nano-HAp (Chen & Sun 2005).

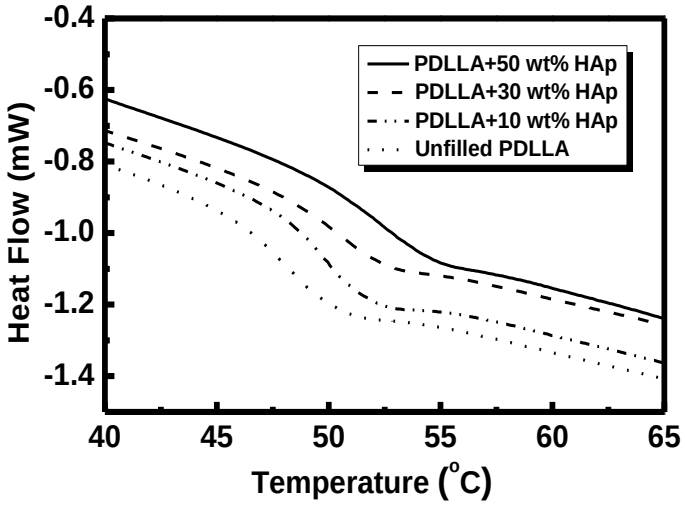

Figure 6.2 DSC thermograms for PDLLA scaffolds with different amounts of nano-HAp filled

6.3.3 Dynamic Mechanical Properties

Dynamic mechanical analysis (DMA, Perkin Elmer Diamond DMA lab system) was conducted under a nitrogen atmosphere, using a compression mode at a fixed frequency of 1 Hz. The temperature was swept at a heating rate of 5 °C/min from 0 to 100 °C. The specimens were of rectangular shape with dimensions of 5.5 mm in length, 5 mm in width and 4 mm in thickness.

Figure 6.3 presents the storage modulus (*E'*) and loss factor (*tanδ*) of the scaffolds as a function of temperature. All the specimens experienced T_g when *tanδ* sharply dropped and *E'* suddenly decreased. From the *E'* curves, the *E'* of the PDLLA/nano-HAp composite increased as the nano-HAp content increased, indicating that nano-HAp

acted as a strong reinforcing phase, thereby enhancing the elasticity of the PDLLA/nano-HAp composites. The larger the E is, the harder the material is. T_g also can be defined as the peaks of the *tanδ* curves, as shown in the Figure 6.3. The T_g determined from the DMA were nearly 15 °C higher than the ones from DSC. For example, T_g of PDLLA obtained from DCS and DMA were 50.3, and 66.3 °C, respectively. This is a normal phenomenon due to the different measuring processes between DCS and DMA. The results from both of the measurements are acceptable. T_g slightly shifted to a higher temperature with the addition of nano-HAp particles. Additionally, with a rise in the nano-HAp content, a broadening of the peak on the *tanδ* curve and a lower peak value were observed. These are because the reinforcing effect of the homogeneously dispersed nano-HAp, which obstructs the mobility of the polymer chains and the interfacial interaction between PDLLA and nano-HAp (Zheng et al. 2006). The shape memory performance of an SMPC may be improved by the broadened transition temperature (Miaudet et al. 2007).

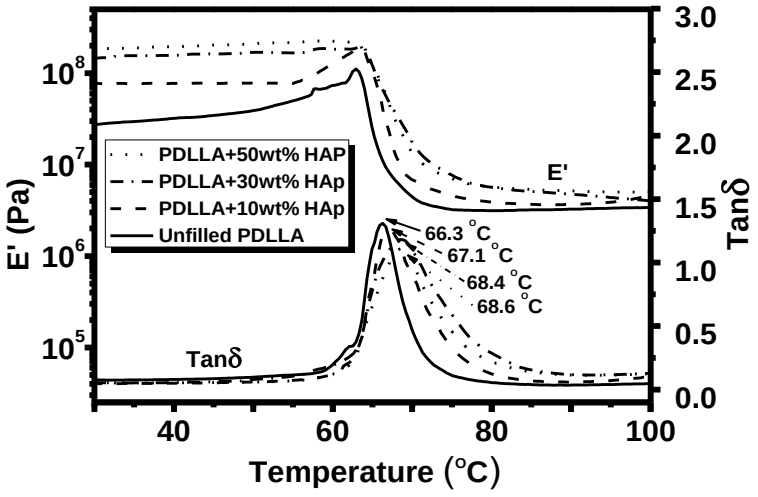

Figure 6.3 DMA thermograms for PDLLA scaffolds with different amounts of nano-HAp filled

6.4 Shape Memory Effect

6.4.1 Cyclic Thermomechanical Compression Test

The thermal condition, kinetics, and type of mechanical deformation influence the shape memory properties. Cyclic thermomechanical experiments can be performed to obtain a full description of these factors and quantify the shape memory properties (Wagermaier et al. 2010). Strain-controlled cyclic thermomechanical compression testing was used to characterize the cyclic shape memory behavior using an electromechanical universal testing machine (MTS, CMT4202) with a heating chamber (Figure 6.4).

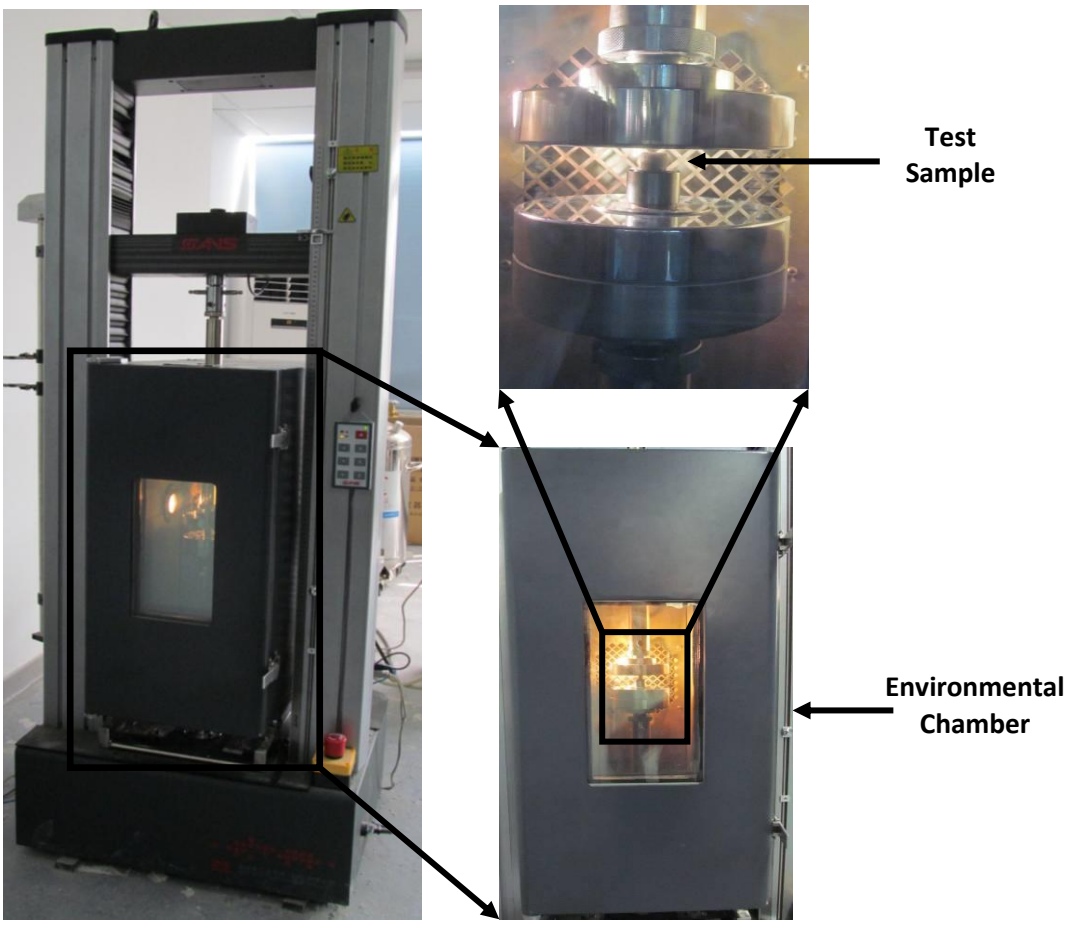

Figure 6.4 Photographs of electromechanical universal testing machine (MTS, CMT4202) with a enviromental chamber

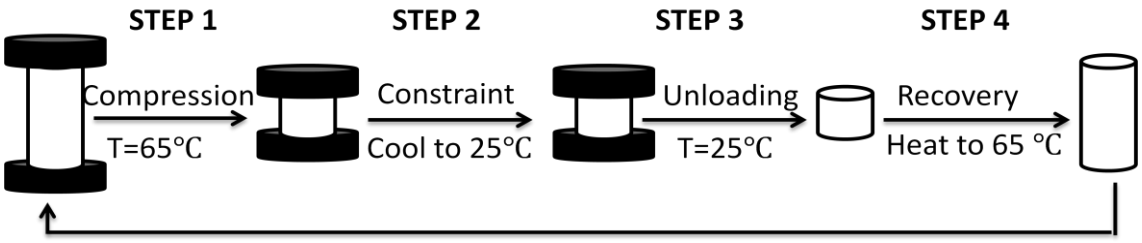

Figure 6.5 Schematic describing of cyclic thermomechanical compression test

In this study, the testing circle, consisting of four steps, is shown in Figure 6.5: (i) The cylinder shaped sample (Φ=10 mm, H=8 mm) was heated to 65 °C (T_g+10K, T_g obtained from the DSC) and kept in an isothermal condition for 10 min; (ii) The specimen was compressed to a certain deformation at ε_m=50% at 65 °C (2 mm/min); (iii) The specimen was rapidly cooled to 25 °C while deformation of ε_u was kept constant as the temporary shape; (iv) After being held at 25 °C for 3 min, the load was released and the shape recovered. To initiate the second cycle, the temperature was ramped to 65 °C again and the final length of the specimen was recorded as ε_p. Four cycles were performed to evaluate the repeatability and the durability of the shape memory behavior. The quantification of the SME was described as the percentage of strain fixing and extent of strain recovery determined in the cyclic thermomechanical tests. The shape fixity ratio, $R_f(N)$, and shape recovery ratio, $R_r(N)$, were determined using Equations 6.1 and 6.2 below:

$$R_f(N) = \frac{\varepsilon_u(N)}{\varepsilon_m} \times 100\% \quad 6.1$$

$$R_r(N) = \frac{\varepsilon_m - \varepsilon_p(N)}{\varepsilon_m - \varepsilon_p(N-1)} \times 100\% \quad 6.2$$

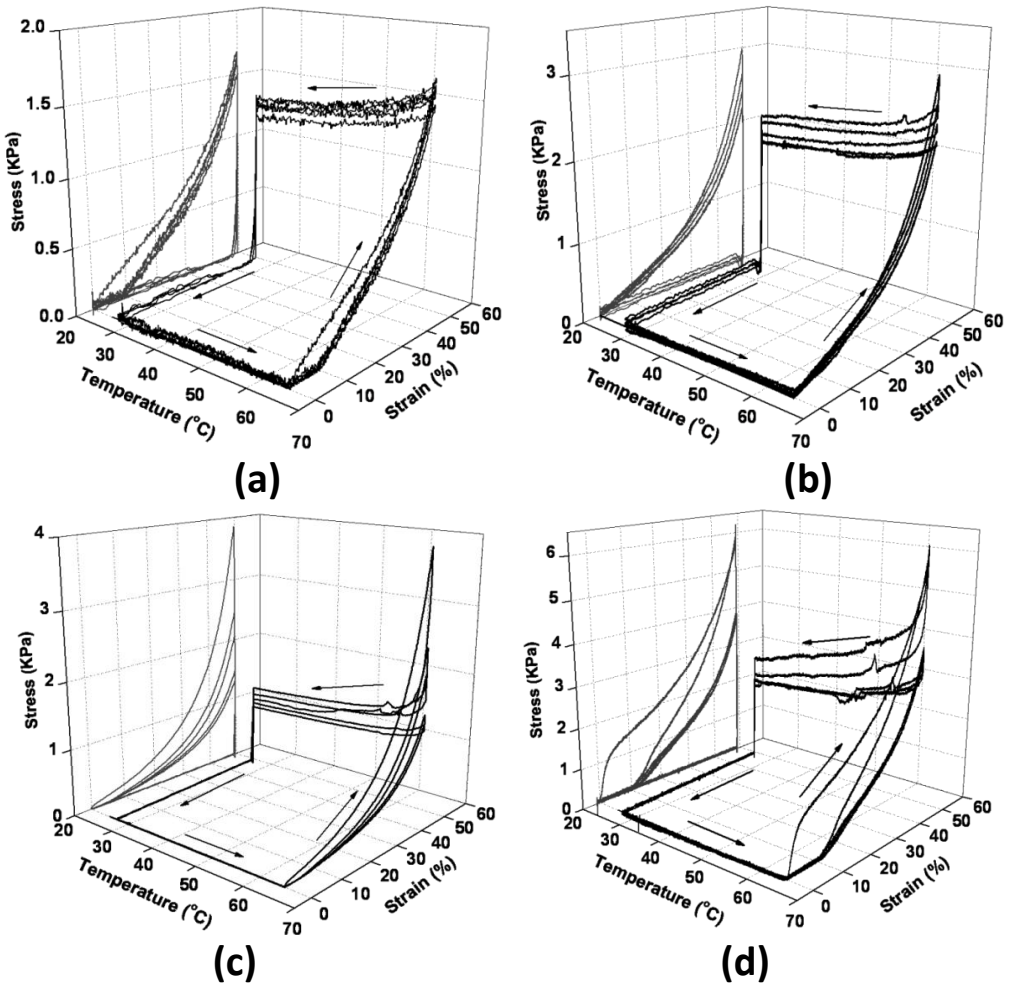

Figure 6.6 3D temperature-strain-stress curves and 2D strain-stress curves of cyclic thermo-mechanical compressive test of (a) unfilled PDLLA scaffolds and scaffolds with (b) 10, (c) 30 and (d) 50 wt% of nano-HAp at mechanical deformation of 50%

The 3D stress-strain-temperature diagrams from the strain-controlled cyclic thermo-mechanical testing at deformations of 50% and 70% are shown in Figures 6.6 and 6.7, respectively. Four cycles were performed to characterize the cyclic shape memory behavior and their shape fixity (R_f) and recovery ratios (R_r) were calculated and are listed in Table 6.1. The increase of stress with increasing fraction of nano-HAp was found in both cases when the ε_m was 50% and 70%, which showed a strong reinforcement of the nano-HAp. The improvement in the mechanical properties of the

scaffolds is a direct consequence of the relatively high modulus of the nano-HAp relative to the polymer matrix. The stress reached was higher for the larger deformation imposed. From the data shown in Table 6.1, it is clear to find that the PDLLA based scaffolds showed a good ability to fix the temporary shape when R_f of all the scaffolds were higher than 85%. Scaffolds with nano-HAp filled exhibited better strain fixation ability compared to the unfilled ones. This indicated that the addition of nano-HAp could improve the shape fixation ability.

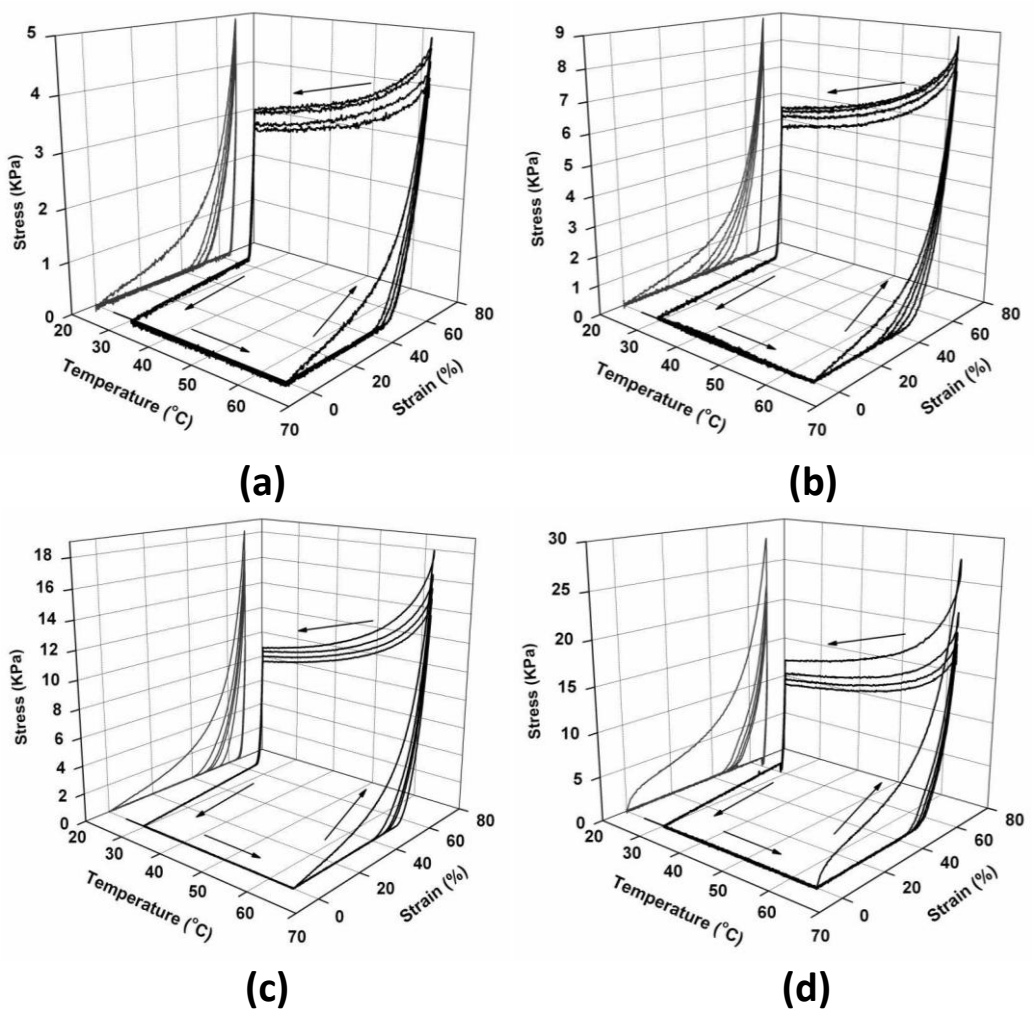

Figure 6.7 3D temperature-strain-stress curves and 2D strain-stress curves of cyclic thermo-mechanical compressive test of (a) unfilled PDLLA scaffolds and scaffolds with (b) 10, (c) 30 and (d) 50 wt% of nano-HAp at mechanical deformation of 70%

Table 6.1 Value for R_f and R_r calculated for the porous scaffolds at mechanical deformation of 50% and 70%

ε_m	Scaffolds	R_f (%)				R_r (%)			
		C1	C2	C3	C4	C1	C2	C3	C4
50%	**1:8**	92.6	90.8	88.6	86.4	85.6	98.4	96.9	97.5
	1:8+10%	99.2	99.0	98.8	96.2	100.0	100.0	99.9	96.6
	1:8+30%	99.6	99.0	98.6	98.0	91.8	98.9	98.8	97.3
	1:8+50%	99.5	99.4	99.4	99.3	79.4	99.7	95.6	99.7
70%	**1:8**	94.9	94.1	93.4	92.4	37.1	84.6	86.4	89.5
	1:8+10%	94.6	94.1	93.4	92.4	57.1	85.1	82.4	78.6
	1:8+30%	94.4	93.6	92.7	91.3	42.9	80.0	91.7	72.7
	1:8+50%	97.3	97.1	96.9	96.6	37.1	88.5	91.3	90.5

When comparing the R_r (1st cycle) of the scaffolds with different amounts of nano-HAp incorporation, scaffolds with 10 wt% of nano-HAp showed a highest R_r of 100% and 57.1% when ε_m was 50% and 70%, respectively. The R_r of the scaffolds decreased when the nano-HAp filled fraction further increased to 30 and 50 wt%. This reduction is due to the disruption of the interactions among the hard segments (e.g. the damage of the struts in the porous structure) under compression and the obstruction of the mobility of PDLLA chain segments. The scaffolds showed good shape recoverability after the first cycle since all the R_r values were higher than 80%. Moreover, the R_f and R_r of the scaffolds at 50% deformation were higher than those at 70%. These results show that the recoverability of the PDLLA/nano-HAp scaffold was sensitive to the nano-HAp filled fraction and the testing factor (e.g. maximum strain).

6.4.2 Physical Shape Memory Test

The physical bending test was performed in a hot water bath at 65 °C to examine the shape memory effects and actuation behavior of the PDLLA scaffolds with different

amounts of nano-HAp. The samples with dimensions 240×4×2.5 mm were bent to a "U" shape at 65 °C, and the deformed shape was fixed by quickly cooling at room temperature while maintaining the deformation load. The samples were then put back into the 65 °C hot water bath and their shape changes and recovery times were recorded.

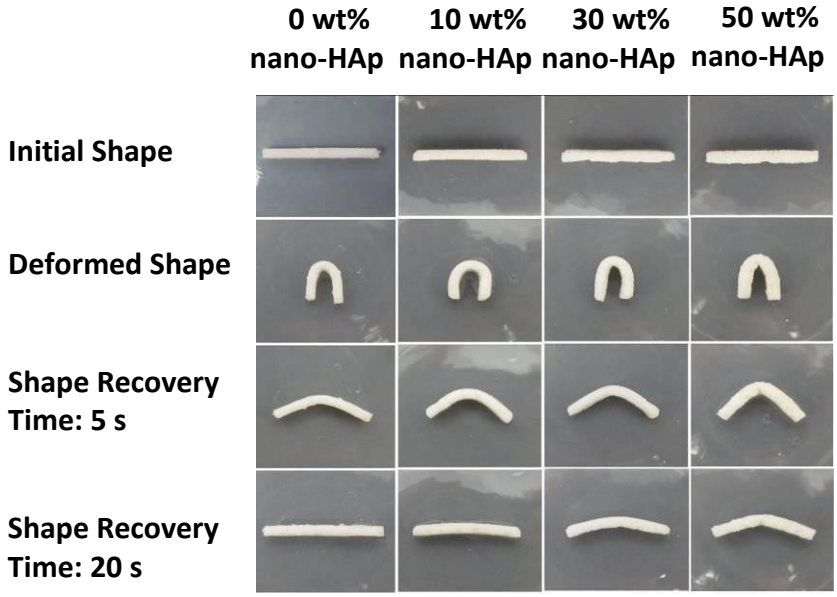

Figure 6.8 The shape recoverability of the porous scaffolds as a function of nano-HAp fraction and time at 65 °C

Images of the whole process of the physical shape memory tests of the porous PDLLA scaffolds with different amounts of nano-HAp fill are presented in Figure 6.8. The first row shows the porous scaffolds with their original shapes. The second row shows the porous scaffolds after being bent around a small mandrel at 65 °C, then constrained and cooled to room temperature. Rows three and four show photographs recording the shape recovery at 5 s and 20 s after the temperature was increased to 65 °C. Unfilled PDLLA and the composite with 10 wt% nano-HAp incorporation showed good shape recoverability since they almost recovered to their original shapes within 20 s. In this

PDLLA/nano-HAp composite system, the nano-HAp and the temporary entanglements of the polymer chains acted as the physical netpoints which could be used for the fixation of the permanent shape. The amorphous PDLLA (switching segments) became flexible when the temperature increase to 65 °C and the composite could be deformed elastically. And the deformed shape could be fixed when the temperature cooled back to room temperature. The permanent shape recovered when the composite was heated up again. However, the scaffolds with 30 and 50 wt% of nano-HAp filled showed irreversible deformations. This is because the larger amount of nano-HAp (>10 wt%) restricted the movement of the amorphous PDLLA chain segments and the damage of the scaffolds under compression. This phenomenon is in a good agreement with the cyclic thermomechanical tests.

Table 6.2 Shape recovery time of the porous scaffolds recovered from "U" shape to their original "I" shape at 65 °C

Scaffolds	**1:8**	**1:8 +10%**	**1:8 +30%**	**1:8 +50%**
Shape Recovery Time (s)	8	4	14	20

The shape recovery times of the scaffolds are shown in Table 6.2. The scaffolds with 10 wt% of nano-HAp recovered faster than the unfilled ones and the scaffolds with higher fraction of nano-HAp. Small amount of nano-HAp (e.g. 10 wt%) act as reinforcing fillers and netpoints in the shape memory composites, not only shortening the shape recovery time but also improving the mechanical properties, shape recoverability and shape fixation ability. Though the transition temperature is 65 ℃ for the PDLLA/nano-HAp, the scaffold still showed a potential as a bone scaffold in bone tissue engineering for minimally invasive surgery. Co-polymers or block-polymers derived from PDLLA

and other polymers may be developed with a lower transition temperature in the next stage of this study.

6.5 Summary

The effect of nano-HAp on the thermal properties and shape memory effect of the porous PDLLA composite were investigated. The T_i and T_g increased with the increasing amounts of nano-HAp particles, which directly affected the mechanical properties and shape memory behavior of the composites by increasing the shape transition temperature. Porous PDLLA/nano-HAp composites fabricated in this study showed desirable shape memory effects from the cyclic thermomechanical test and physical shape memory test. The sample still showed good shape recoverability after 4 cycles. PDLLA with 10 wt% nano-HAp possessed the best shape fixity, recoverability and shortest shape recovery time of only 4 seconds. The addition of nano-HAp (30 and 50 wt%) restricted the movement of the PDLLA chain segments and reduced the crystallinity of the PDLLA chains, which resulted in the residual deformation and slow recovery time. PDLLA/nano-HAp showed a better shape memory effect when the applied maximum strain was 50% than that at 70%. The degree of the SMPCs compressed also is another factor that influences the ability of shape fixation and recovery. The multifunctional PEG/Dex coated porous PDLLA/nano-HAp scaffolds fabricated were confirmed to have controllable interconnected porous structure, improved mechanical properties, good cellular response, bioactivity, degradability, drug release function and great shape memory properties. Therefore, PEG/Dex coated PDLLA/nano-HAp scaffolds have a high potential in bone tissue engineering applications.

Chapter 7. Conclusions and Statement of Originality

7.1 Overall Conclusions

A new technique was developed for bone scaffold fabrication. This technique can independently control the pore size and porosity of the scaffolds by means of particle sizes and the amounts of NaCl, whereas the present gas forming/particulate leaching method has difficulty in controlling the pore size. The solvent residual can be greatly reduced by the polymer coagulation and vacuum drying processes when compared with the conventional solvent casting/particulate leaching method. Moreover, the gel-like polymer based paste formed by coagulation of the polymer in the non-solvent proved easy to mold and produced a more uniform NaCl distribution in the polymer matrix without the formation of a skin layer. Scaffolds having a highly interconnected pore structure and uniform pore distribution can be fabricated using this technique. Unlike the thermal electrospinning and compression molding method, the PC-DC technique is a low temperature approach which can be applied to a wide range of polymer based materials. Compared with SFF, the PC-DC technique can be easily carried out and it does not need costly equipment. Dex is effectively loaded into the matrix, confirming that the subsequent PEG/Dex coating process is a suitable alternative method for drug loading, especially for water soluble drugs. This process avoids a premature drug loss when the drug is incorporated into the scaffold during the scaffold fabrication process. Using this technique, PEG/Dex coated porous PDLLA/nano-HAp porous scaffolds with similar mechanical properties to human cancellous bone, shape memory effect and drug release function were successfully fabricated.

The cellular response on the PDLLA based scaffolds showed that the cell adhesion, proliferation and differentiation were highly influenced by the chemical composition and microstructure of the scaffolds. The PDLLA based composites fabricated by the proposed method, with pore sizes from 200 to 350 μm and porosity from 60% to 80%, demonstrated good ability for supporting the cell attachment and ingrowth. All the samples were covered by a monolayer of cells after 7 days of culture and no cytotoxic responses were observed. Higher porosity of the scaffold, more cell adhesion and faster proliferation rate of the cells on the scaffold were found. Addition of nano-HAp in the PDLLA was proven to facilitate osteogenic differentiation of the osteoblast progenitor MG63 cells. Moreover, bonelike apatite formation on the scaffolds after SBF incubation showed an improved bioactivity by nano-HAp incorporation which could assist bone bonding. Incorporation of nano-HAp slows down the polymer degradation and mass loss of the nano-HAp filled scaffolds. In vitro evaluation of the mechanical properties of the scaffolds showed that the weight loss, polymer plasticization, and degradation of the PDLLA/nano-HAp scaffolds resulted in a reduction of their compressive moduli and strengths. On the other hand, compressive moduli and the strengths of the scaffolds were improved due to the rigid apatite formation on them after the SBF incubation. Moreover, the PDLLA/nano-HAp scaffolds had a pH buffering effect during incubation in the SBF, which reduces the risk of chronic inflammation complications.

The influences of the nano-HAp fraction on the multifunctionalities of the composites have been investigated. PDLLA based composites with larger nano-HAp content had higher initial drug loading amounts and larger total drug release amounts. Higher compressive moduli and strengths could be achieved by the larger amounts of nano-

HAp incorporation. The significant improvement of the wettability of the composites was achieved by the incorporation of nano-HAp particles and the coating of the PEG/Dex films. Desirable shape memory effects of the porous PDLLA/nano-HAp scaffolds fabricated in this study were confirmed by the cyclic thermomechanical and physical shape memory tests. Nano-HAp with 10 wt% in PDLLA was shown to be the best fraction since the scaffold produced possessed the best shape fixity, recoverability and shortest shape recovery time. The addition of nano-HAp (30 and 50 wt%) restricted the movement of PDLLA chain segments and reduced the crystallinity of the PDLLA chains, which resulted in the residual deformation. These indicated that the shape memory effects of the PDLLA scaffolds can be controlled by the nano-HAp filled fraction. All these demonstrate that multifunctional porous PDLLA/nano-HAp composites have a high potential for minimally invasive surgery and bone tissue engineering applications. The PC-DC technique described in this study provides a new route for the fabrication of drug loaded scaffolds for bone tissue engineering.

7.2 Originality and Contributions of the Research Work

This study provides a novel way for the fabrication of multifunctional scaffold material with drug releasing function, shape memory effect and controllable biodegradation rate. The PC-DC technique solves the problem of non-uniform pore distribution within a composite matrix fabricated by the conventional solvent casting/particulate leaching method. Moreover, it shortens the solvent evaporation time and reduces solvent residuals by polymer coagulation and vacuum drying steps. This low temperature fabrication technique prevents the thermal decomposition of drug inclusion and the

polymer contributes to a wider range of choices of drug loadings and polymer matrices for bone scaffold fabrication.

This proposed technique provides the ability to develop multifunctional porous scaffolds which have a similar structure and mechanical properties as human bone. Porous PDLLA/nano-HAp composites were first coated with PEG/Dex film as a model system for bone tissue scaffold materials. The PEG/Dex coated PDLLA/nano-HAp composites then fabricated have many advantages: (a) controllable biodegradability of the scaffold will avoid secondary surgery to take out the implants after tissue recovery; (b) controllable mechanical properties of the scaffold will be in phase with the tissue regeneration; (c) adjustable total drug release amounts provide relatively high therapeutic efficacy to the diseased tissue to obtain a faster recover rate; (d) excellent bioactivity (bone like apatite formation) and biocompatibility of the scaffold facilitates cell adhesion, growth, and differentiation; (e) scaffolds with shape memory effect have the ability to be precisely positioned in the body by minimal invasive techniques in a temporary small shape and then gain their application-relevant shape after implantation; (f) scaffolds have an active cellular response and high potential in bone tissue engineering.

This is the first time the change of the mechanical properties of the porous PDLLA/nano-HAp composite scaffolds during incubation in a SBF has been evaluated. Mechanical properties of bone scaffolds change after implantation by the complex interactions between the scaffolds and the body fluid (e.g. degradation of the scaffolds, bonelike apatite formation on the scaffolds, and plasticization of the polymer matrix).

To evaluate and control the mechanical property changes are of crucial important for the success of a scaffold for bone tissue engineering. The results showed that nano-HAp incorporation and apatite formation made a positive impact on the mechanical properties of the scaffolds; however, plasticization and degradation of PDLLA had a negative impact. An interesting phenomenon was found in that the PDLLA/nano-HAp composites had a fast degradation rate during the first 7 days incubation and the degradation rate slowed down in the following 21 days. This information could facilitate the design and fabrication of porous biodegradable scaffolds for different bone defects.

It is amongst the first attempts to determine the shape memory behavior of the porous PDLLA/nano-HAp composites. Controlling the nano-HAp filling fraction of the scaffold could affect the shape memory effects of the scaffolds. PDLLA with 10 wt% nano-HAp showed the best fixity and recoverability when compared with those filled with 30 and 50 wt% nano-HAp. Moreover, the larger the maximum strain applied to the test sample, the lower the shape recovery ratios. The addition of nano-HAp (30 and 50 wt%) restricted the movement of PDLLA chain segments and reduced the crystallinity of the PDLLA chains, which resulted in the residual deformation.

This research is the first in regard to the cellular response of the PDLLA/nano-HAp composites using a MG63 cell model. The results showed that the PDLLA based scaffolds fabricated in this study are biocompatible and facilitate cell attachment and proliferation. The pore size of the fabricated scaffolds ranged from 200 to 350 μm and the high porosity of 60% to 80% allowed cells to host and penetrate inside the scaffolds.

The whole scaffolds covered by the MG63 cells were observed after 7 days of culture, during which time, the number of cells on the PDLLA based substrates increased. Moreover, the scaffolds with higher porosity were beneficial for cell attachment, growth, migration and differentiation. Nano-HAp incorporation that promoted calcium deposition (cell mineralization/osteoconduction) was also found.

7.3 Research Outputs

Some findings from this study gave rise to the following research outputs:

1. **Chen L**., Tang C.Y., Chen D.Z., Wong C.T., Tsui C.P., Fabrication and characterization of poly-D-L-lactide/nano-hydroxyapatite composite scaffolds with poly(ethylene glycol) coating and dexamethasone releasing, Composites Science and Technology, 2011;71(16):1842-1849.

2. **Chen L.**, Tang C.Y., Tsui C.P., Chen D.Z., Mechanical properties and *in vitro* evaluation of bioactivity of bioactivity, degradation of dexamethasone-releasing poly-D-L-lactide/nano-hydroxyapatite composite scaffolds, Journal of the Mechanical Behavior of Biomedical Materials, 2013;22:41-50.

3. **Chen L.**, Tang C.Y., Ku H.S.L., Tsui C.P., Chen X., Microwave sintering and characterization of polypropylene/multi-walled carbon nanotube/hydroxyapatite composites, Composite Part B, 2014;56:504-511.

4. **Chen L.**, Tang C.Y., H.S. Ku, Chen D.Z., Tsui C.P., Surface coating of poly-D-L-lactide/nano- hydroxyapatite composite scaffolds for dexamethasone-releasing function

and wettability enhancement, presented at the Materials Science & Technology 2012 Conference & Exhibition, October 7-11, 2012, Pittsburgh, Pennsylvania, USA.

5. **Chen L.**, Tang C.Y., Tsui C.P., Chen D.Z., Fabrication and characterization of nano-HAp reinforced poly-D-L-lactide scaffolds with poly (ethylene glycol)/dexamethasone coatings, presented at the 6th Asia-Europe Symposium on Processing and Properties of Reinforced Polymers, June 2-6, 2013, Wuhan, China

6. **Chen L**., Tang C.Y., Tsui C.P., Chen D.Z., Thermal characterization and shape memory effect of porous poly-D-L-lactide/nano-hydroxyapatite composite scaffolds, under preparation.

7. **Chen L**., Tang C.Y., Tsui C.P., Chen D.Z., Human osteoblast-like cells (MG63) proliferation on poly-D-L-lactide/nano-hydroxyapatite composite scaffolds with poly(ethylene glycol) coating and dexamethasone releasing, under preparation.

7.4 Suggestions for Future Work

In this study, PEG/Dex coated PDLLA/nano-HAp composite scaffolds have been fabricated using the newly developed technique. Despite the microstructures, degradability, drug release behavior, mechanical properties, shape memory effects, bioactivity and *in vitro* cellular investigation of the scaffolds being extensively studied, there are some related issues worthy of further investigation, as follows:

i. Surface modification of the PEG/Dex coating by incorporating some other bioactive

organic components, such as collagen, Arg-Gly-Asp tripeptide, and growth factors, may be undertaken to further improve the cell adhesion and osteoconductivity of the scaffolds and promote cellular adhesion, growth and differentiation.

ii. Microcapsules with bioactive drugs inside may be developed and coated on the scaffolds for a controllable drug delivery system. The drug release rate can be controlled by the thickness and degradation rate of the microcapsules.

iii. Co-polymers or block-polymers derived from PDLLA with controllable shape memory effect and transition temperatures close to the human body temperature may be developed, and may show a higher potential for bone tissue engineering.

iv. Preclinical studies, such as animal model experiments, may be conducted in vivo to further evaluate and ascertain the performance of the PDLLA/nano-HAp scaffolds with PEG/Dex coatings. The experiments should begin with small animals and proceed to larger animals after some positive results emerge.

v. Based on the relationship between the shape memory behavior, drug release profile, degradation, apatite formation and mechanical properties changes of the produced composites, a finite element model can be developed to simulate the behavior of the materials implanted into a human body. This finite element model may facilitate the design and manufacture of multifunctional composite bone scaffolds and provide a powerful tool to develop the material and meet patient-specific functional requirements.

References

Adams S.B.J., Shamji M.F., Nettles D.L., Hwang P., Setton L.A. 2009, "Sustained Release of Antibiotics From Injectable and Thermally Responsive Polypeptide Depots", *Journal of Biomedical Materials Research Part B-Applied biomaterials,* vol. 90B, no. 1, pp. 67-74.

Agarwal, S., Wendorff, J.H., Greiner, A. 2008, "Use of electrospinning technique for biomedical applications", *Polymer,* vol. 49, no. 26, pp. 5603-5621.

Agrawal, C.M., Ray, R.B. 2001, "Biodegradable polymeric scaffolds for musculoskeletal tissue engineering", *Journal of Biomedical Materials Research,* vol. 55, no. 2, pp. 141-150.

Albrektsson, T., Johansson, C. 2001, "Osteoinduction, osteoconduction and osseointegration", *European Spine Journal,* vol. 10, no. 2, pp. 96-101.

Aleksendrić, D., Balac, I., Tang C,Y,, Tsui, C.P., Ushokovic, P.S., Ushokovic, D.P. 2010, "Surface characterisation of PLLA polymer in HAp/PLLA biocomposite material by means of nanoindentation and artificial neural networks". *Advances in Applied Aeramics,* vol. 109, no. 2, pp.65-70.

Ang, K.C., Leong, K.F., Chua, C.K., Chandrasekaran, M. 2007, "Compressive properties and degradability of poly(e-caprolatone)/ hydroxyapatite composites under accelerated hydrolytic degradation", *Journal of Biomedical Materials Research - Part A,* vol. 80, no. 3, pp. 655-660.

Anklekar, R.M., Agrawal, D.K., Roy, R.B. 2001, "Microwave sintering and mechanical properties of PM copper steel", *Powder Metallurgy,* vol. 44, no. 4, pp. 355-362.

Anselme, K. 2000, "Osteoblast adhesion on biomaterials", *Biomaterials,* vol. 21, no. 7, pp. 667-681.

Anselme, K., Ponche, A., Bigerelle, M. 2010, "Relative influence of surface topography and surface chemistry on cell response to bone implant materials. Part 2: Biological aspects", *Proceedings of the Institution of Mechanical Engineers, Part H: Journal of Engineering in Medicine,* vol. 224, no. 12, pp. 1487-1507.

Anthony Atala, "Printing a human kidney", Filmed on March 2011 at TED2011, http://www.ted.com/talks/anthony_atala_printing_a_human_kidney

Armentano, I., Dottori, M., Fortunati, E., Mattioli, S., Kenny, J.M. 2010, "Biodegradable polymer matrix nanocomposites for tissue engineering: A review", *Polymer Degradation and Stability,* vol. 95, no. 11, pp. 2126-2146.

Assouline, E., Wachtel, E., Grigull, S., Lustiger, A., Wagner, H.D., Marom, G. 2001, "Lamellar twisting in a isotactic polypropylene transcrystallinity investigated by synchrotron microbeam X-ray diffraction", *Polymer,* vol. 42, no. 14, pp. 6231-6237.

Babensee, J.E., Anderson, J.M., McIntire, L.V., Mikos, A.G. 1998, "Host response to tissue engineered devices", *Advanced Drug Delivery Reviews,* vol. 33, no. 1-2, pp. 111-139.

Baer, G.M., Small IV, W., Wilson, T.S., Benett, W.J., Matthews, D.L., Hartman, J., Maitland, D.J. 2007, "Fabrication and in vitro deployment of a laser-activated shape memory polymer vascular stent", *BioMedical Engineering Online,* vol. 6. art. no. 43.

Bao, T.Q., Franco, R.A., Lee, B.T. 2011, "Preparation and characterization of novel poly(e-caprolactone)/ biphasic calcium phosphate hybrid composite microspheres", *Journal of Biomedical Materials Research - Part B Applied Biomaterials,* vol. 98 B, no. 2, pp. 272-279.

Behrend, M., Kluge, E., Schüttler, W. 2006, "On the use of unsealed polypropylene mesh as tracheal replacement", *ASAIO Journal,* vol. 52, no. 3, pp. 328-333.

Bhattacharyya, A.R., Sreekumar, T.V., Liu, T., Kumar, S., Ericson, L.M., Hauge, R.H., Smalley, R.E. 2003, "Crystallization and orientation studies in polypropylene/single wall carbon nanotube composite", *Polymer,* vol. 44, no. 8, pp. 2373-2377.

Bianco, A., Di Federico, E., Moscatelli, I., Camaioni, A., Armentano, I., Campagnolo, L., Dottori, M., Kenny, J.M., Siracusa, G., Gusmano, G. 2009, "Electrospun poly(e-caprolactone)/Ca-deficient hydroxyapatite nanohybrids: Microstructure, mechanical properties and cell response by murine embryonic stem cells", *Materials Science and Engineering C,* vol. 29, no. 6, pp. 2063-2071.

Biondi M., Ungaro F., Quaglia F., Netti P.A. 2008, "Controlled drug delivery in tissue engineering", *Advanced Drug Delivery Reviews,* vol. 60, pp. 229-242.

Black, J., Hastings, G. 1998, *Handbook of Biomaterial Properties,* Chapman & Hall, London.

Blaker, J.J., Bismarck, A., Boccaccini, A.R., Young, A.M., Nazhat, S.N. 2010, "Premature degradation of poly(α-hydroxyesters) during thermal processing of Bioglass®-containing composites", *Acta Biomaterialia,* vol. 6, no. 3, pp. 756-762.

Blaker, J.J., Maquet, V., Jérôme, R., Boccaccini, A.R., Nazhat, S.N. 2005, "Mechanical properties of highly porous PDLLA/Bioglass® composite foams as scaffolds for bone tissue engineering", *Acta Biomaterialia,* vol. 1, no. 6, pp. 643-652.

Blaker, J.J., Nazhat, S.N., Maquet, V., Boccaccini, A.R. 2011, "Long-term in vitro degradation of PDLLA/Bioglass® bone scaffolds in acellular simulated body fluid", *Acta Biomaterialia,* vol. 7, no. 2, pp. 829-840.

Blau, H.M., Brazelton, T.R., Weimann, J.M. 2001, "The evolving concept of a stem cell: Entity or function?", *Cell,* vol. 105, no. 7, pp. 829-841.

Boccaccini, A.R., Blaker, J.J., Maquet, V., Day, R.M., Jérôme, R. 2005, "Preparation and characterisation of poly(lactide-co-grycolide) (PLGA) and PLGA/Bioglass® composite tubular foam scaffolds for tissue engineering applications", *Materials Science and Engineering C,* vol. 25, no. 1, pp. 23-31.

Boland, E., Wnek, G., Simpson, D., Pawlowski, K., Bowlin, G. 2001, "Tailoring tissue engineering scaffolds using electrostatic processing techniques: A study of poly(glycolic acid) electrospinning", *Journal of Macromolecular Science-pure and Applied Chemisry,* vol. 38, no. 12, pp. 1231-1243.

Bose, S., Roy, M., Bandyopadhyay, A. 2012, "Recent advances in bone tissue engineering scaffolds", *Trends in Biotechnology,* vol. 30, no. 10, pp. 546-554.

Bucholz, R. 2002, "Nonallograft osteoconductive bone graft substitutes", *Clinical Orthopaedics and Related Research,* vol. 395, pp. 44-52.

Burr, D.B. & Akkus, O. 2014, "Bone Morphology and Organization" in *Basic and Applied Bone Biology*, eds. D.B. Burr & M.R. Allen, Academic Press, San Diego, pp. 3-25.

Buttery, L.D.K., Bourne, S., Xynos, J.D., Wood, H., Hughes, F.J., Hughes, S.P.F., Episkopou, V., Polak, J.M. 2001, "Differentiation of osteoblasts and in Vitro bone formation from murine embryonic stem cells", *Tissue Engineering,* vol. 7, no. 1, pp. 89-99.

Cai, B.L., Chang, Y.G., Mei, J.H., Ji, W.W., Yi, F.P., Yang, D.Z., Guo, Z.L., Ma, L.G., Wang, K., Ming, J.T., Yu, Q.W., Qian, Z.Y. 2008, "Thermoreversible gel-sol behavior of biodegradable PCL-PEG-PCL triblock copolymer in aqueous solutions", *Journal of Biomedical Materials Research - Part B Applied Biomaterials,* vol. 84, no. 1, pp. 165-175.

Calandrelli, L., Calarco, A., Laurienzo, P., Malinconico, M., Petillo, O., Peluso, G. 2008, "Compatibilized polymer blends based on PDLLA and PCL for application in bioartificial liver", *Biomacromolecules,* vol. 9, no. 6, pp. 1527-1534.

Campanelli, G., Catena, F. & Ansaloni, L. 2008, "Prosthetic abdominal wall hernia repair in emergency surgery: From polypropylene to biological meshes", *World Journal of Emergency Surgery,* vol. 3, no. 1.

Caplan, A.I. 1994, "The mesengenic process", *Clinics in Plastic Surgery*, vol. 21, no. 3, pp. 429-435.

Cartmell, S., Huynh, K., Lin, A., Nagaraja, S., Guldberg, R. 2004, "Quantitative microcomputed tomography analysis of mineralization within three-dimensional

scaffolds in vitro". *Journal of Biomedical Materials Research-Part A*, vol. 69, no. 1, pp. 97-104.

Causa, F., Netti, P.A., Ambrosio, L., Ciapetti, G., Baldini, N., Pagani, S., Martini, D., Giunti, A. 2006, "Poly-e-caprolactone/hydroxyapatite composites for bone regeneration: In vitro characterization and human osteoblast response", *Journal of Biomedical Materials Research - Part A*, vol. 76, no. 1, pp. 151-162.

Causa, F., Netti, P.A., Ambrosio, L. 2007, "A multi-functional scaffold for tissue regeneration: The need to engineer a tissue analogue", *Biomaterials*, vol. 28, no. 34, pp. 5093-5099.

Charlesby, A. (ed) 1960, *Atomic Radiation and Polymers*, Pergamon Press, New York.

Chen, G.P., Ushida, T., Tateishi, T. 2001, "Development of biodegradable porous scaffolds for tissue engineering", *Materials Science and Engineering C*, vol. 17, no. 1-2, pp. 63-69.

Chen, D.Z., Tang, C.Y., Chan, K.C., Tsui, C.P., Yu, P.H.F., Leung, M.C.P., Uskokovic, P.S. 2007, "Dynamic mechanical properties and in vitro bioactivity of PHBHV/HA nanocomposite", *Composites Science and Technology*, vol. 67, no. 7-8, pp. 1617-1626.

Chen, Y., Mak, A., Li, J., Wang, M., Shum, A. 2005, "Formation of apatite on poly(alpha-hydroxy acid) in an accelerated biomimetic process", *Journal of Biomedical Materials Research,Part B*, vol. 73B, no. 1, pp. 9-9.

Chen, B., Sun, K. 2005, "Poly (e-caprolactone)/hydroxyapatite composites: Effects of particle size, molecular weight distribution and irradiation on interfacial interaction and properties", *Polymer Testing*, vol. 24, no. 1, pp. 64-70.

Chen, G., Ushida, T., Tateishi, T. 2002, "Scaffold design for tissue engineering", *Macromolecular Bioscience*, vol. 2, no. 2, pp. 67-77.

Chen, J., Mwenifumbo, S., Langhammer, C., McGovern, J.P., Li, M., Beye, A., Soboyejo, W.O. 2007, "Cell/surface interactions and adhesion on Ti-6Al-4V: Effects of surface texture", *Journal of Biomedical Materials Research, Part B*, vol. 82B, no. 2, pp. 360-373.

Chen, L., Tang, C.Y., Chen, D.Z., Wong, C.T., Tsui, C.P. 2011, "Fabrication and characterization of poly-D-L-lactide/nano-hydroxyapatite composite scaffolds with poly (ethylene glycol) coating and dexamethasone releasing", *Composites Science and Technology*, vol. 71, no. 16, pp. 1842-1849.

Chen, L., Tang, C.Y., Tsui, C.P., Chen, D.Z. 2013, "Mechanical properties and in vitro evaluation of bioactivity and degradation of dexamethasone-releasing poly-D-L-

lactide/nano-hydroxyapatite composite scaffolds", *Journal of the Mechanical Behavior of Biomedical Materials*, vol. 22, pp. 41-50.

Chen, V.J., Smith, L.A., and Ma, P.X. 2006, "Bone regeneration on computer-designed nano-fibrous scaffolds", *Biomaterials*, vol. 27, no. 21, pp. 3973-3979.

Chou, Y., Chiou, W., Xu, Y., Dunn, J., Wu, B. 2004, "The effect of pH on the structural evolution of accelerated biomimetic apatite", *Biomaterials*, vol. 25, no. 22, pp. 9-9.

Chuenjitkuntaworn, B., Inrung, W., Damrongsri, D., Mekaapiruk, K., Supaphol, P., Pavasant, P. 2010, "Polycaprolactone/Hydroxyapatite composite scaffolds: Preparation, characterization, and in vitro and in vivo biological responses of human primary bone cells", *Journal of Biomedical Materials Research part A*, vol. 94A, no. 1, pp. 241-251.

Chung, H.J., Park, T.G. 2007, "Surface engineered and drug releasing pre-fabricated scaffolds for tissue engineering", *Advanced Drug Delivery Reviews*, vol. 59, no. 4-5, pp. 249-262.

Coleman, J.N., Khan, U., Gun'ko, Y.K. 2006, "Mechanical reinforcement of polymers using carbon nanotubes", *Advanced Materials*, vol. 18, no. 6, pp. 689-706.

Cooke, M.N., Fisher, J.P., Dean, D., Rimnac, C., Mikos, A.G. 2003, "Use of stereolithography to manufacture critical-sized 3D biodegradable scaffolds for bone ingrowth", *Journal of Biomedical Materials Research Part B*, vol. 64, no. 2, pp. 65-69.

Cooper, A., Bhattarai, N., Zhang, M. 2011, "Fabrication and cellular compatibility of aligned chitosan-PCL fibers for nerve tissue regeneration", *Carbohydrate Polymers*, vol. 85, no. 1, pp. 149-156.

Cooper, J.A., Lu, H.H., Ko, F.K., Freeman, J.W., Laurencin, C.T. 2005, "Fiber-based tissue-engineered scaffold for ligament replacement: Design considerations and in vitro evaluation", *Biomaterials*, vol. 26, no. 13, pp. 1523-1532.

Cosson, M., Debodinance, P., Boukerrou, M., Chauvet, M.P., Lobry, P., Crépin, G., Ego, A. 2003, "Mechanical properties of synthetic implants used in the repair of prolapse and urinary incontinence in women: Which is the ideal material?", *International Urogynecology Journal and Pelvic Floor Dysfunction*, vol. 14, no. 3, pp. 169-178.

Cowins, S.C. 1989, "Mechanics of Materials" in *Bone Mechanics*, ed. S.C. Cowins, pp. 15-42.

Currey, J.D. 2002, *Bones: Structure and Mechanics*, 1st edn, Princeton University Press, Princeton, USA.

Darney, P.D., Monroe, S.E., Klaisle, C.M., Alvarado, A. 1989, "Clinical evaluation of the Capronor contraceptive implant: Preliminary report", *American Journal of Obstetrics and Gynecology*, vol. 160, no. 5, pp. 1292-1295.

De Tayrac, R., Devoldere, G., Renaudie, J., Villard, P., Guilbaud, O., Eglin, G., Bénifla, J., Demaria, F., Blanchot, J., Broux, P., Cosson, M., Lucot, J., Delporte, P., Fernandez, H., Frayret, C., Hacquin, F., Maaliki, K., Marpeau, L., Sergent, F. 2007, "Prolapse repair by vaginal route using a new protected low-weight polypropylene mesh: 1-year functional and anatomical outcome in a prospective multicentre study", *International Urogynecology Journal and Pelvic Floor Dysfunction*, vol. 18, no. 3, pp. 251-256.

Deng, X.M., Hao, J.Y., Wang, C.S. 2001, "Preparation and mechanical properties of nanocomposites of poly(D,L-lactide) with Ca-deficient hydroxyapatite nanocrystals", *Biomaterials*, vol. 22, no. 21, pp. 2867-2873.

Deng, C., Weng, J., Lu, X., Zhou, S.B., Wan, J.X., Qu, S.X., Feng, B. & Li, X.H. 2008, "Preparation and in vitro bioactivity of poly(d,l-lactide) composite containing hydroxyapatite nanocrystals", *Materials Science and Engineering: C*, vol. 28, no. 8, pp. 1304-1310.

Deplaine, H., Ribelles, J.L.G., Ferrer, G.G. 2010, "Effect of the content of hydroxyapatite nanoparticles on the properties and bioactivity of poly(l-lactide)-Hybrid membranes", *Composites Science and Technology*, vol. 70, no. 13, pp. 1805-1812.

Dicesare, P., Fox, W.M., Hill, M.J., Krishnan, G.R., Yang, S., Sarkar, D. 2013, "Cell-material interactions on biphasic polyurethane matrix", *Journal of Biomedical Materials Research , Part A*, vol. 101 A, no. 8, pp. 2151-2163.

Donaruma, L.G. 1988, "Definitions in biomaterials, D. F. Williams, Ed., Elsevier, Amsterdam, 1987, 72 pp.", *Journal of Polymer Science, Part C*, vol. 26, no. 9, pp. 414-414.

Dorati, R., Colonna, C., Genta, I., Modena, T., Conti, B. 2010, "Effect of porogen on the physico-chemical properties and degradation performance of PLGA scaffolds", *Polymer Degradation and Stability*, vol. 95, no. 4, pp. 694-701.

Dordunoo, S.K., Jackson, J.K., Arsenault, L.A., Oktaba, A.M.C., Hunter, W.L., Burt, H.M. 1995, "Taxol encapsulation in poly(e-caprolactone) microspheres", *Cancer Chemotherapy and Pharmacology*, vol. 36, no. 4, pp. 279-282.

Dos Santos, E.A., Farina, M., Soares, G.A.,Anselme, K. 2009, "Chemical and topographical influence of hydroxyapatite and β-tricalcium phosphate surfaces on human osteoblastic cell behavior", *Journal of Biomedical Materials Research, Part A*, vol. 89, no. 2, pp. 510-520.

Douglas, T., Pamula, E., Hauk, D., Wiltfang, J., Sivananthan, S., Sherry, E., Warnke, P.H. 2009, "Porous polymer/hydroxyapatite scaffolds: Characterization and biocompatibility investigations", *Journal of Materials Science: Materials in Medicine,* vol. 20, no. 9, pp. 1909-1915.

Du, C., Cui, F.Z., Zhu, X.D., De Groot, K. 1999, "Three-dimensional nano-HAp/collagen matrix loading with osteogenic cells in organ culture", *Journal of Biomedical Materials Research,* vol. 44, no. 4, pp. 407-415.

Duarte, A.R.C., Mano, J.F., Reis, R.L. 2009, "Dexamethasone-loaded scaffolds prepared by supercritical-assisted phase inversion", *Acta Biomaterialia,* vol. 5, no. 6, pp. 2054-2062.

Esawi, A.M.K., Salem, H.G., Hussein, H.M., Ramadan, A.R. 2010, "Effect of processing technique on the dispersion of carbon nanotubes within polypropylene carbon nanotube-composites and its effect on their mechanical properties", *Polymer Composites,* vol. 31, no. 5, pp. 772-780.

Filho, O.P., La Torre, G.P., Hench, L.L. 1996, "Effect of crystallization on apatite-layer formation of bioactive glass 45S5", *Journal of Biomedical Materials Research,* vol. 30, no. 4, pp. 509-514.

Fisher, J.P., Dean, D., Mikos, A.G. 2002, "Photocrosslinking characteristics and mechanical properties of diethyl fumarate/poly(propylene fumarate) biomaterials", *Biomaterials,* vol. 23, no. 22, pp. 4333-4343,

Fu, S.Y., Feng, X.Q., Lauke, B., Mai, Y.W. 2008, "Effects of particle size, particle/matrix interface adhesion and particle loading on mechanical properties of particulate-polymer composites", *Composites, Part B,* vol. 39, no. 6, pp. 933-961.

Fung, Y.C. 1993, *Biomechanics mechanical properties of living tissue,* 2nd edn, Springer-Verlag New York, Inc., New York, USA.

Galli, R., Borello, U., Gritti, A., Minasi, M.G., Bjornson, C., Coletta, M., Mora, M., Cusella De Angelis, M.G., Fiocco, R., Cossu, G., Vescovi, A.L. 2000, "Skeletal myogenic potential of human and mouse neural stem cells", *Nature Neuroscience,* vol. 3, no. 10, pp. 986-991.

Gartland, A., Buckley, K.A., Dillon, J.P., Curran, J.M., Hunt, J.A., Gallagher, J.A. 2005, "Isolation and culture of human osteoblasts" in *Human Cell Culture Protocols,* ed. J. Picot, 2nd edn, Humana Press, Totowa, New Jersey, pp. 29-54.

Gartland, A., Buckley, K.A., Dillon, J.P., Curran, J.M., Hunt, J.A., & Gallagher, J.A. 2005, "Isolation and culture of human osteoblasts" in *Human cell culture protocols*, ed. J. Picot, 2nd edn, Humana Press, Totowa, New Jersey, pp. 29-54.

Geethamma, V.G., Kalaprasad, G., Groeninckx, G., Thomas, S. 2005, "Dynamic mechanical behavior of short coir fiber reinforced natural rubber composites", *Composites Part A: Applied Science and Manufacturing,* vol. 36, no. 11, pp. 1499-1506.

German R.M. 1989, *Particle packing characteristics,* Metal powder industries federation, Princeton, NJ.

Giannoudis, P.V., Dinopoulos, H., Tsiridis, E. 2005, "Bone substitutes: an update.", *Injury,* vol. 36 Suppl 3, pp. S20-27.

Giesen, E.B.W., Ding, M., Dalstra, M., Van Eijden, T.M.G.J. 2001, "Mechanical properties of cancellous bone in the human mandibular condyle are anisotropic", *Journal of Biomechanics,* vol. 34, no. 6, pp. 799-803.

Gollwitzer, H., Thomas, P., Diehl, P., Steinhauser, E., Summer, B., Barnstorf, S., Gerdesmeyer, L., Mittelmeier, W., Stemberger, A. 2005, "Biomechanical and allergological characteristics of a biodegradable poly(D, L-lactic acid) coating for orthopaedic implants", *Journal of Orthopaedic Research,* vol. 23, no. 4, pp. 802-809.

Gomes, M.E., Salgado A.J., Reis, R.L. 2002, *Polymer Based Systems on Tissue Engineering, Replacement and Regeneration,* 1st edition, Kluwer, Dordrecht, Netherlands.

Gong, X.H., Tang, C.Y., Wong, C.T., LU, W.W.J., Zhang, Y.G., Lam, W.M., Wu, S.P., Liu, J.N. 2010, "Fabrication of poly(lactic acid) scaffolds by a modified solvent casting/porogen leaching method". *E-Polymer,* no. 113, pp.1-9.

Guarino, V., Causa, F., Salerno, A., Ambrosio, L., Netti, P.A. 2008, "Design and manufacture of microporous polymeric materials with hierarchal complex structure for biomedical application", *Materials Science and Technology,* vol. 24, no. 9, pp. 1111-1117.

Gunatillake, P., Mayadunne, R., Adhikari, R. 2006, "recent developments in biodegradable synthetic polymers". *Biotechnology Annual Review,* vol. 12, pp. 301-347.

Gunes, I.S., Jana, S.C. 2008, "Shape memory polymers and their nanocomposites: A review of science and technology of new multifunctional materials", *Journal of Nanoscience and Nanotechnology,* vol. 8, no. 4, pp. 1616-1637.

Harris, L.D., Kim, B.S., Mooney, D.J. 1998, "Open pore biodegradable matrices formed with gas foaming", *Journal of Biomedical Materials Research,* vol. 42, no. 3, pp. 396-402.

He, W., Ma, Z.W., Yong, T., Teo, W.E., Ramakrishna, S. 2005, "Fabrication of collagen-coated biodegradable polymer nanofiber mesh and its potential for endothelial cells growth", *Biomaterials,* vol. 26, no. 36, pp. 7606-7615.

Hearon, K., Singhal, P., Horn, J., Small, W., Olsovsky, C., Maitland, K.C., Wilson, T.S., Maitland, D.J. 2013, "Porous shape-memory polymers", *Polymer Reviews,* vol. 53, no. 1, pp. 41-75.

Heath, C.A. 2000, "Cells for tissue engineering", *Trends in biotechnology,* vol. 18, no. 1, pp. 17-19.

Hench, L.L. 1998, "Bioceramics", *Journal of the American Ceramic Society,* vol. 81, no. 7, pp. 1705-1728.

Hench LL, Wilson J, editors. An introduction to bioceramics. 2nd ed. London: Word Scientific; 1999.

Hile, D.D., Doherty, S.A., Trantolo, D.J. 2004, "Prediction of resorption rates for composite polylactide/hydroxylapatite internal fixation devices based on initial degradation profiles", *Journal of Biomedical Materials Research,* vol. 71B, no. 1, pp. 201-205.

Holland, T.A., Mikos, A.G. 2006, "Review: Biodegradable polymeric scaffolds. Improvements in bone tissue engineering through controlled drug delivery." *Tissue Engineering I: Advances in Biochemical Engineering/Biotechnology*, vol. 102, pp. 161-185.

Hollister, S.J. 2005, "Porous scaffold design for tissue engineering", *Nature Materials,* vol. 4, no. 7, pp. 518-524.

Holly, C.E., Schoichet, M.S., Davies, J.E. 2000, "Engineering three-dimensional bone tissue *in vitro* using biodegradable scaffolds: Investigating initial cell-seeding density and culture period", *Journal of Biomedical Materials Research*, vol. 51, pp. 376-382.

Hong, S.J., Yu, H.S., Kim, H.W. 2009, "Tissue engineering polymeric microcarriers with macroporous morphology and bone-bioactive surface", *Macromolecular Bioscience,* vol. 9, no. 7, pp. 639-645.

Hong, Z., Zhang, P., He, C., Qiu, X., Liu, A., Chen, L., Chen, X., Jing, X. 2005, "Nano-composite of poly(L-lactide) and surface grafted hydroxyapatite: Mechanical properties and biocompatibility", *Biomaterials,* vol. 26, no. 32, pp. 6296-6304.

Horbett, T.A. 2004, "The role of adsorbed proteins in tissue response to biomaterials" in *Biomaterials science, an introduction to materials in medicine,* ed. Ratner BD, Hoffman, A.S., Schoen, F.J., Lemons, J.E., 2nd edn, pp. 237-246.

Hou Q.P., Grijpma, D.W., Feijen, J. 2003, "Porous polymeric structures for tissue engineering prepared by a coagulation, compression moulding and salt leaching technique", *Biomaterials,* vol. 24, no. 11, pp. 1937-1947.

Huang, W.D., Zheng, Q.X., Sun, W.Q., Xu, H., Yang, X. 2007, "Levofloxacin implants with predefined microstructure fabricated by three-dimensional printing technique", *International journal of pharmaceutics,* vol. 339, no. 1-2, pp. 33-38.

Huang, W.D., Sun, W.Q., Zheng, Q.X., Guo, X.D., Yu, D.G., Liu, W., Xu, H.B., Yang, X.L. 2005, "Design and fabrication of drug delivery devices with complex architectures based onthree-dimensional printing technique", *Journal of Wuhan University of Technology (Materials science edition),* vol. 21, no. z1.

Huang, W.M., Ding, Z., Wang, C.C., Wei, J., Zhao, Y., Purnawali, H. 2010, "Shape memory materials", *Materials Today,* vol. 13, no. 7-8, pp. 54-61.

Hulse, G.K., Stalenberg, V., McCallum, D., Smit, W., O'Neil, G., Morris, N., Tait, R.J. 2005, "Histological changes over time around the site of sustained release naltrexone-poly(DL-lactide) implants in humans", *Journal of Controlled Release,* vol. 108, no. 1, pp. 43-55.

Hutmacher DW 2000, "Scaffolds in tissue engineering bone and cartilage", *Biomaterials,* vol. 21, no. 24, pp. 2529-2543.

Hutmacher, D.W. 2001, "Scaffold design and fabrication technologies for engineering tissues - State of the art and future perspectives", *Journal of Biomaterials Science, Polymer Edition,* vol. 12, no. 1, pp. 107-124.

Hutmacher, D.W., Schantz, J.T., Lam, C.X., Tan, K.C., Lim, T.C. 2007, "State of the art and future directions of scaffold-based bone engineering from a biomaterials perspective.", *Journal of Tissue Engineering and Regenerative Medicine,* vol. 1, no. 4, pp. 245-260.

Hutmacher, D.W., Schantz, J.T., Zein, I., Ng, K.W., Teoh, S.H.,Tan, K.C. 2001, "Mechanical properties and cell cultural response of polycaprolactone scaffolds designed and fabricated via fused deposition modeling", *Journal of Biomedical Materials Research,* vol. 55, no. 2, pp. 203-216.

Ichioka, N., Inaba, M., Kushida, T., Esumi, T., Takahara, K., Inaba, K., Ogawa, R., Iida, H., Ikehara, S. 2002, "Prevention of senile osteoporosis in SAMP6 mice by intrabone marrow injection of allogeneic bone marrow cells", *Stem Cells,* vol. 20, no. 6, pp. 542-551.

Inzana, J.A., Olvera, D., Fuller, S.M., Kelly, J.P., Graeve, O.A., Schwarz, E.M., Kates, S.L., Awad, H.A., 2014 "3D printing of composite calcium phosphate and collagen scaffolds for bone regeneration", *Biomaterials*, vol.35, no.13, , pp.4026-4034,

Lee, J.B, Lee, S.H., Yu, S.M., Park, J.C., Choi, J.B., Kim, J.K. 2008, "PLGA scaffold incorporated with hydroxyapatite for cartilage regeneration", *Surface & Coating Technology*, vol.202, pp. 5757-5761.

Li, J.l., Stocum, D.L. 2014, "Fracture Healing" in *Basic and Applied Bone Biology*, eds. D.B. Burr , M.R. Allen, Academic Press, San Diego, pp. 205-223.

Iolascon, G., Di Pietro, G., Capaldo, A., Gioia, C., Gatto, S., Gimigliano, F. 2010, "Periprosthetic bone density as outcome of therapeutic response", *Clinical Cases in Mineral and Bone Metabolism,* vol. 7, no. 1, pp. 27-31.

Ismail, F.S.M., Rohanizadeh, R., Atwa, S., Mason, R.S., Ruys, A.J., Martin, P.J., Bendavid, A. 2007, "The influence of surface chemistry and topography on the contact guidance of MG63 osteoblast cells", *Journal of Materials Science: Materials in Medicine,* vol. 18, no. 5, pp. 705-714.

Jaiswal, N., Haynesworth, S.E., Caplan, A.I., Bruder, S.P. 1997, "Osteogenic differentiation of purified, culture-expanded human mesenchymal stem cells in vitro", *Journal of Cellular Biochemistry*, vol. 64, no. 2, pp. 295-312.

Jeon, O., Krebs, M., Alsberg, E. 2011, "Controlled and sustained gene delivery from injectable, porous PLGA scaffolds", *Journal of Biomedical Materials Research - Part A,* vol. 98 A, no. 1, pp. 72-79.

Jeschke, B., Meyer, J., Jonczyk, A., Kessler, H., Adamietz, P., Meenen, N.M., Kantlehner, M., Goepfert, C. & Nies, B. 2002, "RGD-peptides for tissue engineering of articular cartilage", *Biomaterials*, vol. 23, no. 16, pp. 3455-3463.

Jones, J.R., Hench, L.L. 2001, "Biomedical materials for new millennium: Perspective on the future", *Materials Science and Technology*, vol. 17, no. 8, pp. 891-900.

Jose, M.V., Thomas, V., Johnson, K.T., Dean, D.R., Nyairo, E. 2009, "Aligned PLGA/HA nanofibrous nanocomposite scaffolds for bone tissue engineering", *Acta Biomaterialia*, vol. 5, no. 1, pp. 305-315.

Juhasz, J.A., Best, S.M., Bonfield, W., Kawashita, M., Miyata, N., Kokubo, T. Nakamura, T. 2003, "Apatite-forming ability of glass-ceramic apatite-wollastonite - Polyethylene composites: Effect of filler content", *Journal of Materials Science: Materials in Medicine,* vol. 14, no. 6, pp. 489-495.

Karageorgiou, V., Kaplan, D. 2005, "Porosity of 3D biornaterial scaffolds and osteogenesis", *Biomaterials*, vol. 26, no. 27, pp. 5474-5491.

Kawase, T., Bruce, J.N., Kaye, A.H. 2006, "Fibrin glue and polyglycolic acid nonwoven fabric as a biocompatible dural substitute: Commentary", *Neurosurgery*, vol. 58, no. SUPPL. 1.

Kearns, J.C., Shambaugh, R.L. 2002, "Polypropylene fibers reinforced with carbon nanotubes", *Journal of Applied Polymer Science,* vol. 86, no. 8, pp. 2079-2084.

Keselowsky, B.G., Collard, D.M., Garc ía, A.J. 2005, "Integrin binding specificity regulates biomaterial surface chemistry effects on cell differentiation", *Proceedings of the National Academy of Sciences of the United States of America,* vol. 102, no. 17, pp. 5953-5957.

Khademhosseini, A., Langer, R. 2007, "Microengineered hydrogels for tissue engineering", *Biomaterials,* vol. 28, no. 34, pp. 5087-5092.

Kim, B., Mooney, D.J. 1998, "Development of biocompatible synthetic extracellular matrices for tissue engineering", *Trends in Biotechnology,* vol. 16, no. 5, pp. 224-230.

Kim, H., Kim, H.W., Suh, H. 2003, "Sustained release of ascorbate-2-phosphate and dexamethasone from porous PLGA scaffolds for bone tissue engineering using mesenchymal stem cells", *Biomaterials,* vol. 24, no. 25, pp. 4671-4679.

Kim, H.D., Valentini, R.F. 2002, "Retention and activity of BMP-2 in hyaluronic acid-based scaffolds in vitro". *Journal of Biomedical Materials Research*, vol.59, no.3, pp. 573–84.

Kim, H.W, Knowles, JC, Kim, H.E. 2004, "Hydroxyapatite/poly(epsilon-caprolactone) composite coatings on hydroxyapatite porous bone scaffold for drug delivery", *Biomaterials,* vol. 25, no. 7-8, pp. 1279-1287.

Kim, H.W., Himeno, T., Kokubo, T., Nakamura, T. 2005, "Process and kinetics of bonelike apatite formation on sintered hydroxyapatite in a simulated body fluid", *Biomaterials,* vol. 26, no. 21, pp. 4366-4373.

Kim, H.W., Knowles, J.C., Kim, H.E. 2005, "Hydroxyapatite porous scaffold engineered with biological polymer hybrid coating for antibiotic Vancomycin release", *Journal of Materials Science: Materials in Medicine,* vol. 16, no. 3, pp. 189-195.

Kim, J.Y., Cho, D. 2009, "Blended PCL/PLGA scaffold fabrication using multi-head deposition system", *Microelectronic Engineering,* vol. 86, no. 4-6, pp. 1447-1450.

Kim, K., Yeatts, A., Dean, D., Fisher, J.P, 2010, "Stereolithographic bone scaffold design parameters: osteogenic differentiation and signal expression". *Tissue Engineering Part B Review.* vol. 16, no. 5, pp. 523-539.

Kim, K., Yu, M., Zong, X.H., Chiu, J., Fang, D.F., Seo, Y.S., Hsiao, B.S., Chu, B., Hadjiargyrou, M. 2003, "Control of degradation rate and hydrophilicity in electrospun non-woven poly(D,L-lactide) nanofiber scaffolds for biomedical applications", *Biomaterials,* vol. 24, no. 27, pp. 4977-4985.

Kim, S.S., Park, M. S., Jeon, O., Choi,Y.C., Kim, B.S. 2006, "Poly(lactide-co-glycolide)/hydroxyapatite composite scaffolds for bone tissue engineering", *Biomaterials*, vol. 27, no. 8, pp. 1399-1409.

Kim, S.S., Utsunomiya, H., Koski, J.A., Wu, B.M., Cima, M.J., Sohn, J., Mukai, K., Griffith, L.G., Vacanti, J.P. 1998, "Survival and function of hepatocytes on a novel three-dimensional synthetic biodegradable polymer scaffold with an intrinsic network of channels", *Annals of Surgery*, vol. 228, no. 1, pp. 8-13.

Kingshott, P., Griesser, H.J. 1999, "Surfaces that resist bioadhesion", *Current Opinion in Solid State and Materials Science*, vol. 4, no. 4, pp. 403-412.

Kissel W., Han J., Meyer J. 1999, "Polypropylene: structure, properties, manufacturing processes, and applications" in *Handbook of Polypropylene and Polypropylene Composites*, ed. Karian H., Marcel Dekker, Inc, pp. 15-38.

Koegler, W.S., Griffith, L.G. 2004, "Osteoblast response to PLGA tissue engineering scaffolds with PEO modified surface chemistries and demonstration of patterned cell response", *Biomaterials* vol. 25, no. 14, pp. 2819-2830.

Kokubo, T., Takadama, H. 2006, "How useful is SBF in predicting in vivo bone bioactivity?", *Biomaterials*, vol. 27, no. 15, pp. 2907-2915.

Kokubo, T. 1991, "Bioactive glass ceramics: properties and applications", *Biomaterials*, vol. 12, no. 2, pp. 155-163.

Kolan, K.C.R., Leu, M.C., Hilmas, G.E., Velez, M. 2012, "Effect of material, process parameters, and simulated body fluids on mechanical properties of 13-93 bioactive glass porous constructs made by selective laser sintering", *Journal of the Mechanical Behavior of Biomedical Materials*, vol. 13, no. 0, pp. 14-24.

Kothapalli, C.R., Shaw, M.T., Wei, M. 2005, "Biodegradable HA-PLA 3-D porous scaffolds: Effect of nano-sized filler content on scaffold properties", *Acta Biomaterialia*, vol. 1, no. 6, pp. 653-662.

Kovačević, V., Vrsaljko, D., Blagojević, S.L., Leskovac, M. 2008, "Adhesion parameters at the interface in nanoparticulate filled polymer systems", *Polymer Engineering and Science*, vol. 48, no. 10, pp. 1994-2002.

Kruyt, M.C., De Bruijn, J.D., Wilson, C.E., Oner, F.C., Van Blitterswijk, C.A., Verbout, A.J., Dhert, W.J.A. 2003, "Viable osteogenic cells are obligatory for tissue-engineered ectopic bone formation in goats", *Tissue Engineering*, vol. 9, no. 2, pp. 327-336.

Kuboki, Y., Takita, H., Kobayashi, D., Tsuruga, E., Inoue, M., Murata, M., Nagai, N., Dohi, Y., Ohgushi, H. 1998, "BMP-induced osteogenesis on the surface of hydroxyapatite with geometrically feasible and nonfeasible structures: Topology of

osteogenesis", *Journal of Biomedical Materials Research,* vol. 39, no. 2, pp. 190-199.

Landers, R., Hübner, U., Schmelzeisen, R., Mülhaupt, R. 2002a, "Rapid prototyping of scaffolds derived from thermoreversible hydrogels and tailored for applications in tissue engineering", *Biomaterials,* vol. 23, no. 23, pp. 4437-4447.

Landers, R., Pfister, A., Hübner, U., John, H., Schmelzeisen, R., Mülhaupt, R. 2002b, "Fabrication of soft tissue engineering scaffolds by means of rapid prototyping techniques", *Journal of Materials Science,* vol. 37, no. 15, pp. 3107-3116.

Langer, R. 1998, "Drug delivery and targeting", *Nature,* vol. 392, no. 6679 SUPPL., pp. 5-10.

Langer, R., Tirrell, D.A. 2004, "Designing materials for biology and medicine", *Nature,* vol. 428, no. 6982, pp. 487-492.

Langer, R., Vacanti, J.P. 1993, "Tissue Engineering", *Science,* vol. 260, no. 5110, pp. 920-926.

Laurencin, C.T., Ambrosio, A.M.A., Borden, M.D., Cooper Jr., J.A. 1999, *Tissue Engineering: Orthopedic Applications*.

Lee, J.B., Lee, S.H., Yu, S.M., Park, J.-., Choi, J.B. & Kim, J.K. 2008, "PLGA scaffold incorporated with hydroxyapatite for cartilage regeneration", *Surface and Coatings Technology,* vol. 202, no. 22-23, pp. 5757-5761.

Lee, K.W., Wang, S., Fox, B.C., Ritman, E.L., Yaszemski, M.J., and Lu, L. 2007, "Poly(propylene fumarate) bone tissue engineering scaffold fabrication using stereolithography: effects of resin formulations and laser parameters", *Biomacromolecules,* vol. 8, no. 4, pp. 1077-1084.

Lendlein, A., Langer, R. 2002, "Biodegradable, elastic shape-memory polymers for potential biomedical applications", *Science,* vol. 296, no. 5573, pp. 1673-1676.

Leng, J., Lan, X., Liu, Y., Du, S. 2011, "Shape-memory polymers and their composites: Stimulus methods and applications", *Progress in Materials Science,* vol. 56, no. 7, pp. 1077-1135.

Leong, K.F., Cheah, C.M., Chua, C.K. 2003, "Solid freeform fabrication of three-dimensional scaffolds for engineering replacement tissues and organs", *Biomaterials,* vol. 24, no. 13, pp. 2363-2378.

Li, H., Chang, J. 2005, "pH-compensation effect of bioactive inorganic fillers on the degradation of PLGA", *Composites Science and Technology,* vol. 65, no. 14, pp. 2226-2232.

Li, W.J., Jiang, Y.J., Tuan, R.S. 2008, "Cell-nanofiber-based cartilage tissue engineering using improved cell seeding, growth factor, and bioreactor technologies", *Tissue Engineering - Part A.*, vol. 14, no. 5, pp. 639-648.

Li, X., Liu, H., Wang, J., Li, C. 2012, "Preparation and characterization of poly(e-caprolactone) nonwoven mats via melt electrospinning", *Polymer,* vol. 53, no. 1, pp. 248-253.

Li, Y., Han, R., Wang, F. 2006, "Application of mesenchymal stem cells in bone and cartilage tissue engineering", *Chinese Journal of Clinical Rehabilitation,* vol. 10, no. 5, pp. 121-124.

Liang, J.Z., Yang, J., Tang, C.Y. 2010, "Die-swell behavior of PP/Al(OH)3/Mg(OH)2 flame retardent composite melts". *Polymer Testing*, vol. 29, pp.624-628 (2010)

Liao, S., Wang, W., Uo, M., Ohkawa, S., Aksaka, T., Tamura, K., Cui, F., Watari, F. 2005, "A three-layered nano-carbonated hydroxyapatite/collagen/PLGA composite membrane for guided tissue regeneration", *Biomaterials*, vol. 26, no. 36, pp. 7564.

Lin, A.S.P., Barrows, T.H., Cartmell, S.H., Guldberg, R.E. 2003, "Microarchitectural and mechanical characterization of oriented porous polymer scaffolds", *Biomaterials,* vol. 24, no. 3, pp. 481-489.

Lin, C.Y., Wirtz, T., LaMarca, F., Hollister, S.J. 2007, "Structural and mechanical evaluations of a topology optimized titanium interbody fusion cage fabricated by selective laser melting process", Journal of Biomedical Materials Research Part A, vol.83, no. 2, pp. 272-279.

Lincks, J., Boyan, B.D., Blanchard, C.R., Lohmann, C.H., Liu, Y., Cochran, D.L., Dean, D.D., Schwartz, Z. 1998, "Response of MG63 osteoblast-like cells to titanium and titanium alloy is dependent on surface roughness and composition", *Biomaterials,* vol. 19, no. 23, pp. 2219-2232.

Liu, C., Xia, Z., Czernuszka, J.T. 2007, "Design and development of three-dimensional scaffolds for tissue engineering", *Chemical Engineering Research and Design*, vol. 85, no. A7, pp. 1051-1064.

Liu, H., Lee, I., Wang, J., Yang, S., Young, T. 2004, "Preparation of PLLA membranes with different morphologies for culture of MG-63 Cells", *Biomaterials*, vol. 25, no. 18, pp. 4047-4056.

Liu, Y., Gall, K., Dunn, M. L., McCluskey, P. 2004, "Thermomechanics of shape memory polymer nanocomposites," *Mechanics of Materials,* vol. 36, pp. 929-940.

Liu, Y.G., Zhou, C.R. & Sun, Y. 2012, "A biomimetic strategy for controllable degradation of chitosan scaffolds", Journal of Materials Research, vol. 27, no. 14, pp. 1859-1868.

Lv, Q., Nair, L., Laurencin, C.T. 2009, "Fabrication, characterization, and *in vitro* evaluation of poly(lactic acid glycolic acid)/nano-hydroxyapatite composite microsphere-based scaffolds for bone tissue engineering in rotating bioreactors.", *Journal of Biomedical Materials Research - Part A*, vol. 91A, no. 3, pp. 679-691.

Ma, P.X., Zhang, R. 2001, "Microtubular architecture of biodegradable polymer scaffolds", *Journal of Biomedical Materials Research*, vol. 56, no. 4, pp. 469-477.

Ma, P.X. 2008, "Biomimetic materials for tissue engineering", *Advanced Drug Delivery Reviews*, vol. 60, no. 2, pp. 184-198.

Ma, X., Wu, T., Robich, M.P. 2012, "Drug-eluting stent coatings", *Interventional Cardiology*, vol. 4, no. 1, pp. 73-83.

Mandoli, C., Mecheri, B., Forte, G., Pagliari, F., Pagliari, S., Carotenuto, F., Fiaccavento, R., Rinaldi, A., Di Nardo, P., Licoccia, S., Traversa, E. 2010, "Thick soft tissue reconstruction on highly perfusive biodegradable scaffolds", *Macromolecular Bioscience*, vol. 10, no. 2, pp. 127-138.

Mano, J.f., Sousa, R.A., Boesel, L.F., Neves, N.M., Reis, R.L. 2004, "Bioinert, biodegradable and injectable polymeric matrix composites for hard tissue replacement: State of the art and recent developments", *Composites Science and Technology*, vol. 64, no. 6, pp. 789-817.

Maquet, V., Boccaccini, A.R., Pravata, L., Notingher, I., Jérôme, R. 2004, "Porous poly(α-hydroxyacid)/Bioglass® composite scaffolds for bone tissue engineering. I: Preparation and in vitro characterisation", *Biomaterials*, vol. 25, no. 18, pp. 4185-4194.

Marie, P.J. 2008, "Transcription factors controlling osteoblastogenesis", *Archives of Biochemistry and Biophysics*, vol. 473, no. 2, pp. 98-105.

Maspero, F.A., Ruffieux, K., Muller, B., Wintermantel, E. 2002, "Resorbabledefect analog PLGA scaffolds using CO_2 as solvent:structural characterization". *Journal of Biomedical Materials Research*, vol. 62, no.1, pp.89-98.

Matsuo, K., Irie, N. 2008, "Osteoclast-osteoblast communication", *Archives of Biochemistry and Biophysics*, vol. 473, no. 2, pp. 201-209.

Medtronic Inc., 2013, "Orthobiologics Market (Allografts, Viscosupplements, DBM, BMP, Stem Cell and Others) is Expected to Reach USD 5,519.9 Million Globally in 2019" *Transparency Market Research*, NY, PR Newswire Association LLC

Meng, Q., Hu, J. 2009, "A review of shape memory polymer composites and blends", *Composites Part A: Applied Science and Manufacturing*, vol. 40, no. 11, pp. 1661-1672.

Meyer, U.,Wiesmann, H.P. 2006, "Bone and cartilage" in *Bone and cartilage engineering*, eds. U. Meyer, H.P. Wiesmann, Springer, Germany, pp. 7-46.

Miaudet, P., Derré, A., Maugey, M., Zakri, C., Piccione, P.M., Inoubli, R., Poulin, P. 2007, "Shape and temperature memory of nanocomposites with broadened glass transition", *Science*, vol. 318, no. 5854, pp. 1294-1296.

Middleton, J.C., Tipton, A.J. 2000, "Synthetic biodegradable polymers as orthopedic devices", *Biomaterials*, vol. 21, no. 23, pp. 2335-2346.

Mikos, A.G., Sarakinos, G., Leite, S.M., Vacanti, J.P., Langer, R. 1993, "Laminated three-dimensional biodegradable foams for use in tissue engineering", *Biomaterials*, vol. 14, no. 5, pp. 323-330.

Mikos, A.G., Temenoff, J.S. 2000, "Formation of highly porous biodegradable scaffolds for tissue engineering", *Electronic Journal of Biotechnology*, vol. 3, no. 2, pp. 114-119.

Miller, R.A., Brady, J.M., Cutright, D.E. 1977, "Degradation rates of oral resorbable implants (polylactates and polyglycolates): Rate modification with changes in PLA/PGA copolymer ratios", *Journal of Biomedical Materials Research*, vol. 11, no. 5, pp. 711-719.

Mironov, V., Boland, T., Trusk, T., Forgacs, G., Markwald, R.R. 2003,"Organ printing: computer-aided jet-based 3D tissue engineering", *Trends in Biotechnology*, vol. 21, no. 4, pp. 157-161.

Mironov, V., Kasyanov, V., Drake, C., Markwald, R.R. 2008, "Organ printing: promises and challenges", *Regenative Medicine*, vol. 3, no.1, pp.93-103.

Mondal, S., Hu, J.L. 2006, "Temperature stimulating shape memory polyurethane for smart clothing", *Indian Journal of Fibre and Textile Research*, vol. 31, no. 1, pp. 66-71.

Mooney, D.J., Baldwin, D.F., Suh, N.P., Vacanti, J.P., Langer, R. 1996, "Novel approach to fabricate porous sponges of poly(D,L-lactic-co-glycolic acid) without the use of organic solvents", *Biomaterials*, vol. 17, no. 14, pp. 1417-1422.

Mourino, V., Boccaccini, A.R. 2010, "Bone tissue engineering therapeutics: controlled drug delivery in three-dimensional scaffolds", *Journal of The Royal Society Interface*, vol. 7, no. 43, pp. 209-227.

Nair, L.S., Laurencin, C.T. 2007, "Biodegradable polymers as biomaterials", *Progress in Polymer Science (Oxford)*, vol. 32, no. 8-9, pp. 762-798.

Nam, Y.S., Yoon, J.J., Park, T.G. 2000, "A novel fabrication method of macroporous biodegradable polymer scaffolds using gas foaming salt as a porogen additive", *Journal of Biomedical Materials Research,* vol. 53, no. 1, pp. 1-7.

Nazarov, R., Jin, H.J., Kaplan, D.L. 2004, "Porous 3-D scaffolds from regenerated silk fibroin". *Biomacromolecules*, vol.5, no.3, pp. 718-26.

Neffe, A.T., Hanh, B.D., Steuer, S., Lendlein, A. 2009, "Polymer networks combining controlled drug release, biodegradation, and shape memory capability", *Advanced Materials*, vol.22, pp. 3394–3398.

Ngabonziza, Y., Li, J., Barry, C.F. 2011, "Electrical conductivity and mechanical properties of multiwalled carbon nanotube-reinforced polypropylene nanocomposites", *Acta Mechanica*, vol. 220, no. 1-4, pp. 289-298.

Nikpour, M.R., Rabiee, S.M., Jahanshahi, M. 2012, "Synthesis and characterization of hydroxyapatite/chitosan nanocomposite materials for medical engineering applications", *Composites Part B,* vol. 43, no. 4, pp. 1881-1886.

Nukavarapu, S.P., Kumbar, S.G., Brown, J.L., Krogman, N.R., Weikel, A.L., Hindenlang, M.D., Nair, L.S., Allcock, H.R., Laurencin, C.T. 2008, "Polyphosphazene/nano-hydroxyapatite composite microsphere scaffolds for bone tissue engineering", *Biomacromolecules*, vol. 9, no. 7, pp. 1818-1825.

Ochi, K., Chen, G., Ushida, T., Gojo, S., Segawa, K., Tai, H., Ueno, K., Ohkawa, H., Mori, T., 2003, "Use of isolated mature osteoblasts in abundance acts as desired-shaped bone regeneration in combination with a modified poly-DL-lactic-Co-glycolic acid (PLGA)-collagen sponge", *Journal of Cellular Physiology*, vol. 194, no. 1, pp. 45-53.

Olevsky, E.A. 1998, "Theory of sintering: From discrete to continuum", *Materials Science and Engineering R: Reports*, vol. 23, no. 2, pp. 41-100.

Olivier, J.C. 2005, "Drug transport to brain with targeted nanoparticles", *NeuroRx*, vol. 2, no. 1, pp. 108-119.

Orthopedic Biomaterials, The World Market, PR Newswire, New York, 03 Nov 2011.

Otsuka, H., Nagasaki, Y., Kataoka, K. 2003, "PEGylated nanoparticles for biological and pharmaceutical applications", *Advanced Drug Delivery Reviews*, vol. 55, no. 3, pp. 403-419.

Ott, A., Irlinger, F. 2009, "Hydroxyapatite powder used for rapid prototyping in medical engineering", *International Journal of Computer Applications in Technology*, vol. 36, no. 1, pp. 32-37.

Oyane, A., Kim, H.M., Furuya, T., Kokubo, T., Miyazaki, T., Nakamura, T. 2003, "Preparation and assessment of revised simulated body fluids", *Journal of Biomedical Materials Research Part A*, vol. 65A, no. 2, pp. 188-195.

Park, J.B., Lakes, R.S. 1992, *Biomaterials: an introduction*, Plenum Press, New York.

Patel, Z.S., Ueda, H., Yamamoto, M, Tabata, Y., Mikos, A.G. 2008, "In vitro and in vivo release of vascular endothelial growth factor from gelatin microparticles and biodegradable composite scaffolds", *Pharmaceutical Research*, vol. 25, no. 10, pp. 2370-2378.

Patel, P., Mundargi, R.C., Babu, V.R., Jain, D., Rangaswamy, V., Aminabhavi, T.M. 2008, "Microencapsulation of doxycycline into poly(lactide-co-glycolide) by spray drying technique: Effect of polymer molecular weight on process parameters", *Journal of Applied Polymer Science*, vol. 108, no. 6, pp. 4038-4046.

Peltoniemi, H., Ashammakhi, N., Kontio, R., Waris, T., Salo, A., Lindqvist, C., Grätz, K., Suuronen, R. 2002, "The use of bioabsorbable osteofixation devices in craniomaxillofacial surgery", *Oral surgery, Oral Medicine, Oral Pathology, Oral Radiology, and Endodontics*, vol. 94, no. 1, pp. 5-14.

Peter, S.J., Miller, M.J., Yasko, A.W., Yaszemski, M.J., Mikos, A.G. 1998, "Polymer concepts in tissue engineering", *Journal of Biomedical Materials Research*, vol. 43, no. 4, pp. 422-427.

Pizzoferrato, A., Arciola, C.R., Cenni, E. 1995, "Biocampatibility of implant materials: a quantitative approach." in *Encyclopedic Handbook of Biomaterials and Bioengineering*, ed. D.L. Wise, Marcel Dekker, , pp. 329-370.

Platt, J.L. 1996, "The immunological barriers to xenotransplantation", *Critical Reviews in Immunology*, vol. 16, no. 4, pp. 331-358.

Pompe, W., Worch, H., Epple ,M.,Friess, W., Gelinsky, M., Greil, P., Hempele, U., Scharnwebera, D., Schulte, K. 2003, "Functionally graded materials for biomedical applications", *Materials Science and Engineering A*, vol. 362, no. 1-2, pp. 40-60.

Prabaharan, M., Rodriguez-Perez, M.A., De Saja, J.A., Mano, J.F. 2007, "Preparation and characterization of poly(L-lactic acid)-chitosan hybrid scaffolds with drug release capability", *Journal of Biomedical Materials Research, Part B*, vol. 81, no. 2, pp. 427-434.

Preston, S.L., Alison, M.R., Forbes, S.J., Direkze, N.C., Poulsom, R., Wright, N.A. 2003, "The new stem cell biology: Something for everyone", *Journal of Clinical Pathology - Molecular Pathology*, vol. 56, no. 2, pp. 86-96.

Qing L., Lakshmi N., Cato T.L., 2009, "Fabrication, characterization, and in vitro evaluation of poly(lactic acid glycolic acid)/nano-hydroxyapatite composite

microsphere-based scaffolds for bone tissue engineering in rotating bioreactors", Joural of Biomedical Materials Research Part A, vol 91, no. 3, pp. 679-691.

Ratner, B.D., Hoffman AS, Schoen FJ, Lemons JE 2004, *Biomaterials Science,* , London.

Ratner, B.D. 2002, "Reducing capsular thickness and enhancing angiogenesis around implant drug release systems", *Journal of Controlled Release,* vol. 78, no. 1-3, pp. 211-218.

Raucci, M.G., Guarino, V. & Ambrosio, L. 2010, "Hybrid composite scaffolds prepared by sol-gel method for bone regeneration", *Composites Science and Technology,* vol. 70, no. 13, pp. 1861-1868.

Rauwendaal, C. 2001, *Polymer Extrusion,* 4th edn, Carl Hanser Verlag, Munich.

Ravichandran, R., Sundarrajan, S., Venugopal, J.R., Mukherjee, S., Ramakrishna, S. 2012, "Advances in polymeric systems for tissue engineering and biomedical applications", *Macromolecular Bioscience,* vol. 12, no. 3, pp. 286-311.

Razaq, S. 2003, "The effect of extracellular pH on matrix turnover by cells of the bovine nucleus pulposus", *European Spine Journal,* vol. 12, no. 4, pp. 341-349.

Ren, J., Zhao, P., Ren, T.B., Gu, S.Y., Pan, K.F. 2008, "Poly (D,L-lactide)/nano-hydroxyapatite composite scaffolds for bone tissue engineering and biocompatibility evaluation", *Journal of Materials Science-Materials in Medicine,* vol. 19, no. 3, pp. 1075-1082.

Rezwan, K., Chen, Q.Z., Blaker, J.J., Boccaccini, A.R. 2006, "Biodegradable and bioactive porous polymer/inorganic composite scaffolds for bone tissue engineering", *Biomaterials,* vol. 27, no. 18, pp. 3413-3431.

Robey, P.G. 1989, "The biochemistry of bone", *Endocrinology and Metabolism Clinics of North America,* vol. 18, no. 4, pp. 859-902.

Rose, F.R.A.J., Oreffo, R.O.C. 2002, "Bone tissue engineering: Hope vs hype", *Biochemical and Biophysical Research Communications,* vol. 292, no. 1, pp. 1-7.

Roy, T.D., Simon, J.L., Ricci, J.L., Rekow, E.D., Thompson, V.P., Parsons, J.R. 2003, "Performance of hydroxyapatite bone repair scaffolds created via three-dimensional fabrication techniques", *Journal of Biomedical Materials Research, Part A,* vol. 67, no. 4, pp. 1228-1237.

Russias, J., Saiz, E., Nalla, R.K., Gryn, K., Ritchie, R.O., Tomsia, A.P. 2006, "Fabrication and mechanical properties of PLA/HA composites: A study of in vitro degradation", *Materials Science and Engineering C,* vol. 26, no. 8, pp. 1289-1295.

Russo, G., Vittoria, V., Lamberti, G., Titomanlio, G. 2010, "Electrospinning of drug-loaded polymer systems: Preparation, characterization and drug release", *Journal of Applied Polymer Science,* vol. 122, no. 6, pp. 316.

Ryan, G., Pandit, A., Apatsidis, D.P. 2006, "Fabrication methods of porous metals for use in orthopaedic applications", *Biomaterials,* vol. 27, no. 13, pp. 2651-2670.

Sabir, M.I., Xu, X.X., Li, L. 2009, "A review on biodegradable polymeric materials for bone tissue engineering applications", *Journal of Materials Science,* vol. 44, no. 21, pp. 5713-5724.

Sachs, E., Cima, M., Williams, P., Brancazio, D., Cornie, J. 1992, "Three dimensional printing. Rapid Tooling and prototypes directly from a CAD model", *Journal of Engineering for Industry,* vol. 114, no. 4, pp. 481-488.

Salerno, A., Zeppetelli, S., Oliviero, M., Battista, E., Di Maio, E., Iannace, S., Netti, P.A. 2012, "Microstructure, degradation and in vitro MG63 cells interactions of a new poly(e-caprolactone), zein, and hydroxyapatite composite for bone tissue engineering", *Journal of Bioactive and Compatible Polymers,* vol. 27, no. 3, pp. 210-226.

Salgado, A.J., Coutinho, O.P., Reis, R.L. 2004, "Bone tissue engineering: State of the art and future trends", *Macromolecular Bioscience,* vol. 4, no. 8, pp. 743-765.

Schiller, C., Rasche, C., Wehmöller, M., Beckmann, F., Eufinger, H., Epple, M., Weihe, S. 2004, "Geometrically structured implants for cranial reconstruction made of biodegradable polyesters and calcium phosphate/calcium carbonate", *Biomaterials,* vol. 25, no. 7-8, pp. 1239-1247.

Schiller, C., Siedler, M., Peters, F., Epple, M. 2001, "Functionally graded materials of biodegradable polyesters and bone-like calcium phosphates for bone replacement ", *Ceramic Transactions (USA),* vol. 114, pp. 97-108.

Schiller, C., Epple, M. 2003, "Carbonated calcium phosphates are suitable pH-stabilising fillers for biodegradable polyesters", *Biomaterials,* vol. 24, no. 12, pp. 2037-2043.

Schmidmaier, G., Wildemann, B., Bail, H., Lucke, M., Fuchs, T., Stemberger, A., Flyvbjerg, A., Haas, N.P., Raschke, M. 2001a, "Local application of growth factors (insulin-like growth factor-1 and transforming growth factor-β1) from a biodegradable poly(D,L-lactide) coating of osteosynthetic implants accelerates fracture healing in rats", *Bone,* vol. 28, no. 4, pp. 341-350.

Schmidmaier, G., Wildemann, B., Stemberger, A., Haas, N.P., Raschke, M. 2001b, "Biodegradable poly(D,L-lactide) coating of implants for continuous release of growth factors", *Journal of Biomedical Materials Research,* vol. 58, no. 4, pp. 449-455.

Setzer, B., Bächle, M., Metzger, M.C., Kohal, R.J. 2009, "The gene-expression and phenotypic response of hFOB 1.19 osteoblasts to surface-modified titanium and zirconia", *Biomaterials*, vol. 30, no. 6, pp. 979-990.

Shalaby, W.S., Karen, J.L.B. 2003, *Absorbable and Biodegradable Polymers*, Series:Advances in Polymeric Biomaterials edn, CRC Press.

Shang, Q., Wang, Z., Liu, W., Shi, Y., Cui, L., Cao, Y. 2001, "Tissue-engineered bone repair of sheep cranial defects with autologous bone marrow stromal cells", *Journal of Craniofacial Surgery*, vol. 12, no. 6, pp. 586-593.

Sheridan, M.H., Shea, L.D., Peters, M.C., Mooney, D.J. 2000, "Bioadsorbable polymer scaffolds for tissue engineering capable of sustained growth factor delivery", *Journal of Controlled Release*, vol. 64, no. 1-3, pp. 91-102.

Sherwood, J.K., Riley, S.L., Palazzolo, R., Brown, S.C., Monkhouse, D.C., Coates, M., Griffith, L.G., Landeen, L.K., Ratcliffe, A. 2002, "A three-dimensional osteochondral composite scaffold for articular cartilage repair", *Biomaterials*, vol. 23, no. 24, pp. 4739-4751.

Shikinami, Y. 2001, *Shape-Memory, Biodegradeble and absorbable material*, 523/105 edn, A61L 17/12, US.

Shikinami, Y., Okuno, M. 2001, "Bioresorbable devices made of forged composites of hydroxyapatite (HA) particles and poly L-lactide (PLLA). Part II: Practical properties of miniscrews and miniplates", *Biomaterials*, vol. 22, no. 23, pp. 3197-3211.

Shin, H., Jo, S., Mikios, A.G. 2003, "Biomimetic materials for tissue engineering", *Biomaterials*, vol. 24, pp. 4353-4363

Shum, A.W.T., Mak, A.F.T. 2003, "Morphological and biomechanical characterization of poly(glycolic acid) scaffolds after in vitro degradation", *Polymer Degradation and Stability*, vol. 81, no. 1, pp. 141-149.

Sinha, V.R., Bansal, K., Kaushik, R., Kumria, R., Trehan, A. 2004, "Poly-e-caprolactone microspheres and nanospheres: An overview", *International Journal of Pharmaceutics*, vol. 278, no. 1, pp. 1-23.

Shinzato, S., Nakamura, T., Ando, K., Kokubo, T. & Kitamura, Y. 2002, "Mechanical properties and osteoconductivity of new bioactive composites consisting of partially crystallized glass beads and poly(methyl methacrylate)", *Journal of Biomedical Materials Research*, vol. 60, no. 4, pp. 556-563.

Small IV, W., Gjersing, E., Herberg, J.L., Wilson, T.S., Maitland, D.J. 2009, "Magnetic resonance flow velocity and temperature mapping of a shape memory polymer foam device", *BioMedical Engineering Online*, vol. 8.

Smith, J.L., Jin, L., Parsons, T., Turek, T., Ron, E., Philbrook, C.M., Kenley, R.A., Marden, L., Hollinger, J., Bostrom, M.P.G., Tomin, E., Lane, J.M. 1995, "Osseous regeneration in preclinical models using bioabsorbable delivery technology for recombinant human bone morphogenetic protein 2 (rhBMP-2)", *Journal of Controlled Release*, vol. 36, no. 1-2, pp. 183-195.

Sohier, J., Haan, R.E., de Groot, K., Bezemer, J.M., 2003, "A novel method to obtain protein release from porous polymer scaffolds: emulsion coating", *Journal of Controlled Release*, vol.87, pp. 57 – 68.

Sommerfeldt, D.W., Robin, C.T. 2001, "Biology of bone and how it orchestrates the form and function of the skeleton", *European Spine Journal*, vol. 10, pp. S86-S95.

Son, J.S., Appleford, M., Ong, J.L., Wenke, J.C., Kim, J.M., Choi, S.H., Oh, D.S. 2011, "Porous hydroxyapatite scaffold with three-dimensional localized drug delivery system using biodegradable microspheres", *Journal of Controlled Release*, vol. 153, no. 2, pp. 133-140.

Song, W., Jun, Y., Han, Y., Hong, S. 2004, "Biomimetic apatite coatings on micro-arc oxidized titania", *Biomaterials*, vol. 25, no. 17, pp. 3341-3349.

Söntjens, S.H.M., Engels, T.A.P., Smit, T.H., Govaert, L.E. 2012, "Time-dependent failure of amorphous poly-d,l-lactide: Influence of molecular weight", *Journal of the Mechanical Behavior of Biomedical Materials*, vol. 13, no. 0, pp. 69-77.

Sopyan, I., Mel, M., Ramesh, S., Khalid, K.A. 2007, "Porous hydroxyapatite for artificial bone applications", *Science and Technology of Advanced Materials*, vol. 8, no. 1-2, pp. 116-123.

Srinivasan, S., Jayasree, R., Chennazhi, K.P., Nair, S.V. Jayakumar, R. 2012, "Biocompatible alginate/nano bioactive glass ceramic composite scaffolds for periodontal tissue regeneration", *Carbohydrate Polymers*, vol. 87, no. 1, pp. 274-283.

Starr, C., McMillan, B. 2012, *Human biology*, 9th edn, Yolanda Cossio.

Suwanprateeb, J., Sanngam, R., Suvannapruk, W., Panyathanmaporn, T. 2009, "Mechanical and in vitro performance of apatite-wollastonite glass ceramic reinforced hydroxyapatite composite fabricated by 3D-printing", *Journal of Materials Science: Materials in Medicine*, vol. 20, no. 6, pp. 1281-1289.

Swetha, M., Sahithi, K., Moorthi, A., Srinivasan, N., Ramasamy, K., Selvamurugan, N. 2010, "Biocomposites containing natural polymers and hydroxyapatite for bone tissue engineering", *International Journal of Biological Macromolecules*, vol. 47, no. 1, pp. 1-4.

Tanahashi, M., Yao, T., Kokubo, T., Minoda, M., Miyamoto, T. 1994, "Apatite coating on organic polymers by a biomimetic process", *Journal of the American Ceramic Society*, vol. 77, no. 11, pp. 2805-2808.

Teng, X.R., Ren, J., Gu, S.Y. 2007, "Preparation and characterization of porous PDLLA/HA composite foams by supercritical carbon dioxide technology", *Journal of Biomedical Materials Research part B*, vol. 81B, no. 1, pp. 185-193.

Terasaka, S., Iwasaki, Y., Shinya, N., Uchida, T. 2006, "Fibrin glue and polyglycolic acid nonwoven fabric as a biocompatible dural substitute", *Neurosurgery*, vol. 58, no. SUPPL. 1.

Tessmar, J., Holland, T.A., Mikos, A.G. 2006, "Salt leaching for polymer scaffolds: laboratory scale manufacture of cell carriers" in *Scaffolding in tissue engineering*, eds. P.X. Ma & J. Elisseeff, 1st edn, CRC Press, Boca Raton, FL, USA, pp. 111-123.

Tessmar, J., Mikos, A., Göpferich, A. 2003, "The use of poly(ethylene glycol)-block-poly(lactic acid) derived copolymers for the rapid creation of biomimetic surfaces", *Biomaterials*, vol. 24, no. 24, pp. 4475-4486.

Tessmar, J., Göpferich, A. 2007, "Matrices and scaffolds for protein delivery in tissue engineering", *Advanced Drug Delivery Reviews*, vol. 59, no. 4-5, pp. 274-291.

Thomas S., Y.W. 2009, *Advances in polymer processing: from macro-to nano-scales*, Woodhead Publishing.

Thomas, V., Jagani, S., Johnson, K., Jose, M.V., Dean, D.R., Vohra, Y.K., Nyairo, E. 2006, "Electrospun bioactive nanocomposite scaffolds of polycaprolactone and nanohydroxyapatite for bone tissue engineering", *Journal of Nanoscience and Nanotechnology*, vol. 6, no. 2, pp. 487-493.

Thridandapani, R.R., Folgar, C.E., Kulp, A., Folz, D.C., Clark, D.E. 2011, "Effect of direct microwave sintering on structure and properties of 8 mol% Y_2O_3-ZrO_2", *International Journal of Applied Ceramic Technology*, vol. 8, no. 5, pp. 1229-1236.

Toma, J.G., Akhavan, M., Fernandes, K.J.L., Barnabé-Heider, F., Sadikot, A., Kaplan, D.R., Miller, F.D. 2001, "Isolation of multipotent adult stem cells from the dermis of mammalian skin", *Nature Cell Biology*, vol. 3, no. 9, pp. 778-784.

Uskokovic, P.S., Tang, C.Y., Tsui, C.P., Ignjatovic, N., Uskokovic, D.P. 2007, "Micromechanical properties of a hydroxyapatite/poly-l-lactide biocomposite using nanoindentation and modulus mapping", *Journal of the European Ceramic Society*, vol. 27, no. 2-3, pp. 1559-1564.

Uttarwar M, A.P. 2008, "Fabrication of porous, drug-releasing, biodegradable, polymer scaffolds for sustained drug release", *Journal of Biomedical Materials Research, Part B*, vol. 87B, no. 1, pp. 121-131.

Väänänen, H.K., Laitala-Leinonen, T. 2008, "Osteoclast lineage and function", *Archives of Biochemistry and Biophysics*, vol. 473, no. 2, pp. 132-138.

Valentini, L., Biagiotti, J., Kenny, J.M., Santucci, S. 2003, "Effects of single-walled carbon nanotubes on the crystallization behavior of polypropylene", *Journal of Applied Polymer Science*, vol. 87, no. 4, pp. 708-713.

Van Dijk, M., Göransson, S.A., Strömblad, S. 2013, "Cell to extracellular matrix interactions and their reciprocal nature in cancer", *Experimental Cell Research*, vol. 319, no. 11, pp. 1663-1670.

Verrier, S., Blaker, J.J., Maquet, V., Hench, L.L., Boccaccini, A.R. 2004, "PDLLA/Bioglass® composites for soft-tissue and hard-tissue engineering: an in vitro cell biology assessment", *Biomaterials*, vol. 25, no. 15, pp. 3013-3021.

Wadhawan, A., Garrett, D., Perez, J.M. 2003, "Nanoparticle-assisted microwave absorption by single-wall carbon nanotubes", *Applied Physics Letters*, vol. 83, no. 13, pp. 2683-2685.

Wagermaier, W., Kratz, K., Heuchel, M., Lendlein, A. 2010, *Characterization methods for shape-memory polymers*. *Advances in Polymer Science*, vol. 226, pp. 97-145.

Wan, Y., Qu, X., Lu, J., Zhu, C., Wan, L., Yang, J., Bei, J., Wang, S. 2004, "Characterization ofsurface property of poly(lactide-co-glycolide) after oxygen plasma treatment", *Biomaterials*, vol. 25, no. 23, pp. 4777-4783.

Wang, X.Q., Wenk, E., Zhang, X.H., Meinel, L., Vunjak-Novakovic, G., Kaplan, D.L. 2009, "Growth factor gradients via microsphere delivery in biopolymer scaffolds for osteochondral tissue engineering", *Journal of Controlled Release*, vol. 134, no. 2, pp. 81-90.

Wang, C., Chen, T., Chang, S., Cheng, S., Chin, T. 2007, "Strong carbon-nanotube-polymer bonding by microwave irradiation", *Advanced Functional Materials*, vol. 17, no. 12, pp. 1979-1983.

Wang, J.H., Wei, C.W., Liu, H.C., Young, T.H. 2003, "Behavior of MG-63 cells on nylon/chitosan-blended membranes", *Journal of Biomedical Materials Research - Part A*, vol. 64, no. 4, pp. 606-615.

Wang, M., Ladizesky, N.H., Tanner, K.E., Ward, I.M.,Bonfield, W. 2000, "Hydrostatically extruded HAPEXTM", *Journal of Materials Science*, vol. 35, no. 4, pp. 1023-1030.

Wang, Y., Chen, F.B., Li, Y.C., Wu, K.C. 2004, "Melt processing of polypropylene/clay nanocomposites modified with maleated polypropylene compatibilizers", *Composites Part B: Engineering*, vol. 35, no. 2, pp. 111-124.

Wang, Y.J, Shi, X.T., Ren, L., Wang, C.M., Wang, D.A. 2009, "Porous poly (lactic-co-glycolide) microsphere sintered scaffolds for tissue repair applications", *Materials Science and Engineering C,* vol. 29, no. 8, pp. 2502-2507.

Wang, Y.J, Shi, X.T, Ren, L., Yao, Y., Zhang, F., Wang, D.A. 2010, "Poly(lactide-co-glycolide)/titania composite microsphere-sintered scaffolds for bone tissue engineering applications", *Journal of Biomedical Materials Research , Part B,* vol. 93, no. 1, pp. 84-92.

Warnke, P.H., Seitz, H., Warnke, F., Becker, S.T., Sivananthan, S., Sherry, E., Liu, Q., Wiltfang, J., Douglas, T. 2010, "Ceramic scaffolds produced by computer-assisted 3D printing and sintering: Characterization and biocompatibility investigations", *Journal of Biomedical Materials Research, Part B,* vol. 93, no. 1, pp. 212-217.

Watari, F., Yokoyama, A., Omori, M., Hirai, T., Kondo, H., Uo, M., Kawasaki, T. 2004, "Biocompatibility of materials and development to functionally graded implant for bio-medical application", *Composites Science and Technology,* vol. 64, no. 6, pp. 893-908.

Webster TJ, Schadler LS, Siegel RW, Bizios R. 2001, "Mechanisms of enhanced osteoblast adhesionon nanophase alumina involve vitronectin", *Tissue Engineering*, vol. 7, no.3, pp.291-301.

Williams, D.F. 2008, "On the mechanisms of biocompatibility", *Biomaterials,* vol. 29, no. 20, pp. 2941-2953.

Wischke, C., Lendlein, A. 2010, "Shape-memory polymers as drug carriers-a multifunctional system", *Pharmaceutical research,* vol. 27, no. 4, pp. 527-529.

Wischke, C., Neffe, A.T., Steuer, S. Lendlein A. 2009, "Evaluation of a degradable shape-memory polymer network as matrix for controlled drug release", *Journal of Control Release* vol. 138**,** pp. 243–250.

Wu, L.B., Ding, J.D. 2004, "In vitro degradation of three-dimensional porous poly(D,L-lactide-co-glycolide) scaffolds for tissue engineering", *Biomaterials,* vol. 25, no. 27, pp. 5821-5830.

Wu, D., Sun, Y., Wu, L., Zhang, M. 2008a, "Linear viscoelastic properties and crystallization behavior of multi-walled carbon nanotube/ polypropylene composites", *Journal of Applied Polymer Science,* vol. 108, no. 3, pp. 1506-1513.

Wu, H., Wan, Y., Cao, X., Wu, Q. 2008b, "Proliferation of chondrocytes on porous poly(dl-lactide)/chitosan scaffolds", *Acta Biomaterialia,* vol. 4, no. 1, pp. 76-87.

Xu, L., Xiong, Z.C., Yang, D.J., Zhang, L.F., Chang, J., Xiong, C.D. 2009, "Preparation and in vitro degradation of novel bioactive polylactide/wollastonite scaffolds", *Journal of Applied Polymer Science,* vol. 114, no. 6, pp. 3396-3406.

Xu, Z.H., Wu, Q.Y. 2009, "Effect of lecithin content blend with poly (L-lactic acid) on viability and proliferation of mesenchymal stem cells", *Materials science and engineering C,* vol. 29, no. 5, pp. 1593-1598.

Xynos, I.D., Edgar, A.J., Buttery, L.D.K., Hench, L.L., Polak, J.M. 2000, "Ionic products of bioactive glass dissolution increase proliferation of human osteoblasts and induce insulin-like growth factor II mRNA expression and protein synthesis", *Biochemical and BIophysical Research Communications,* vol. 276, no. 2, pp. 461-465.

Yamamoto, M., Kato, K., Ikada, Y. 1996, "Effect of the structure of bone morphogenetic protein carriers on ectopic bone regeneration", *Tissue Engineering,* vol. 2, no. 4, pp. 315-326.

Yang, B., Huang, W.M., Li C., Chor, J.H. 2005, "Effects of moisture on the glass transition temperature of polyurethane shape memory polymer filled with nano-carbon powder," *European Polymer Journal,* vol. 41, pp. 1123-1128.

Yang, X.B., Bhatnagar, R.S., Li, S., Oreffo, R.O. 2004. "Biomimetic collagen scaffolds for human bone cell growth and differentiation". Tissue Engineering, vol. 10, pp. 1148–59.

Yang, Y.Y., Chung, T.S., Ng, N.P. 2001, "Morphology, drug distribution, and in vitro release profiles of biodegradable polymeric microspheres containing protein fabricated by double-emulsion solvent extraction/evaporation method", *Biomaterials,* vol. 22, no. 3, pp. 231-241.

Yoon, J.J., Kim, J.H., Park, T.G. 2003, "Dexamethasone-releasing biodegradable polymer scaffolds fabricated by a gas-foaming/salt-leaching method", *Biomaterials,* vol. 24, no. 13, pp. 2323-2329.

Yoon, J.J., Park, T.G. 2001, "Degradation behaviors of biodegradable macroporous scaffolds prepared by gas foaming of effervescent salts", *Journal of Biomedical Materials Research,* vol. 55, no. 3, pp. 401-408.

Zaidi, M. 2007, "Skeletal remodeling in health and disease.", *Nature Medicine,* vol. 13, pp. 791-801.

Zein, I., Hutmacher, D.W., Tan, K.C., Teoh, S.H. 2002, "Fused deposition modeling of novel scaffold architectures for tissue engineering applications", *Biomaterials,* vol. 23, no. 4, pp. 1169-1185.

Zeltinger, J., Sherwood, J.K., Graham, D.A. 2001, "Effect of pore size and void fraction on cellular adhesion, proliferation, and matrix deposition", Tissue engineering, vol. 7, no. 5, pp. 557-572.

Zelzer, M., Majani, R., Bradley, J.W., Rose, F.R.A.J., Davies, M.C., Alexander, M.R. 2008, "Investigation of cell-surface interactions using chemical gradients formed from plasma polymers", *Biomaterials*, vol. 29, no. 2, pp. 172-184.

Zhang, D.J., Zhang, L.F., Xiong, Z.C., Bai, W., Xiong, C.D. 2009, "Preparation and characterization of biodegradable poly(d,l-lactide) and surface-modified bioactive glass composites as bone repair materials", *Journal of Materials Science-Materials in Medicine*, vol. 20, no. 10, pp. 1971-1978.

Zhang, L.F., Yang, D.J., Chen, H.C., Sun, R., Xu, L., Xiong, Z.C., Govender, T., Xiong, C.D. 2008, "An ionically crosslinked hydrogel containing vancomycin coating on a porous scaffold for drug delivery and cell culture", *International Journal of Pharmaceutics*, vol. 353, no. 1-2, pp. 74-87.

Zhang, L.F., Sun, R., Xu, L., Du, J., Xiong, Z.C., Chen, H.C., Xiong, C.D. 2008, "Hydrophilic poly (ethylene glycol) coating on PDLLA/BCP bone scaffold for drug delivery and cell culture", *Materials science and engineering C*, vol. 28, no. 1, pp. 141-149.

Zhang, M.Q. 2004, "Biocompatibility of materials" in *Biomaterials and Tissue Engineering*, ed. D. Shi, 2004 edition edn, pp. 83-143.

Zhang, C., Hu, Y.Y., Zhang, S.M., Xiong, Z., Yan, Y.N., Cui, F.Z. 2004, "Application of 3-dimensional porous hydroxyapatite/collagen-poly(L-lactic acid) in tissue engineering of bone: (I)fabrication of 3-dimensional porous hydroxyapatite/collagen-poly(L-lactic acid)", *Chinese Journal of Biomedical Engineering*, vol. 23, no. 5.

Zhang, M., Ye, L., Gao, Y., Lv, X., Chang, J. 2009, "Effects of hydrolysis on dodecyl alcohol modified β-$CaSiO_3$ particles and PDLLA/modified β-$CaSiO_3$ composite films", *Composites Science and Technology*, vol. 69, no. 15-16, pp. 2547-2553.

Zhang, R., Ma, P.X. 1999, "Porous poly(L-lactic acid)/apatite composites created by biomimetic process", *Journal of Biomedical Materials Research*, vol. 45, no. 4, pp. 285-293.

Zhang, Y.Z., Wang, X., Feng, Y., Li, J., Lim, C.T., Ramakrishna, S. 2006. "Coaxial electrospinning of (fluorescein isothiocyanate-conjugated bovine serum albumin)-encapsulated poly(e-caprolactone) nanofibers for sustained release", *Biomacromolecules*, vol. 7, pp. 1049-1057.

Zhao, J., Guo, L.Y., Yang, X.B., Weng, J. 2008a, "Preparation of bioactive porous HA/PCL composite scaffolds", *Applied Surface Science*, vol. 255, no. 5 Part 2, pp. 2942-2946.

Zhao, L., He, C., Gao, Y., Cen, L., Cui, L., Cao, Y. 2008b, "Preparation and cytocompatibility of PLGA scaffolds with controllable fiber morphology and

diameter using electrospinning method", *Journal of Biomedical Materials Research, Part B*, vol. 87, no. 1, pp. 26-34.

Zheng, X., Zhou, S., Li, X., Weng, J. 2006, "Shape memory properties of poly(d,l-lactide)/hydroxyapatite composites", *Biomaterials*, vol. 27, no. 24, pp. 4288-4295.

Zhmayev, E., Cho, D., Joo, Y.L. 2010, "Nanofibers from gas-assisted polymer melt electrospinning", *Polymer*, vol. 51, no. 18, pp. 4140-4144.

Zhou, S.B., Zheng, X.T., Yu, X.J., Wang, J.X., Weng, J., Li, X.H., Feng, B., Yin, M. 2007, "Hydrogen bonding interaction of poly(D,L-lactide)/hydroxyapatite nanocomposites", *Chemistry of Materials*, vol. 19, no. 2, pp. 247-253.

Zolnik, B.S., Burgess, D.J. 2008, "Evaluation of in vivo-in vitro release of dexamethasone from PLGA microspheres", *Journal of Controlled Release*, vol. 127, no. 2, pp. 137-145.

Appendix: Feasibility Study on Fabrication of Polymer Biocomposite by Microwave Sintering

A1. Introduction

Biodegradable Dex-releasing PDLLA/nano-HAp scaffolds were successfully fabricated by the newly developed PC-DC technique in the previous parts of this study. This technique has the advantage of independently controlling the pore size and porosity level of the scaffold, avoiding decomposition of the polymer matrix and bioactive inclusions, low cost and easy operation. However, the processing time of this technique is about one week including complete salt leaching and vacuum drying. Therefore, a study to explore a faster processing way for polymer composite fabrication was carried out in this part of study.

Nowadays, microwave processing has attracted great research interest for composite fabrication because it can greatly reduce energy consumption and processing time (Thomas 2009), and avoids dissolving problems by direct coupling with materials, under two conditions, i.e., direct (Thridandapani et al. 2011) and hybrid sintering (Anklekar et al. 2001). Direct microwave sintering takes the materials themselves as the only susceptors, while hybrid sintering uses both the fabricating materials and external susceptors with high dielectric loss to absorb the microwave energy. In addition to the time and energy saving, microwave sintering can enhance the bonding strength of the fabricated composite, because of the soldering effect between the filler and the matrix of different dielectric constants (Wang et al. 2007). However, this method is limited to polymeric materials which generally have low dielectrics (Esawi et

al. 2010). Polypropylene (PP) is a type of non-degradable polymer that has been commonly used in the construction, automotive and fiber manufacturing industries because of its dimensional stability, low density, and high chemical resistance (Kissel et al. 1999, Liang et al. 2010). In addition to these industrial applications, PP also has some biomedical applications, such as abdominal wall hernia repair, urinary incontinence, prolapsed repair and tracheal replacement (Behrend et al. 2006, De Tayrac et al. 2007, Campanelli et al. 2008). The advantages of using PP for tissue replacement include non-biodegradability, durability, high dimensional stability as well as good chemical resistivity (Cosson et al. 2003). In this part of the study, PP was chosen as a model material for the feasibility study on microwave sintering of biocomposites due to its low dielectrics and low microwave absorption rate. Therefore, a microwave susceptor should be selected and incorporated into PP to assist microwave sintering of low dielectrics PP. Carbon nanotubes (CNTs) with superior electromagnetic absorbing properties and extraordinary mechanical properties (Wadhawan et al. 2003) could be a promising candidate to act as susceptors to assist microwave sintering. Bhattacharyya et al. (2003) pointed out that CNTs acted as nucleating sites for PP crystallization, and an addition of 0.8 wt% of single-walled carbon nanotubes (SWCNTs) increased the PP crystallization rate by more than an order of magnitude. Another study conducted by Valentini et al. (2003) showed that there was an increasing nucleating effect with increasing SWCNTs loading, which was followed by saturation. In addition to the nucleating effects in the PP/CNTs composites, mechanical enhancement of the composites was also observed after incorporation of CNTs into PP (Kearns & Shambaugh 2002). HAp, a typical bioactive ceramic, has attracted great research interest due to its chemical similarity to the mineral component of bone and its

good ability in generating strong bonding with growing tissue (Nikpour et al. 2012). It also has the ability to stiffen composites and increase their elastic moduli (Wang et al. 2000). Therefore, a composite combining PP, MWCNTs, and HAp with improved mechanical and bioactivity was selected as a model system for the feasibility study on microwave sintering of polymer based composite for potential biomedical applications.

In this part of the study, microwave sintering was conducted to fabricate PP/MWCNT/HAp composites. To overcome the main barrier in microwave sintering of microwave transparent PP, dielectric MWCNTs were chosen as the microwave susceptors and incorporated in the PP matrix. Moreover, MWCNTs also act as the reinforcing inclusions for the PP matrix. Meanwhile, the addition of HAp particles is expected to provide good bioactivity, and enhance the stiffness of the composites. XRD, SEM, and EDX were used to characterize the sintered PP/MWCNT/HAp composites in terms of chemical compositions, HAp distributions, and microstructures of the composites. The results of this work have been accepted for publication in the journal Composites Part B.

A2. Sample Preparation

The PP powders were obtained from Goonvean Fibres (Devon, UK), with a density of 0.9 g/cm^3 and particle sizes ranging from 50 to 80 μm. The melting point of the PP was in the range of 150-170 °C. The MWCNTs (catalog no. S-MWNT-1020) were purchased from the Shenzhen Nano-Tech Port Co., Ltd. (Shenzhen, China), with purity > 95%. The outer diameter and the length of MWCNTs were 10-20 nm and 5-15 μm, respectively. The as-received MWCNTs were treated with 38% hydrochloric acid for

purification for 24 hours. The nano-sized HAp particles, obtained from Kingo Advanced Materials R&D Co., Ltd. (Ningbo, China), were irregular-plate-shaped of size 400-2000 nm along the longest direction and nearly 20 nm in thickness.

A combination of ultrasonication and mechanical stirring in a solution based condition was selected to uniformly disperse the MWCNTs. A ultrasonicator (CP 2600, Crest Ultrasonic Powersonic), with an average power of 300 W and a frequency of approximate 45 kHz and a magnetic stirrer (SP18420, Nuova Stir Plate) were adopted. A schematic diagram with detailed parameters values for the powder dispersion process is shown in Figure A.1. First, the three types of particles were ultrasonicated in de-ionized water or ethanol suspension respectively. Second, the three separated suspensions were mixed together by ultrasonication for 30 minutes. Finally, the mixed suspension was further dispersed by a magnetic stirrer until homogenous dispersion was achieved.

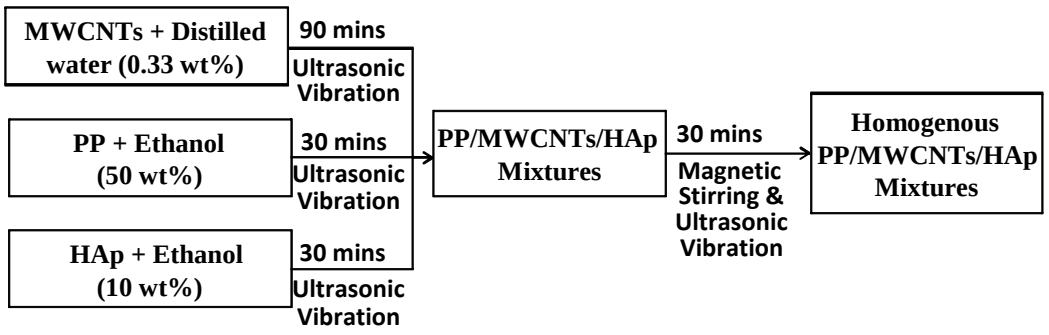

Figure A.1 Schematic diagram for the procedures of powder dispersion

The well-dispersed mixtures were dried for compaction. Since the particles tended to agglomerate during the drying process, a powder sieving procedure was applied to narrow down the range of the particle size distribution. The particles were sieved by a sieve with opening sizes of 75-120 μm in diameter, and then added into a highly polished mould with an internal diameter of 20 mm and lubricant on its inner surface. A 1-Hz sinusoidal load ranging from 10 to 20 N was applied to the mould for particle rearrangement, i.e., from the loosely arrayed condition to a closer packing for increasing the density of the green compact. After particle rearrangement, the PP/MWCNT/HAp powder compaction was conducted at a peak load of 40 kN, i.e., 127 MPa, in order to enable the PP particles to go through plastic deformation, followed by a holding time of 200 s. German (1989) suggested that a smaller thickness-to-diameter ratio resulted in a more uniform stress distribution along the axial direction within the sample. In this study, green compacts with an appropriate ratio of thickness to diameter (i.e. 20 mm in diameter and 3 mm in thickness) were prepared.

The acid-treated MWCNTs, the as-received PP and HAp powders were weighed in a ratio of "PP (wt%):MWCNTs (wt%):HAp (wt%)" as: 100:1:0, 100:1:5, 100:1:15, and 100:1:30 (the ratios used as designated below). Each green compact obtained was placed in a ceramic crucible for sintering in a microwave oven (1100 W, 2.45 GHz frequency magnetron) at full power. The sintering time of each sample was recorded. After sintering, both the oven cavity and the crucible were cooled down to room temperature for next sample sintering.

A3. Processing and Properties of PP/MWCNT/HAp Composites

A3.1 Sintering Time

The sintering time for PP/MWCNT/HAp composites recorded during the experiment are listed in Table A.1. All the composite samples were sintered within 1 minute. This method has led to a significant reduction in heating time, as compared with conventional polymer processing methods such as the extrusion process which needs 30-120 minutes in a single procedure of heating the materials to the peak temperature (Rauwendaal 2001). These suggest that MWCNTs, as microwave susceptors, show a great ability to assist in microwave sintering of PP/MWCNT/HAp composites by enhancing the energy absorption. Another interesting finding is the trend of the sintering time decreasing with an increase of HAp content. This is probably due to the relative reduction of the microwave transparency of PP.

Table A.1 Time required for microwave sintering of PP/MWCNT/HAp composites with different compositions

Samples PP:MWCNT:HA (wt%)	100:1:0	100:1:5	100:1:15	100:1:30
Sintering time (s)	50	25	23	22

A3.2 Morphology of PP/MWCNT/HAp Composites

The samples were fractured after being immersed in liquid nitrogen to effect brittle fractures of the PP matrix and fix the morphology of the composites after fracture. Field emission scanning electron microscopy (FE-SEM, Jeol JSM-6335F) was adopted to examine the fracture surfaces of the microwave sintered samples at high magnification. For comparison, unmodified PP plates (Changzhou No.3 Plastic Co., Ltd., China)

fabricated from extrusion moulding were used as control. Secondary electron imaging scanning electron microscopy (SEI-SEM, Jeol JSM-6490) was conducted to examine the morphology of the pores on the fracture surfaces of the microwave sintered samples at low magnification. 20 kV was selected as the observation voltage.

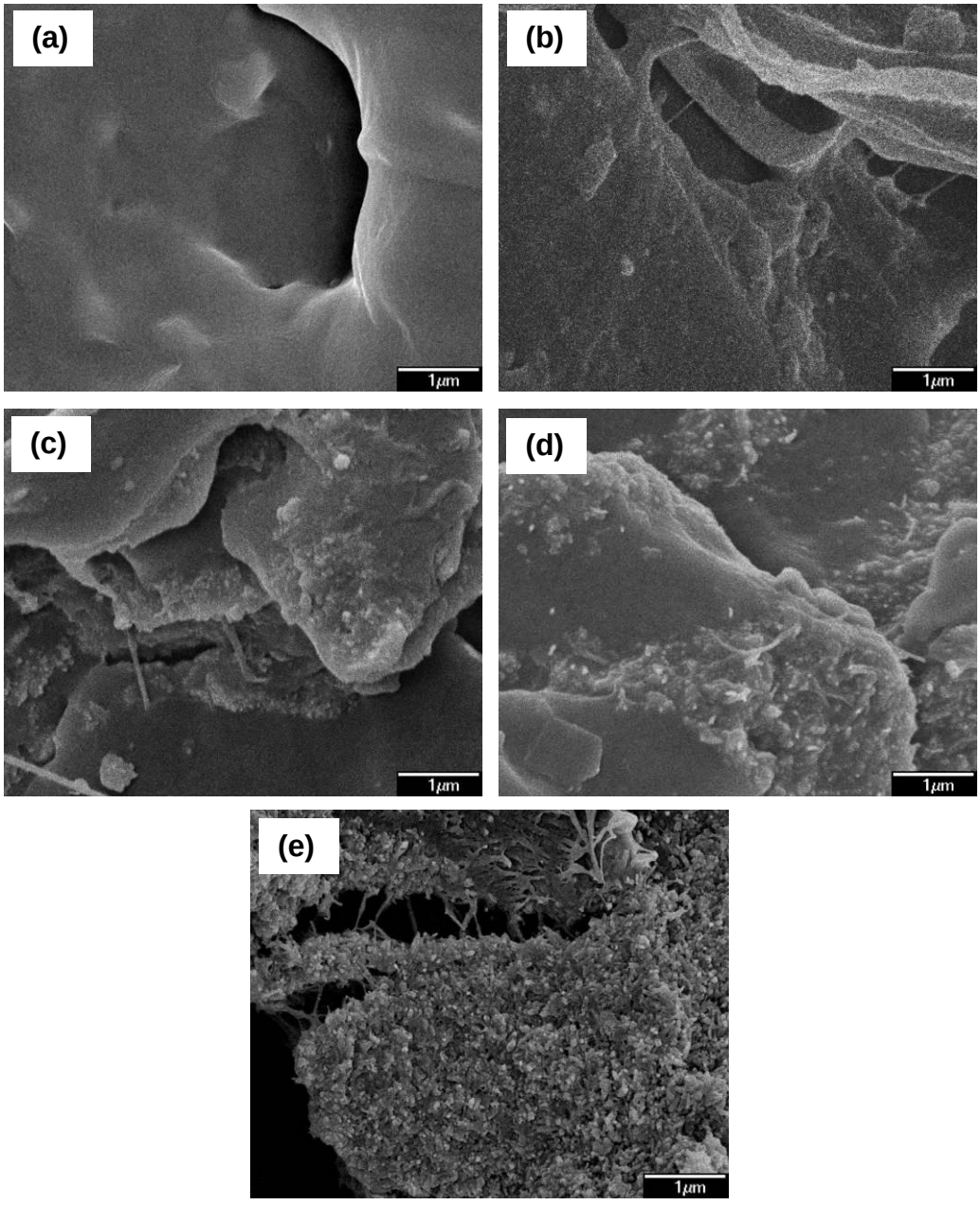

Figure A.2 FE-SEM micrographs of the fractured surfaces: (a) unfilled PP, sintered PP/MWCNT/HAp composites of (b) 100:1:0, (c) 100:1:5, (d) 100:1:15 and (e) 100:1:30.

Figure A.2 shows the FE-SEM images of the unfilled and CNTs/HAp filled PP samples. Unfilled PP shows a smoother surface compared to the composites. Crack bridging effect is observed at the fracture sites for all the PP/MWCNT/HAp composites. The bridging elements are probably due to the breakage of the sintered PP and the stretched MWCNTs. This bridging effect can improve the mechanical properties such as elastic modulus, yield and tensile strengths. Similar images and results can be found in the literature (Coleman et al. 2006). The roughness extent of the fracture surfaces increases with increasing amount of HAp, as shown in Figures A.2(b)-(e).

A porous structure is one of the key factors that influence the mechanical and biological performance of a biomedical component (Olevsky 1998). SEI-SEM images are presented in Figure A.3. It can be seen that pores were generated in all the sintered PP/MWCNT/HAp samples, while there were no pores observed in the unfilled PP plate. From Figure A.3(b) to (e), the average diameter of the pores firstly reaches a peak of nearly 100 μm at 100:1:0 then decreases to 50 μm at 100:1:5 and 10 μm at 100:1:15, and finally increases to 20 μm at 100:1:30. The initial cavities of the green compact may be the reason for pore generation in the sintered PP/MWCNT/HAp composites, because some cavities may exist among PP particles even when they were tightly compacted. As the PP particle size is much bigger than that of the MWCNT and HAp, the MWCNT and HAp powders tended to appear in these cavities and attach to the surface of the PP powders after compaction. The cavities in the composites without the HAp addition are bigger in size than those of the PP/MWCNT/HAp composites, resulting in bigger pores, with diameters of 100 μm generated in the sintered 100:1:0 composites. The diameter of the pores decreased with the increase of HAp content and

reached to a minimum value of 10 μm at a weight ratio of 100:1:15. When the HAp content further increased for a ratio of 100:1:30, the cavities may be fully filled by the HAp, and some extra HAp may be created in other cavities.The diameter of the pores increased to approximately 20 μm in the sintered 100:1:30 samples, as shown in Figure A.3 (e).

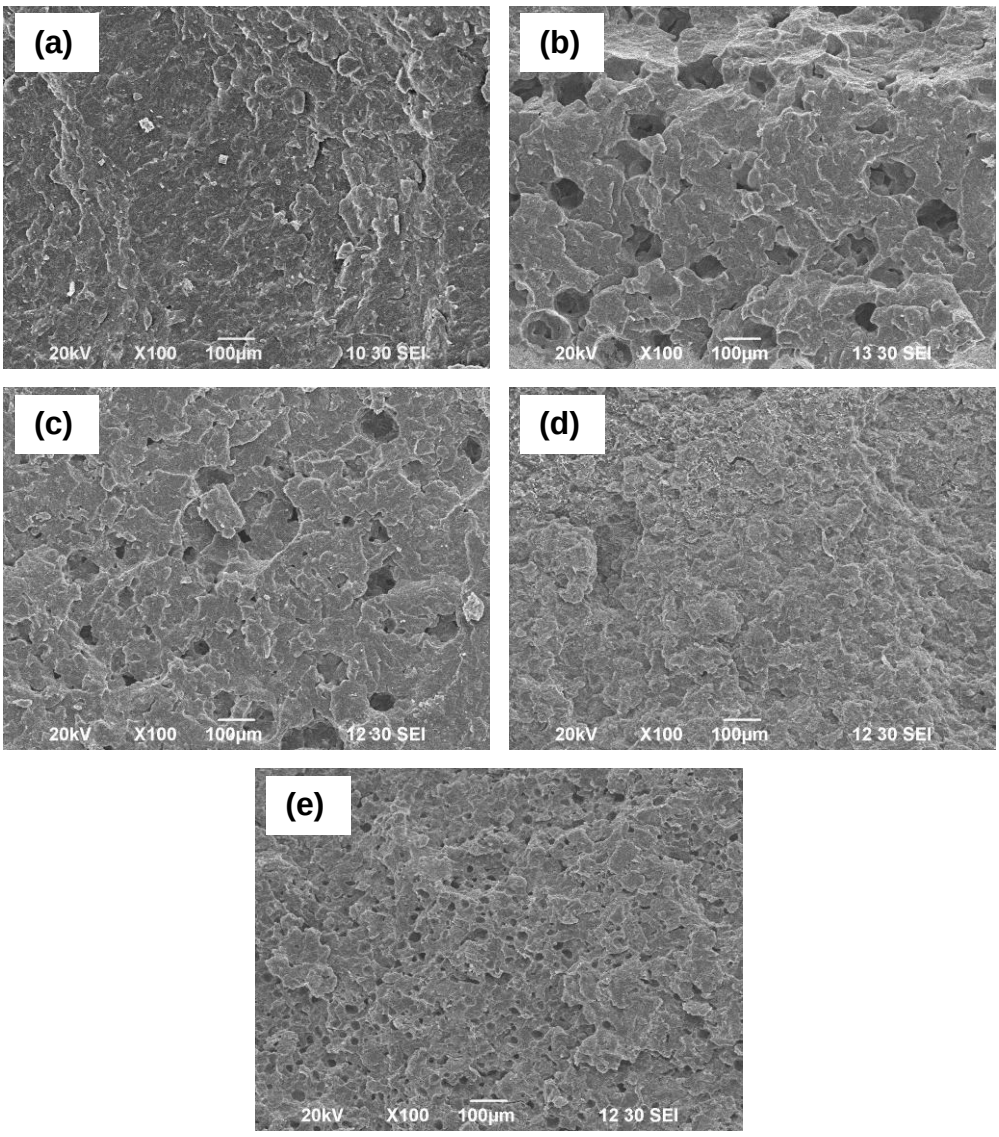

Figure A.3 SEI-SEM micrographs of the fracture surfaces: (a) unfilled PP, and sintered PP/MWCNT/HAp composites of (b) 100:1:0, (c) 100:1:5, (d) 100:1:15 and (e) 100:1:30

A3.3 Composition Characterization

Over-sintering may lead to decomposition of PP. The X-ray diffractometer (XRD, Bruker D8 Discover) was used to investigate decomposition and phase change of PP. Scanning occurred over a 2 theta rang from 10 to 55 degrees at a rate of 1 degree/min. XRD patterns of microwave sintered composites are shown in Figure A.4. The peaks of the PP/MWCNT/HAp composites fit the standard HAp peaks (JCPDS 9-432) and PP peaks (Assouline et al. 2001) without observing any extra peaks. Therefore, no HAp and PP phase transition during the microwave sintering could be confirmed.

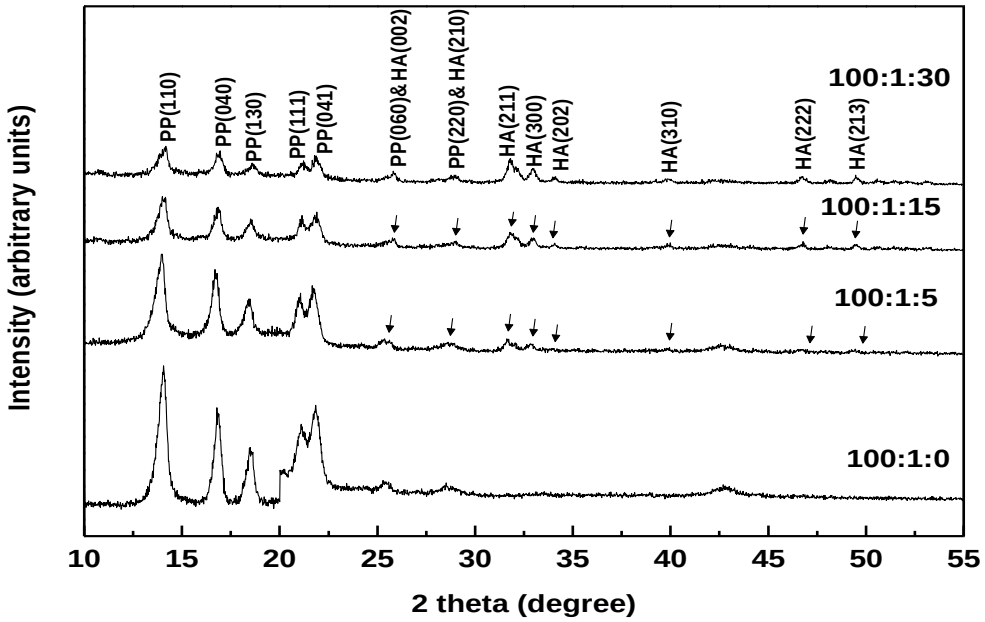

Figure A.4 XRD patterns of the microwave sintered PP/MWCNT/HAp composites with different compositions

A3.4 HAp Distribution in the Composites

Back scattered scanning electron microscopy (BS-SEM, Jeol JSM-6490) was used to investigate the HAp distribution in the PP matrix. The samples were polished and

placed on a stub, and carbon was coated to enhance their conductivity. The examination was conducted at 20 kV. In order to determine the elemental composition of the samples, an energy dispersive X-ray (EDX, Oxford, INCA 250 Energy System) examination was conducted.

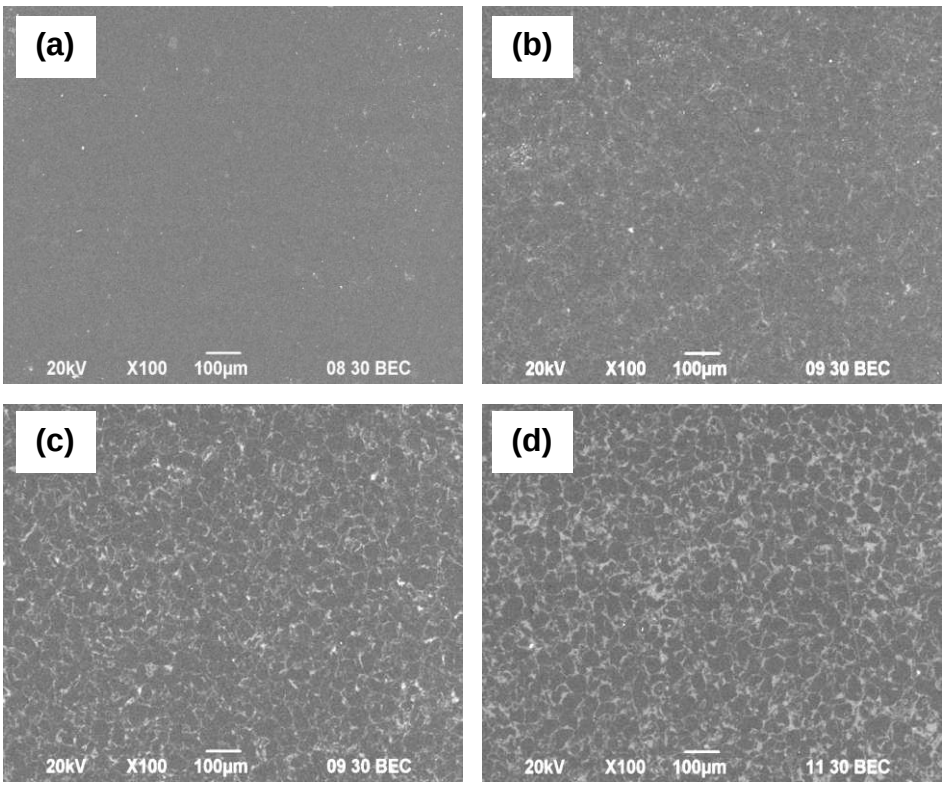

Figure A.5 BS-SEM micrographs of polished surfaces of sintered PP/MWCNT/HAp composites of (a) 100:1:0, (b) 100:1:5, (c) 100:1:15 and (d) 100:1:30

The BS-SEM micrographs of the microwave sintered samples are shown in Figure A.5. The EDX test result for the 100:1:30 composite at the selected region indicated in Figure A.6(a) is shown in Figure A.6(b). It can be observed that the white color phase as shown in Figure A.6(a) represents the HAp, since the spectra in Figure A.6(b)

indicates that the atomic ratio of Ca/P is 1.54, which is close to the claimed ratio of 1.67 for HAp. As shown in the BS-SEM micrographs from 100:1:5 to 100:1:30 in Figures A.5(b-d), the HAp particles increased with HAp fraction in the composites. HAp is uniformly distributed in the PP matrix by attaching to the surface of the PP powders during the dispersion process. This also indicates that HAp has been successfully incorporated.

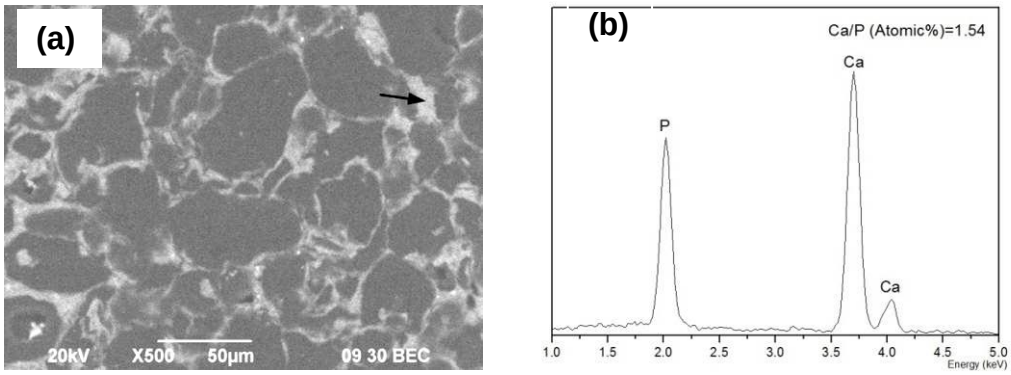

Figure A.6 (a) Magnified BS-SEM micrograph of polished surface of 100:1:30, (b) EDX spectra of the area in micrograph (a) as pointed by the arrow

A4. Summary

The PP/MWCNT/HAp composites were successfully fabricated by the microwave sintering technique. The heating time was reduced to less than 1 minute which was a significant reduction compared to the conventional polymeric material processing methods. Incorporation of the MWCNTs into the PP matrix helped the microwave energy absorption of the composites and hence reduced the sintering time. The results of the material characterization tests show that the HAp was uniformly distributed within the composites, suggesting that the dispersion method, with a combination of

ultrasonication and mechanical stirring, was effective. Pores were generated in the sintered PP/MWCNT/HAp composites and the smallest pores occurred at 100:1:15. The outcomes of the study have demonstrated the feasibility of fabricating the PP based composite, with the addition of HAp and MWCNTs fillers as a model system, by microwave sintering. This method has high potential applications in fabricating similar polymer based composite materials.

Further research may be conducted to investigate the application of the microwave sintering technique in fabricating porous polymer based composites. Surface treatments maybe carried out to improve the interfacial bonding between the particles and matrix and hence improve the mechanical properties of the composites. Moreover, in vitro and in vivo tests are also suggested for further investigation of their bioactivity.